MAX-PLANCK-INSTITUT FÜR MOLEKULARE PFLANZENPHYSIOLOGIE

AG MOLECULAR MECHANISMS OF PLANT ADAPTATION – DR. ROOSA LAITINEN

Understanding the impact of heterozygosity on metabolism, growth and hybrid necrosis within a local *Arabidopsis thaliana* collection site

Dissertation

zur Erlangung des akademischen Grades

“doctor rerum naturalium“

(Dr. rer. nat.)

In der Wissenschaftsdisziplin “Molekularbiologie“

eingereicht an der

Mathematisch-Naturwissenschaftlichen Fakultät

Der Universität Potsdam

von

ANDRÉS EDUARDO RODRÍGUEZ CUBILLOS

Potsdam, September 2018

Published online at the
Institutional Repository of the University of Potsdam:
URN urn:nbn:de:kobv:517-opus4-416753
http://nbn-resolving.de/urn:nbn:de:kobv:517-opus4-416753

Declaration

I hereby declare that the work presented in this thesis has been carried out by myself and does not incorporate any material previously submitted for another degree at any university. To the best of my knowledge, it does not concern any material previously written by another person, except where reference is made in the text.

Selbständigkeitserklärung

Hiermit erkläre ich, dass ich die vorliegende Arbeit selbständig und unter Verwendung keiner anderen als den von mir angegeben Quellen und Hilfsmitteln verfasst habe. Ferner erkläre ich, dass ich bisher weder an der Universität Potsdam noch anderweitig versucht habe eine Dissertation einzureichen oder mich einer Doktorprüfung zu unterziehen.

Potsdam, 10th of April 2018

Andrés Rodríguez

Acknowledgements

I would like to thank Dr. Roosa Laitinen for believing in me and giving me the opportunity to embark on these scientific projects, together with all the members from AG Laitinen for being supportive and contributing to a pleasant working environment. Specifically, I would like to thank Dr. Markus Nurmi for his assistance during the protein-related experiments; Dr. Björn Plötner, for his help and support in all the institute and German-related processes (and for teaching me the importance of bananas in our lives); Dema Alhajturki, for her openness and willingness to discuss about different challenges in the scientific life; Arkadiusz Guzinski and Max Birkl, for their assistance in different technical-related processes of specific experiments; Dr. Neha Vaid, for her theoretical support in the Y2H experiments; and Dr. Jing Yu, for her sweet and caring attitude throughout my PhD.

Additionally, I would like to thank Dr. Francisco de Abreu e Lima for sharing his time to introduce me to the R programming language; Dr. Arun Sampathkumar, for teaching me how to use a confocal laser scanning microscope; Dr. Mutsumi Watanabe, Franziska Brückner and Dr. Rainer Höfgen for their support during the ion measurements; Dr. Saleh Alseekh and Alexander Erban for annotating the metabolites generated in the first and second project, respectively; and Dr. Alisdair Fernie and Dr. Joachim Kopka for their assistance with the metabolic measurements.

I would also like to thank my PhD advisory committee (PAC), Dr. Alexander Graf and Dr. Zoran Nikoloski, for their advice and guidance throughout the development of these projects, as well as the Greenteam, IT-Service, Media Kitchen and Administration Department of the MPIMP for their constant support and services provided.

Finally, I would like to thank my parents and Dr. Magdalena Swiadek for their emotional support throughout this journey; for believing in me even during tough times and reminding me that I am part of a family. Life is not just science; it's also love and unity.

Table of Contents

Abstract

Plants are unable to move away from unwanted environments and therefore have to locally adapt to changing conditions. *Arabidopsis thaliana* (Arabidopsis), a model organism in plant biology, has been able to rapidly colonize a wide spectrum of environments with different biotic and abiotic challenges. In recent years, natural variation in Arabidopsis has shown to be an excellent resource to study genes underlying adaptive traits and hybridization's impact on natural diversity. Studies on Arabidopsis hybrids have provided information on the genetic basis of hybrid incompatibilities and heterosis, as well as inheritance patterns in hybrids. However, previous studies have focused mainly on global accessions and yet much remains to be known about variation happening within a local growth habitat. In my PhD, I investigated the impact of heterozygosity at a local collection site of Arabidopsis and its role in local adaptation. I focused on two different projects, both including hybrids among Arabidopsis individuals collected around Tübingen in Southern Germany. The first project sought to understand the impact of hybridization on metabolism and growth within a local Arabidopsis collection site. For this, the inheritance patterns in primary and secondary metabolism, together with rosette size of full diallel crosses among seven parents originating from Southern Germany were analyzed. In comparison to primary metabolites, compounds from secondary metabolism were more variable and showed pronounced non-additive inheritance patterns. In addition, defense metabolites, mainly glucosinolates, displayed the highest degree of variation from the midparent values and were positively correlated with a proxy for plant size.

In the second project, the role of ACCELERATED CELL DEATH 6 (ACD6) in the defense response pathway of Arabidopsis necrotic hybrids was further characterized. Allelic interactions of *ACD6* have been previously linked to hybrid necrosis, both among global and local Arabidopsis accessions. Hence, I characterized the early metabolic and ionic changes induced by ACD6, together with marker gene expression assays of physiological responses linked to its activation. An upregulation of simple sugars and metabolites linked to non-enzymatic antioxidants and the TCA cycle were detected, together with putrescine and acids linked to abiotic stress responses. Senescence was found to be induced earlier in necrotic hybrids and cytoplasmic calcium signaling was unaffected in response to temperature. In parallel, GFP-tagged constructs of ACD6 were developed.

This work therefore gave novel insights on the role of heterozygosity in natural variation and adaptation and expanded our current knowledge on the physiological and molecular responses associated with ACD6 activation.

Keywords: *Arabidopsis thaliana*, diallel crosses, non-additive inheritance, hybrid necrosis, ACD6, metabolism, variation, adaptation

Zusammenfassung

Pflanzen sind sessile Organismen, die nicht in der Lage sind sich unerwünschten Lebensräumen zu entziehen, sodass sie sich an verschiedene Umweltbedingungen anpassen müssen. *Arabidopsis thaliana* (Arabidopsis) als Modellorganismus der Pflanzenbiologie war in der Lage eine Vielzahl von Lebensräumen zu kolonisieren und dabei verschiedenen biotischen und abiotischen Problemen zu trotzen. Natürliche Variation in Arabidopsis hat sich in den letzten Jahren als Mittel bewährt, um Gene zu analysieren, welche für adaptive Eigenschaften und natürliche Vielfalt verantwortlich sind. Studien über Arabidopsis-Hybride haben Erkenntnisse über die genetische Basis von Hybridinkompatibilitäten, Heterosis und Vererbungsmustern von Hybriden geliefert. Jedoch haben diese sich bisher lediglich mit globalen ökotyp befasst, sodass noch viele Informationen über Variation in einem lokalen Wachstumsgebiet fehlen.

In meiner Doktorarbeit habe ich den Einfluss von Heterozygotie in einer lokalen Arabidopsis-Population und deren Rolle bei der Adaption untersucht. Dabei habe ich mich auf zwei Themen fokussiert. Beide Themen beinhalteten Arabidopsis-Hybride zwischen Individuen, welche in der Region um Tübingen in Deutschland gesammelt wurden. Das erste Projekt zielte darauf ab, den Einfluss der Hybridisierung auf den Metabolismus und das Wachstum der Pflanzen in einer lokalen Arabidopsis-Population zu verstehen. Dafür wurden das Vererbungsmuster von Primär- und Sekundärmetaboliten, sowie die Rosettengröße von diallelen Kreuzungen zwischen sieben Elternpflanzen analysiert. Im Vergleich zum Primärstoffwechsel variierten Sekundärmetabolite stärker und zeigten nicht-additive Vererbungsmuster. Zusätzlich zeigten Abwehrstoffe – hauptsächlich Glukosinolate – die höchste Abweichung vom Mittelwert beider Eltern und waren in positiver Korrelation mit der Größe der Pflanzen.

In dem zweiten Projekt wurde die Rolle von ACCELERATED CELL DEATH 6 (ACD6) im Abwehrsignalweg von nekrotischen Arabidopsis-Hybriden detaillierter charakterisiert. Da die genetische Interaktion zwischen *ACD6*-Allelen von globalen und lokalen Arabidopsis-ökotypen bereits mit Hybridnekrose verknüpft wurde, habe ich frühe Metaboliten-, Ionen- und Expressionsänderungen von Markergenen charakterisiert, welche durch die Aktivierung von ACD6 induziert wurden. Eine Erhöhung von einfachen Zuckern und Metaboliten nicht-enzymatischer

Antioxidantien und dem TCA-Zyklus wurde detektiert, sowie von Putrescin und anderen Säuren abiotischer Stressantworten. Es wurde nachgewiesen, dass Seneszenz früher in nekrotischen Hybriden induziert und zytoplasmatisches Calcium-Signaling nicht durch Temperatur beeinflusst wurde. Zusätzlich wurden GFP-markierte Konstrukte von ACD6 generiert.

Zusammenfassend kann gesagt werden, dass diese Arbeit weitere Erkenntnisse über die Rolle von Heterozygotie in natürlicher Variation und Adaptation liefert und sie unser Wissen über die physiologischen und molekularen Veränderungen, verursacht durch die ACD6-Aktivierung, erweitert.

Stichworte: *Arabidopsis thaliana*, diallele Kreuzungen, nicht-additive Vererbung, Hybridnekrose, ACD6, Metabolismus, Variation, Adaptation

Abbreviations

ul	Microliter
ºC	Degree Celsius
ABA	Abscisic acid
ACD6	Accelerated cell death 6
Alt	Altenriet (localization of Tübingen population; name of Arabidopsis wild accession)
amiRNA	Artificial microRNA
ANK	Ankyrin
Bod	Bodelshausen (localization of Tübingen population; name of Arabidopsis wild accession)
bp	Base pairs
cm	Centimeter
Col-0	C*olumbia-0*; Arabidopsis ecotype
Ca	Calcium
C_T	Threshold cycle
CV	Coefficient of variation
DNA	Deoxyribonucleic acid
EDTA	Ethylenediaminetetraacetic acid
et al.	*et alia* (and others)
FDR	False discovery rate
FW	Fresh weight
GC	Gas chromatography
GC-MS	Gas chromatography with mass spectrometry
GC-TOF-MS	Gas chromatography coupled with time-of-flight mass spectrometry
GFP	Green-fluorescent protein
CFP	Cyan-fluorescent protein
GLS	Glucosinolate
h	Hour
HR	Hypersensitive response
IAA	Indole-3-acetic acid
JA	Jasmonic acid
Kb	Kilobase pairs
LB	Lysogeny broth medium
LC-MS	Liquid chromatography with mass spectrometry
LIR	Leaf initiation rate
M	Molar

m/z	Mass to charge ratio
mM	Milimolar
Mbp	Megabase pairs
mg	Milligram
min	Minute
ml	Mililiter
mm	Milimeter
MPD	Midparental deviation
MPV	Midparent value
ms	Millisecond
MS/MS	Tandem mass spectrometry
NAD	Nicotinamide adenine dinucleotide
NF-YA	HAP2 subunit of the CCAAT-binding Heme Activator Protein (HAP) transcription factor complex
ng	Nanogram
PAL1	Phenylalanine ammonia-lyase I
PC	Principal component
PCA	Principal component analysis
PCD	Programmed cell death
PCR	Polymerase chain reaction
pH	Decimal logarithm of the reciprocal of the hydrogen ion activity
qRT-PCR	Quantitative real-time reverse transcription PCR
rcf	Relative centrifugal force
RLK	Receptor-like kinase
RNA	Ribonucleic acid
ROS	Reactive oxygen species
RT	Room temperature
SA	Salicylic acid
TAIR	Arabidopsis Information Resource
TM	Transmembrane
Tris	Tris(hydroxymethyl)aminomethane
UPLC-MS	Ultra performance liquid chromatography coupled with mass spectrometry
WT	Wild type
YEB	Yeast extract broth medium

1. Introduction

1.1 Natural variation in *Arabidopsis thaliana*

As sessile organisms, plants are exposed to different stresses in their local habitats. Natural environments therefore contain spatial and temporal heterogeneity, key factors influencing differential selection and the emergence of local adaptation. Although the importance of local adaptation in plant survival and diversification is widely recognized, its genetic basis is still not well understood (Fournier-Level et al., 2011). In order to improve data acquisition and interpretation efficiency, biologists have relied on the use of model organisms. In plant biology, *Arabidopsis thaliana* (Arabidopsis) has been the most studied organism, with more resources being allocated to its research than to well-known staple crops. With its ease of maintenance, short generation time, small space requirements and simple chromosomal structure, the number of biologists working with Arabidopsis has increased from around 25 researchers since the 1970s to more than 16,000 worldwide by the end of 2004 (Leonelli, 2007). Friedrich Laibach was the first scientist to be intrigued by the extraordinary amount of natural variation observed within individuals from this species; an observation that fuelled his systematic collection and classification of wild-type mutants since 1937 (Laibach, 1943). Parallel to Arabidopsis*'s* ample genetic diversity is its wide geographical distribution, with native global accessions growing throughout the northern hemisphere in Europe, North America, central Asia and Africa (Koornneef, Alonso-Blanco, & Vreugdenhil, 2004). The number of climatically different areas Arabidopsis has been able to colonize, from North Scandinavia to the mountains of Tanzania and Kenya, exceeds those encountered by almost any other well-investigated species of *Brassicaceae,* making it a suitable model to analyse variation in adaptive traits (Hoffmann, 2002; Koornneef et al., 2004). In fact, it has been shown that large-effect sequence polymorphisms affect approximately 9.4% of Arabidopsis protein-coding genes, with most changes accumulating in regions coding for genes interacting with environmental stresses (Clark et al., 2007). Additionally, the 1001 genomes consortium was able to identify extreme pair-wise divergences among global Arabidopsis accessions not correlated with geographic distance (The 1001 Genomes

Consortium et al., 2016), giving further insights into the global pattern of polymorphisms found within Arabidopsis.

The geographical diversity of Arabidopsis has led to regional differentiation and the appearance of different “ecotypes”. Ecotypes are populations of the same species adapted to their local environmental conditions, although nowadays this term has been replaced with “accession” to refer to plants collected at a specific location (Koornneef et al., 2004). Joe Hereford found that local populations of plants and animals usually show a 45% advantage over non-local individuals (Hereford, 2009). Yet, even though local adaptation is necessary for species to thrive amid rapid environmental changes and across different geographical regions, we still don’t understand its molecular basis (Fournier-Level et al., 2011). Studies on natural variation among global accessions have already helped us understand genetic mechanisms underlying differential fitness traits in hybrids (Weigel, 2012). Due to the wide geographical distribution of Arabidopsis individuals, phenotypic variation of physiological and morphological traits is abundant within global accessions of Arabidopsis (Koornneef et al., 2004). However, less is known about natural variation occurring within accessions from a same collection site. Even though Arabidopsis is mainly a self-fertilizing plant with an average outcrossing rate of 2% to 4% for urban or rural stands respectively, outcrossing rates can reach up to 20% depending on geographical location (Abbott & Gomes, 1989; Bomblies et al., 2010; Platt et al., 2010). Therefore, there can be considerable variation among local groups and haplotypes attributed to outcrossing (Platt et al., 2010). In fact, cases of heritable genetic variation leading to local adaptation have already been described. Of particular interest, it was recently shown that Arabidopsis accessions with different life-cycle strategies differed in their responses to different stresses; while winter annuals showed more resistance against drought, aphids and thrips, summer annuals fared better against *P. rapae* and *P. xylostella* caterpillars (Davila Olivas et al., 2017). Together, these findings suggest that heterozygosity can add to the genetic variation already present in a local habitat. Therefore, studies of local natural variation will not only help characterize the observed differences among local groups of accessions, but also enable us to uncover the mechanisms generating and maintaining this variability (Hedrick, 2006; Koornneef et al., 2004).

1.2 Metabolism and growth

The ability of a plant to survive and grow in different environmental conditions is linked to its metabolic capacity, which influences the energy resources available for reproduction and defense. In this sense, growth can be regarded as a direct measure of metabolic performance and an indirect measure of fitness linked to adaptation (Meyer et al., 2007). The impact of metabolism on plant growth is well-documented, with primary metabolism and carbon assimilation acting as direct regulators and secondary metabolism and defense compounds acting as indirect regulators (Box et al., 2015; Caldana et al., 2013; Meyer et al., 2007; Sulpice et al., 2009; Züst et al., 2011). In Arabidopsis, significant correlations between biomass and specific metabolite compositions have already been revealed, clarifying the direct link that exists between metabolism and growth (Meyer et al., 2007; Sulpice et al., 2009). In this regard, it is interesting to note that plant biomass could be predicted based on specific metabolite combinations. It has already been demonstrated that predictability of hybrid yield can be almost doubled with metabolomic data when compared to predictions relying solely on genomic information (Xu, Xu, Gong, & Zhang, 2016).

The predictive power of metabolites in plant biomass has been evidenced not only across recombinant inbred lines (RILs), but also across large sets of genotypically diverse Arabidopsis accessions (Sulpice et al., 2009). This should come as no surprise, given the fact that central metabolites comprise the major building blocks for growth and their depletion is an indicator of plant development under favourable conditions (Caldana et al., 2013; Meyer et al., 2007; Sulpice et al., 2009). Going beyond direct relationships between specific groups of metabolites and growth, a study conducted by (Lisec et al., 2011) revealed a negative association between overall metabolic variation and fresh weight heterosis in corn hybrids, thus highlighting a possible link between specific metabolite levels and growth optimization. More in detail, the authors hypothesized that the reduced metabolic variation associated to heterosis could be explained by the existence of optimal fluxes related to faster growth. This further enhances the notion that biomass can be explained by metabolic composition.

Understanding what the sources of variation for different metabolic profiles are, will allow us to comprehend the processes that drive plant adaptation. Taking advantage of high-throughput metabolomics gives the opportunity to understand plants as full

biological systems rather than relying on isolated pieces of information. Consequently, plant metabolomes open the possibility to grasp the complex relationships shaping plant growth; knowledge that could consequently help plant breeding strategies increase crop yields in more efficient ways.

1.3 The impact of hybridization on metabolism

The ubiquitous cause of adaptation across all organisms has been usually linked to random mutations within the genome after replication inaccuracies during mitotic cell divisions. Nevertheless, increased heterozygosity brought by hybridization has shown to be a driving force behind genetic diversity, with self-incompatible populations of *Arabidopsis lyrata* displaying higher levels of heterozygosity and diversity than selfed-seed populations (Mable & Adam, 2007). Furthermore, the contribution of hybridization to secondary metabolite variation and herbivore resistance serves as direct evidence for the existing relationship between hybridization, nonadditive metabolic inheritance and local adaptation (Cheng, Vrieling, & Klinkhamer, 2011).

Metabolic variability is affected, among other things, by parental ancestry. During hybridization, genetic traits in the offspring can be inherited in additive or non-additive ways. Traits inherited in an additive way will produce phenotypes resembling the mean effect of both parental alleles in the progeny. Therefore, the progeny phenotypes will not differ from the average phenotype observed in the parents (midparent phenotype). On the other hand, traits deviating from the midparental phenotype will be inherited in a non-additive way and can be transgressive, or beyond the range of both parents (Ng, Lu, & Chen, 2012; Seymour, Chae, & Grimm, 2016). These midparental deviations can be either beneficial or disadvantageous for the offspring. Decreased fitness in progeny compared to both parents is termed hybrid incompatibility and increased fitness is known as heterosis or hybrid vigour (Charlesworth & Willis, 2009; Schwartz & Laughner, 1969). The main mechanisms related with non-additive inheritance described so far are dominance, over-dominance and epistasis (C. Davenport, 1908; Hull, 1945). The dominance theory states that a phenotypic effect from a deleterious parental allele can be complemented in a hybrid with a dominant allele from the second parent (C. B. Davenport, 1908). In over-dominance, the effect of heterozygosity results in hybrid traits being higher than those observed in either parent. Additionally, hybrids can also

show novel phenotypes due to epistasis, where a gene from one locus influences genes at different loci (Sharp & Agrawal, 2016). Hybridization will therefore affect the inheritance patterns of genetic traits in hybrids, which in turn will influence the molecular and physiological responses of a plant.

The first project of my PhD work aimed to further investigate the causes and molecular mechanisms underlying non-additive inheritance and has the potential to improve hybrid breeding strategies. At the same time, the strength of studying natural variation in Arabidopsis resides in the very large and well-integrated resources of genomic data and molecular tools, which enable more accurate analyses and result comparisons when formulating new hypotheses (Trontin, Tisné, Bach, & Loudet, 2011).

1.4 Hybrid necrosis in A. thaliana

As mentioned in the previous chapter, non-additive inheritance can result in phenotypes that are beneficial or disadvantageous in comparison to the parents. Besides studying non-additive inheritance patterns in the first part of my thesis, the second part focused on investigating a special case of disadvantageous outcome in hybrids, namely hybrid necrosis. When independently diverging genomes meet in hybrids, epistatic interactions between newly introduced alleles might generate detrimental consequences. The developed incompatibilities have been previously described by Bateson, Dobzhansky, and Muller (Coyne & Orr, 2004; Dobzhansky, 1937; Muller, 1942), where complementary changes hypothetically occurring in two different populations can trigger the appearance of reproductive barriers among individuals. Hybrid incompatibilities can be seen as the unwanted by-product of diversification through natural selection. It can be found across most plant species, including important crop species like rice (Chen et al., 2014), and can act as a gene-flow barrier among them; more specifically, a postzygotic barrier (Bomblies & Weigel, 2007). Post zygotic barriers come in many forms, from poor hybrid performance or failure to attract pollinators, to intrinsic genic or chromosomal incompatibilities. In this way, hybrid incompatibilities can also shape speciation and local adaptation by promoting reproductive isolation between diverging populations (Fishman & Sweigart, 2018). These types of deleterious epistatic events have been mostly studied between different populations (Maheshwari & Barbash, 2011; Presgraves, 2010; Rieseberg &

Blackman, 2010), although recent research shows that these events can also occur within a single intermating population (Corbett-Detig, Zhou, Clark, Hartl, & Ayroles, 2013; Hou, Friedrich, de Montigny, & Schacherer, 2014; Seidel, Rockman, & Kruglyak, 2008). When parents from two different populations encounter each other, genes that have evolved independently with divergent functionality, with no deleterious consequences in their respective population, meet and interact in unexpected ways (Bomblies et al., 2007; Bomblies & Weigel, 2007; Chae, Tran, & Weigel, 2016; Coyne & Orr, 2004; Fishman & Sweigart, 2018). For these deleterious interactions to occur within individuals of the same species, a strong selective pressure usually acts on specific loci, triggering a higher degree of polymorphisms that end up in unexpected incompatibilities (Chae et al., 2014). Therefore, increased allelic heterogeneity increases the likelihood of incompatible interactions (Crespi & Nosil, 2013; Cutter, 2012; Lachance & True, 2010). In this sense, high levels of sequence divergence are fuelled by adaptation. For this reason, fast-evolving defense genes have been linked both with adaptation and hybrid incompatibilities in natural accessions of Arabidopsis (Alcazar et al., 2009; Alcázar et al., 2014; Bomblies et al., 2007; Chae et al., 2014; Świadek et al., 2017; Todesco et al., 2014).

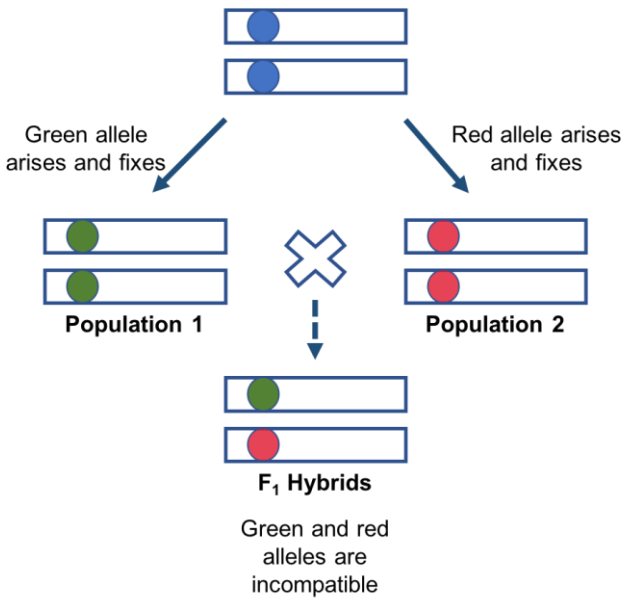

Figure 1. Schematic representation of the Bateson-Dobzhansky-Muller (BDM) model of hybrid incompatibility. Blue circles represent the ancestral alleles, while green and red circles represent the incompatible alleles that are acquired and fixed independently in each population.

Hybrid necrosis was first described in Arabidopsis more than ten years ago (Bomblies et al., 2007). It is a common type of post-zygotic genetic incompatibility in plants characterized by stunted growth, necrotic lesions, cell death, ROS accumulation, *PATHOGENESIS-RELATED* (*PR1*) expression and salicylic acid (SA) build-up, resembling a response elicited by pathogen attack (Alcazar et al., 2009; Alcázar et al., 2014; Bomblies et al., 2007; Bomblies & Weigel, 2007; Chae et al., 2014; Świadek et al., 2017; Todesco et al., 2014). In the first report with more than 850 unique crosses, approximately 2% of F_1 hybrids showed different degrees of necrosis (Bomblies et al., 2007). This was later confirmed by a diallel crossing scheme among 80 accessions with 6409 crosses (Chae et al., 2014). In addition to global accessions, hybrid necrosis may also occur between local accessions of Arabidopsis (Świadek et al., 2017). Most cases of hybrid necrosis described so far are linked with highly polymorphic loci; mostly immune receptor genes with nucleotide binding domains and leucine-rich repeat structures, also termed NLRs (Bakker, Toomajian, Kreitman, & Bergelson, 2006; Bomblies & Weigel, 2007; Chae et al., 2014; Clark et al., 2007; Noel, 1999; Todesco et al., 2014). NLRs are well-characterized proteins involved in the recognition of specific pathogen effectors and the consequent activation of plant defense responses (Alcazar et al., 2009; Bakker et al., 2006; Chae et al., 2014; Thomas Eulgem, 2005; Lodha & Basak, 2012; Maiti, Basak, & Pal, 2014). Additionally to NLRs, receptor-like kinases have also been involved in the elicitation of autoimmune responses (Alcázar et al., 2014). Nevertheless, Alcázar and collaborators were unable to identify incompatible interactions within a local population of Arabidopsis.

An interesting aspect of hybrid necrosis is its temperature-dependency (Alcazar et al., 2009; Alcázar & Parker, 2011; Alcázar et al., 2014; Bomblies et al., 2007; Bomblies & Weigel, 2007; Świadek et al., 2017; Todesco et al., 2010, 2014). It has already been shown that temperature modulates defense signaling in Arabidopsis (Alcázar & Parker, 2011; Y. Wang, Bao, Zhu, & Hua, 2009; Zhu, Qian, & Hua, 2010). Although there is no known universal regulator for this temperature-dependent defense suppression, key regulatory elements have already been identified (Gangappa, Berriri, & Kumar, 2017). Interestingly, the positive roles of incompatible alleles in bestowing pathogen resistance has also been evidenced, offering possible explanations as to their accumulation within populations. Alcázar and collaborators were able to see an increased resistance to *Hyaloperonospora parasitica* both at

14ºC, when the necrotic phenotypes were visible, and at 20ºC where growth defects had been supressed (Alcazar et al., 2009). Yet, although activation of defense responses might be beneficial against pathogen attack, autoimmune responses will undoubtedly have an impact in biomass and yield (Bomblies et al., 2007; C. Chen et al., 2014; Rate, Cuenca, Bowman, Guttman, & Greenberg, 1999; Todesco et al., 2010, 2014). Therefore, the intertwined relationship between defense and hybrid necrosis is a challenge for the optimal balance between growth and resistance; one that even crop breeders have had to encounter. In fact, there is a well-known correspondence between disease resistance selection and cases of hybrid necrosis. Most notably, wheat breeders searching for resistance to rust fungus ended up encountering an increased incidence of hybrid necrosis due to the raised frequency of the necrotic allele Ne_2 (Morrison, 1957; Pukhalskiy, Martynov, & Dobrotvorskaya, 2000).

1.5 The role of ACD6 in hybrid necrosis

Though most genes involved in incompatible interactions, including NLRs, are well-studied resistance genes, many other proteins induced during different defense responses in diverging plant species remain uncharacterized or have yet unknown targets (Maiti et al., 2014). The molecular architecture of necrotic hybrids allows not only to study genes involved in incompatible interactions, but also the identification of novel proteins required for the activation of plant defense responses. In addition to NLRs, the *ACCELERATED CELL DEATH 6* (*ACD6*) gene has been found as a common cause of hybrid necrosis in Arabidopsis (Świadek et al., 2017; Todesco et al., 2014). ACD6 was first identified in the gain-of-function mutant *acd6-1* (Rate et al., 1999). In this case, a single amino acid substitution at the transmembrane (TM) domain was able to induce stunted growth, activation of defense-related genes, accumulation of salicylic acid (SA) and cell death (Rate et al., 1999). A similar phenotype was later identified in the natural accession Est-1, where ACD6 was shown to have two amino acid substitutions at the TM domain (Todesco et al., 2010). It was only recently that ACD6 was linked with hybrid necrosis among global accessions of Arabidopsis (Todesco et al., 2014), although these accessions would never have the opportunity to meet in real life. Nevertheless, with the identification of ACD6-conferred hybrid necrosis among local Arabidopsis accessions (Świadek et al., 2017), the possibilities for allelic variation at this locus to impact adaptation has

become more plausible. ACD6 activation elicits stunted growth, necrotic lesions and cell death linked to elevated reactive oxygen species (ROS), rise in PATHOGENESIS-RELATED PROTEIN 1 (*PR1*) transcripts and SA accumulation in F_1 hybrids (Lu, Liu, & Greenberg, 2005; Lu, Rate, Song, & Greenberg, 2003; Lu et al., 2009; Rate et al., 1999; Todesco et al., 2014). It has also been shown that *ACD6* is both necessary and sufficient to generate hybrid necrosis, both among global and local accessions (Świadek et al., 2017; Todesco et al., 2014).

Unlike most of the genes involved in hybrid necrosis, ACD6 is not characterized and its function remains unknown. In all cases of hybrid necrosis, the phenotype is temperature-dependent, appearing below 17ºC and diminishing at temperatures above 21ºC. This, however, does not hold true in the gain-of-function mutants, where ACD6 is constitutively active due to amino acid substitutions in its transmembrane domain (Lu et al., 2005, 2009; Rate et al., 1999; Todesco et al., 2010). Current evidence supports that ACD6 is involved in a positive feedback loop with SA and that the conferred phenotype is SA-dependent and unrelated to *ACD6* expression levels (Lu et al., 2003, 2009; Rate et al., 1999; Todesco et al., 2010, 2014). It has also been reported that SA triggers the migration of ACD6 to the cellular membrane through the formation of protein complexes (Zhang, Shrestha, Tateda, & Greenberg, 2014). Therefore, the function of ACD6 seems to be tied to its membrane localization and SA. Interestingly, accumulation of SA on its own does not trigger a defense response in plants, suggesting that SA works as a coactivator and needs other signals to induce these responses (Lu et al., 2003; Rate et al., 1999). In line with this, increased apoplastic bacterial growth has been evidenced in Arabidopsis plants grown in the dark when inoculated with avirulent strains of *Pseudomonas syringae* (Genoud, Buchala, Chua, & Métraux, 2002). A very similar study concluded that expression of *PR1* and SA accumulation required light (Zeier, Pink, Mueller, & Berger, 2004). Though not all defense pathways were light-dependent, including jasmonic acid (JA) signaling, expression of ACD6 has been shown to be induced by SA in the presence of light (Lu et al., 2003). However, since hybrid necrosis is a product of incompatible allelic interactions, an increased expression of *ACD6* will not trigger the phenotype (Todesco et al., 2010). In this regard, the *ACD6* mutations responsible for the necrotic phenotypes seem to generate post-translational modifications (Zhang et al., 2014). What exactly are these modifications affecting in terms of the function of ACD6 is not yet well understood. Therefore, more work needs to be done to further

comprehend its role in the plant's defense pathways, and important insights could be gained by understanding how it is able to generate hybrid necrosis in F_1 hybrids. Because this phenotype is detected in a temperature-dependent manner, it offers an opportunity to identify early molecular changes associated with its induction. Characterizing different physiological and molecular phenotypes of necrotic hybrids could therefore enable us to decipher new aspects of plant immunity.

1.6 Defense and senescence

Senescence is an organized loss of cellular functions that occurs at the final stage of leaf development. During this time, the plant recovers and reutilizes important nutrients that would otherwise be lost (Guiboileau, Sormani, Meyer, & Masclaux-Daubresse, 2010). Though developmental senescence is important to maximize viability in the next generation, premature senescence can actually hinder yield and crop quality (Breeze et al., 2011). Therefore, the timing of senescence is not only important for the plant, but also for the offspring. Interestingly, overlapping patterns in gene expression between defense responses and leaf senescence have already been observed (Quirino, Normanly, & Amasino, 1999; Zentgraf, Hinderhofer, & Zentgraf, 2001). A high-resolution temporal transcriptome profiling during Arabidopsis leaf senescence uncovered the upregulation of a diverse family of transcription factors with well-known roles in defense and stress-related responses (Breeze et al., 2011). Among them, members of the bZIP family, NF-YA subunits from the CCAAT box binding family, members from the NAC family, and WRKY family members involved in the regulation of SA- and JA-dependent defense signaling pathways (Thomas Eulgem & Somssich, 2007; Ülker & Somssich, 2004) were recognized. Therefore, pathogen attack and senescence both trigger concomitant molecular pathways.

In order to stop pathogen dispersal, plants usually rely on the production of ROS based on recognition of conserved pathogen molecular patterns (PAMPs) or pathogen effector proteins (Chakravarthy, Velásquez, Ekengren, Collmer, & Martin, 2010; Göhre & Robatzek, 2008; Pombo et al., 2014). For the latter, effector triggered immunity (ETI) is a host-acquired resistance against specialized plant pathogens. It is activated after the recognition of bacterial/fungal effector proteins and induces the production of ROS through SA. This, in turn, generates cell death to control the

dispersal of pathogens at an infected site; a defense mechanism known as the hypersensitive response (HR) (Büttner & Bonas, 2010; Koebnik, Krüger, Thieme, Urban, & Bonas, 2006; Li et al., 2013; K. A. I. Wengelnik & Bonas, 1996; K. Wengelnik, Van den Ackerveken, & Bonas, 1996). In this regard, cell death is a common process of both biotic defense and senescence. SA is also known to induce certain senescence-associated genes, though it is not necessary for leaf senescence to occur (Quirino et al., 1999). Nevertheless, Vogelmann and collaborators showed that SA was indeed necessary and sufficient to trigger early leaf senescence in *senescence-associated ubiquitin ligase1* (*saul1*) Arabidopsis mutants grown in low light conditions (Vogelmann et al., 2012). During this light-dependent early-senescence phenotype, WRKY transcription factors were also significantly increased 24 hours after the transfer to low light. WRKY transcription factors have already been implicated in the regulation of plant defense responses and target conserved W box elements; *cis*-acting regulators that have been found in a large number of plant defense gene promoters (Fukuda & Shinshi, 1994; P. J. Rushton et al., 1996; Paul J. Rushton & Somssich, 1998). Expression of *WRKY* genes is also known to be triggered by the recognition of viral, fungal and bacterial elicitors (Eulgem, Rushton, Robatzek, & Somssich, 2000; Fukuda, 1997; Rushton et al., 1996; Z. Wang, Yang, Fan, & Chen, 1998), as well as in response to wounding (Hara, Yagi, Kusano, & Sano, 2000). Besides the dual role of SA and WRKY transcription factors, activation of defense-related genes during senescence, including the SAR markers *PR1* and *PR5*, has also been reported in numerous studies (Morris et al., 2000; Quirino et al., 1999; Silke Robatzek & Somssich, 2001). This body of evidence serves to highlight the notion of a strong overlap between senescence and defense regulatory mechanisms (Quirino et al., 1999). Therefore, activation of defense pathways seems to play a dual-role in the activation of the leaf senescence response.

1.7 Significance and aims of the work

This work seeks to understand the role heterozygosity plays on plant adaptation through its impact on metabolism and growth. Our study is focused on a local collection site of Arabidopsis because we believe the impact of hybridization to be stronger among natural accessions that have no geographical boundaries between them.

We were also intrigued in studying these accessions further because specific parental combinations yielded hybrid necrosis in the F_1 offspring. The cause of this hybrid incompatibility was connected to allelic interactions at the *ACD6* locus (Świadek et al., 2017). Although certain alleles of *ACD6* were found to be sufficient and necessary to trigger the hybrid necrotic phenotype, its function in plant stress signaling remains unknown. These observations led us to further characterize the role of *ACD6* in the context of hybrid necrosis; information that we believe will complement the existing knowledge about plant immune responses and its connection with other physiological and metabolic processes.

To understand the impact of hybridization on metabolism and growth, we generated a full diallel cross among seven genetically different parents collected in 2007 from a collection site in Tübingen, Germany (Bomblies et al., 2010; Świadek et al., 2017) and monitored the reciprocal hybrids and the seven parents for changes in primary and secondary metabolism. Additionally, we measured growth of all individuals across five different timepoints. The seven individuals used for this study also contained at least three different alleles of *ACD6*, known to influence growth through activated immune responses (Świadek et al., 2017; Todesco et al., 2014). A previous analysis of hybrid performance in heterotic maize hybrids among selected inbred lines showed that the increased fitness in hybrids was associated with a reduced metabolic variation (Lisec et al., 2011). In contrast, we hypothesized that an increased variation due to heterozygosity within a single natural growth habitat, with no prior artificial selection of the parents, could be a beneficial strategy for highly homozygous plants to cope with sudden changes in their surroundings.

To understand the molecular functions of ACD6, we focused on characterizing the early metabolic and ionic changes induced by ACD6 activation in a temperature-dependent manner. Additionally, different GFP-tagged constructs of the protein were developed to identify novel interacting partners through immunoprecipitation assays. The expression pattern of senescence and flowering markers was also monitored across time, both in necrotic hybrids and their corresponding parents, to identify differences in these two physiological responses. Finally, due to the reported plasma membrane localization of ACD6 (Lu et al., 2005; Zhang et al., 2014), we hypothesized it could be a regulatory component situated very high in the signaling hierarchy, and thought it could be mediating this regulation via calcium ions (Ca^{2+}).

Therefore, cytosolic calcium changes in response to cold were measured in necrotic hybrids and their corresponding parents using yellow cameleon sensors.

Consequently, the aims of the first project were:

- Understand the impact of heterozygosity on metabolism and growth
- Investigate the amount of metabolic and phenotypic variability between hybrids and parents coming from a local collection site
- Identify inheritance patterns in primary and secondary metabolism, together with growth taken as rosette radius

The aims of the second project were:

- Characterize the physiological and molecular responses associated to ACD6 activation within necrotic hybrids arising from individuals within the same local collection site.
- Understand the relationship between defense and senescence in necrotic hybrids.
- Identify the very early metabolic changes associated to *ACD6*-conferred hybrid necrosis.
- Compare intracellular calcium signaling in response to temperature between parents and necrotic hybrids.
- Develop N and C-terminal GFP-tagged ACD6 constructs for future pull-down assays.

2. Materials and Methods

2.1 Impact of heterozygosity in a single growth habitat

2.1.1 Plant material, growth conditions and phenotyping

The Altenriet (Alt) accessions 1 to 7 collected around Tübingen in 2007 (Bomblies et al., 2010) were used to determine the impact of hybridization on metabolism and growth. Two plants were used in the full diallel crosses to control the biological variation of individual plants. The same parent was used for all crosses within a replicate and the parent seeds were produced by manual fertilization to avoid random heterotic effects. Plants were grown in randomized individual pots using long day conditions (16 h light/ 8 h dark) in growth chambers with 21°C during the day and 17°C during the night. Each tray (containing 30 pots) was moved and turned every second day to decrease any chamber-dependent effects. Rosette radiuses (from the middle of the rosette to the end of the leaf tip) were measured from 10-leaf stage plants using imageJ (version 1.48). Whole rosettes were harvested for metabolic profiling at the 10-leaf stage in the middle of the day (between 12:00-14:00) to avoid any circadian effects. Analyses were conducted with at least four, and up to eight, biological replicates (the average number of biological replicates used was 7). Additionally, pictures of the same plant material were taken at five different developmental timepoints: 2-leaf, 4-leaf, 6-leaf, 8-leaf, and 10-leaf stage.

2.1.2 Metabolic profiling

Six rosettes of 10-12 leaf stage Arabidopsis plants were harvested and frozen immediately in liquid nitrogen. 50 mg of ground plant material was extracted using 300ul of cold methanol including Ribitol as internal standard, followed by 200ul chloroform and 400ul Bidest double-distilled water. After centrifugation, a 160ul aliquot from the upper polar phase was lyophilized and stored in -80°C until metabolite analysis. The derivatized extracts were analyzed by GC-MS as described previously (Dethloff et al., 2014). Briefly, 70µL of MSTFA and 10µL Pyridine including retention time index standards followed by 40µL methoxymation reagent in pyridine (20mg/mL) were added as described in (Allwood et al., 2009). Splitless injection for chromatograpical analysis was performed as described in (Allwood et al., 2009).

Datamining was performed using TagFinder (Allwood et al., 2009; Luedemann, Strassburg, Erban, & Kopka, 2008) after baseline correction using ChromaTof-Software (Leco) as described (Allwood et al., 2009). Annotation was manual supervised in comparison to the GMD mass-spectral-library. Data was normalized to the internal standard Ribitol and fresh-weight prior to statistical analysis. Extraction and analysis by gas chromatography mass spectrometry (GC-MS) were performed using the same equipment set up and protocol as described in (Lisec, Schauer, Kopka, Willmitzer, & Fernie, 2006). GC-MS spectra were manually evaluated using the ChromaTOF® 4.5 (Leco) and TagFinder 4.2 softwares (Luedemann et al., 2008; Schauer et al., 2005).

Secondary metabolite analysis was performed as previously described by (Tohge & Fernie, 2010) using a high-performance liquid chromatography (HPLC; Surveyor; Thermo Finnigan, USA) coupled to a Finnigan LTQ-XP system (Thermo Finnigan, USA). Metabolites were evaluated on the basis of the peak area of parental ion peaks processed using Xcalibur 2.1 software (Thermo Fisher Scientific, USA). The obtained relative peak areas were normalized by comparison to an internal standard (isovitexin; CAS29702-25-8) and the fresh weight of the sample used for extraction.

2.1.3 Statistical analyses

Metabolite data was first normalized for differences in fresh weight and machine performance using an internal standard. All metabolite intensities were normalized by log10 transformation and each metabolite value was then scaled by its standard deviation to detect outliers. Values with more than five standard deviations away from the mean were replaced with non-analyzed (NA) values and metabolites with more than 20% NA values were eliminated from posterior analyses. The remaining NA values were imputed using the missForest package available in the R software for statistical computing (R). Bonferroni correction was used in R for every multivariate analysis done, and a significance level of 0.05 was used unless otherwise stated.

Correlation analysis

Pearson correlations using matrices with the mean values over the biological replicates were done in the R Statistical Computing Platform. The Pearson

correlation between metabolism and final rosette size contained the average metabolic intensities of both primary and secondary metabolism together with the rosette radius measurements of the final timepoint. The second correlation matrix contained the growth rates and rosette radius measurements for each of the five timepoints analyzed. Percent growth rate was calculated between every two consecutive timepoints as (x-y)/y, where *x* represents the latest and *y* the previous rosette radius.

Principal component analysis

Principal component analyses (PCA) were done using the function PCA from the "FactoMineR" package available for R. Average metabolite intensities per accession were used. To identify differences in the metabolomes of parents and hybrids after the temperature switch, independent PCAs were done for parents and hybrids. Metabolites with significant contributions ($p < 0.05$) to both dimensions were then compared between the two groups.

Coefficients of variation

The coefficient of variation was calculated by dividing the standard deviation of each metabolite over its mean, either across all hybrids (CVh) or all parents (CVp). Hence, the log2 CV-ratio was calculated as log2(CVh / CVp). The mean log2 CV-ratio for primary metabolites, secondary metabolites and size (based on rosette radius) was calculated independently and compared against a random mean CV-ratio. The random mean CV-ratio was generated by assigning new parent and hybrid groups after resampling all observations. This process was repeated 10000 times and a mean CV-ratio was calculated each time to produce a random distribution of mean CV-ratios (for primary metabolites, secondary metabolites and size independently). A shift in the observed mean CV-ratio with respect to the random mean CV-ratio was then assessed.

Analysis of inheritance patterns

To identify the different inheritance patterns across hybrids, the deviations from the midparent values (MPVs) were calculated for each hybrid per

metabolite. The deviation of each hybrid per metabolite was the result of subtracting the observed value from the predicted midparent value. To identify the classes of metabolites that were deviating most from the average midparent value, the relative percentage of deviation from the midparent value (rMPD) was calculated for each metabolite within each hybrid using the formula rMPD = 100d/a, where *d* is the difference between the hybrid and parental mean and *a* is the parental mean. Primary and secondary metabolites were coded from 1-100 and divided into biochemical/functional classes. Metabolites were reordered according to their mean rMPD values across all hybrids using ggplot2. To identify metabolites with non-additive modes of inheritance, empirical p-values were calculated by contrasting the observed deviation per metabolite against a random distribution generated for each individual metabolite by resampling.

2.2 The role of ACD6 in hybrid necrosis

2.2.1 Growth conditions and phenotyping

The individuals Alt-5 and Bodenhausen (Bod) 6, together with their reciprocal hybrids (Alt-5xBod-6 and Bod-6xAlt-5), were grown in individual pots at constant 21°C. Whole rosettes of six biological replicates were sampled at three different timepoints once plants reached the 10-12 leaf stage. In total, 72 plants were used and sampling was always done at midday to avoid circadian rhythm differences. During sampling, plants were switched to constant 17°C and left there either for 15 minutes or 220 minutes before being frozen in liquid nitrogen. A control group, without the switch to 17°C, was also sampled.

2.2.2 Metabolic profiling

Six rosettes of 10-12 leaf stage Arabidopsis plants were harvested and frozen immediately in liquid nitrogen. 50 mg of ground plant material was extracted using 300ul of cold methanol including 13C6-Sorbitol as internal standard, followed by 200ul chloroform and 400ul Bidest double-distilled water. After centrifugation, a 160ul aliquot from the upper polar phase was lyophilized and stored in -80°C until metabolite analysis. The derivatized extracts were analyzed by GC-MS as described

previously (Dethloff et al., 2014). Briefly, 70µL of BSTFA and 10µL Pyridine including retention time index standards followed by 40µL methoxymation reagent in pyridine (20mg/mL) were added as described in (Allwood et al., 2009). Splitless injection for chromatograpical analysis was performed as described in (Allwood et al., 2009). Datamining was performed using TagFinder (Allwood et al., 2009; Luedemann et al., 2008) after baseline correction using ChromaTof-Software (Leco) as described (Allwood et al., 2009). Annotation was manual supervised in comparison to the GMD mass-spectral-library. Data was normalized to the internal standard 13C6-Sorbitol and fresh-weight prior to statistical analysis.

2.2.3 Statistical analyses

Multiple Multivariate Analyses of Variance (MANOVAs) were done in order to determine metabolites affected by temperature in hybrids with significantly different levels from each parent. In the first MANOVA analysis, metabolites were divided into three groups corresponding to both reciprocal hybrids (hybrids), Alt-5 (parent 1), and Bod-6 (parent 2). Consequently, three independent MANOVAs were performed to detect metabolites that were varying significantly between timepoints ($p < 0.05$), with p-values adjusted according to the false discovery rate (FDR). Significant metabolites unique for hybrids were kept and compared against the results of a second analysis. In the second analysis, the metabolic data was divided into two groups, comprising either hybrids and parent1 or hybrids and parent 2. After correcting for the FDR, a list of significantly changing metabolites between hybrids and both parents was obtained and contrasted against the results of the first analysis. This gave us a list of metabolites exclusively affected by temperature in hybrids with different intensities from both parents.

2.2.4 Intracellular calcium signaling

Cytosolic calcium signaling was monitored using yellow cameleon sensors. The parent lines Alt-5 and Bod-6, together with their F_1 hybrid Alt-5xBod-6, were agro-transformed with the construct NES-YC3.6 described in (Krebs et al., 2012). Transformed seedlings were screened via fluorescence microscopy for the emission spectra of yellow fluorescent tags. Six confirmed seedlings from each transformed line were transferred to pots and leaves from the adult plants were sampled when they reached the 8-leaf stage. A small cutting from the youngest leaf was pasted on a

well slide with medical adhesive and leaves were allowed to acclimate with 100ul of room-temperature water for 20 minutes. Afterwards, plants were imaged in a spectral laser scanning confocal motorized microscope (Leica TCS SP5) using the Leica Software “LAS AF”. The imaging parameters were as follows: image dimension (512 x 512), pinhole (3.69 airy units), and line average (2). ECFP was excited using the 458 nm laser line of the Argon laser. The fluorescence intensity values for ECFP (465-500 nm) and cpVenus (520-570 nm) were detected simultaneously in selected regions of interest. Image acquisition was taken every 2.57 seconds and 100ul of cold water was added to the well slide after 60 seconds of data acquisition. Data acquisition was carried out for 416.34 seconds and the generated image data was analysed using Fiji ImageJ 1.51h to retrieve the FRET/CFP ratios for each of the 162 timepoints per biological replicate. Differences between the FRET/CFP ranges between the hybrid and each parent were contrasted against a random distribution generated by permutation resampling with 10000 iterations. Confidence intervals were determined with an alpha of 0.05 and all analyses were done in the R statistical environment (version 3.3.1).

2.2.5 Quantitative real-time PCR

For all experiments, RNA was isolated using TRIzol Reagent from Invitrogen (MA, USA) according to the manufacturer’s instructions. Isolated RNA was treated with DNAse using the TURBO DNA-*free* Kit from Ambion (MA, USA) and the resulting RNA was reverse transcribed using oligo-dT primers from Qiagen (Düsseldorf, Germany). Synthesis of cDNA was carried out using the Maxima Reverse Transcriptase enzyme from Thermo Fisher Scientific (MA, USA) according to the manufacturer’s instructions. The resulting cDNAs were checked on gel prior to the quantitative reverse-transcription polymerase chain reaction (qRT-PCR) runs. For the qRT-PCR, Maxima SYBR Green with low ROX from Thermo Fisher Scientific (MA, USA) was used in the StepOnePlus System from Applied Biosystems (MA, USA) following the manufacturer’s instructions. The threshold cycles (Ct) were quantified by the comparative Ct method and transcript abundances were estimated relative to the reference genes *UBQ5* and *18S rRNA*. Dot plot graphs using the standard error per sample were generated and the statistical significance was estimated by a Wilcoxon test on the open software R. Primers used for the different marker and housekeeping genes are summarized in Table S1.

To further understand the molecular variation present in the local Tübingen population, we evaluated the transcript levels of different marker defense genes for all seven Altenriet parental lines (Alt1 to Alt7). For this purpose, we took leaf tissue samples from each accession grown at 17ºC and a Col-0 wild type line grown under the same conditions. RNA was extracted from leaves three and four when plants reached a 12-leaf stage and the transcript levels of the marker defense genes *enhanced disease susceptibility 1* (*EDS1), phytoalexin deficient 4 (PAD4), pathogenesis-related protein 1 (PR1)*, *nonexpresser of pr genes (NPR1), pathogenesis-related protein 5 (PR5)* and *accelerated cell death 6 (ACD6)* were evaluated by qRT-PCR. The housekeeping genes *ubiquitin 10* and *5 (UBQ10, UBQ5), elongation factor 1 (ef1), tubulin (TUB),* and *acetylated tubulin (AC-TUB)* were tested for each time-point between all accessions. The housekeeping genes that showed less variation were used for the corresponding timepoints and three biological replicates were used per sample.

To characterize how the physiological processes of senescence and flowering were affected by hybrid necrosis, a time-course experiment between the hybrid Alt-5xBod-6 and its corresponding parental lines was conducted. Leaf tissue samples from leaves 3 and 4 were harvested for RNA isolation throughout six timepoints corresponding to the following developmental stages: 4-leaf stage, 8-leaf stage, 16-leaf stage, 24-leaf stage, flowering stage, and the stage “after flowering”. Plants were grown at constant 17ºC to induce hybrid necrosis in hybrid plants (parental lines did not show signs of necrotic lesions throughout the experiment) and five biological replicates were used. The number of days to germination, bolting, and first open flower was recorded and the leaf initiation rate (LIR) was calculated as the rosette-leaf number at bolting stage divided by the number of days to bolt (bolting was defined as a flowering stem of 1cm). The molecular markers used for senescence and flowering time are shown in Table S1.

To better understand how nitrogen metabolism was affected by the activation of ACD6 in hybrids, RNA from the same plants used to identify early metabolic changes induced by ACD6 was extracted. Additionally, as a positive control, RNA from the gain-of-function mutant line *acd6-1* was also harvested. In addition to the molecular markers for nitrogen metabolism, the thermosensory immunity and growth regulator

PIF4 was also tested in parents, the hybrid Alt-5xBod-6, and the gain-of-function mutant *acd6-1*.

2.2.6 Interaction studies using GFP-tagged ACD6 constructs

To identify candidate interacting partners of ACD6, different GFP-tagged versions of the protein were developed. Briefly, the coding sequence of *ACD6* from the Alt-5 accession line was amplified and cloned by double-restriction enzyme ligation into the entry Gateway® vector pJL-Blue using the FastDigest® enzymes NotI and XhoI from Thermo Fisher Scientific (MA, USA). Two versions of the gene, one with and one without its stop codon were cloned and transferred respectively by LR reactions to the destination vectors pUBN-GFP and pUBC-GFP described in (Grefen et al., 2010). All selected constructs were verified by gel electrophoresis and sequencing to confirm the presence of the desired gene. Afterwards, the final vector was isolated from the *E. coli* strain DH5α and transformed into *Agrobacterium tumefaciens* strain GV3101. Agrobacterium-mediated transformation of the Arabidopsis accession Bod-6 was done using the floral dip method (Bent & Clough, 1998) and T1 seeds containing the GFP constructs were BASTA® selected. Seedlings were then screened for GFP signal using the confocal motorized microscope Leica TCS SP5 with the Leica software “LAS AF”.

2.2.7 Protein extraction, pull-down and Western blot

Isolation of a plasma membrane-containing microsomal fraction was done from mechanically disrupted leaf tissue as described in (Santoni, 2007). Col-0 was used as a negative control and the plasma membrane protein *LOW TEMPERATURE INDUCED 6B* (*LTI6B*) tagged to GFP was used as a positive control. The resulting microsomal fractions were enriched for GFP-bound proteins using the Spin column protocol for GFP-Trap®_A from Chromotek. The enriched protein extract was separated on gel by SDS-PAGE and blotted to Whatman® chromatography paper (3mm). The western blot was run for 1 hour at a constant current (mA) equivalent to the volume of the gel. Tween tris-buffered saline solution (T-TBS) was used for the washing steps and 5% milk for blocking non-specific binding of the antibodies to the membrane. Blotting of the primary antibody (anti-GFP) was done overnight and the gel was washed afterwards three times with T-TBS before being incubated for 2 hours with the secondary antibody (anti-rat). Clarity® Western ECL Blotting from Bio-

Rad was used as the chemiluminescent detection agent and the membrane was revealed on Super RX-N medical x-ray film from Fujifilm (Tokyo, Japan).

2.2.8 Yeast two-hybrid assay

To find out candidate interacting partners of ACD6, the coding sequence of *ACD6* from the gain-of-function mutant *acd6-1* and the Alt-5 accession was cloned into the pGBKT7-BD vector from Clontech's Matchmaker® Gold Yeast Two-Hybrid System (Takara Holdings, Kyoto, Japan). Competent yeast cells were prepared and the pGBKT7-BD::ACD6 constructs were transformed to Y2HGold yeast cells using the Frozen-EZ Yeast Transformation II® protocol from Zymo Research (CA, USA). In parallel, the empty vector pGADT7-AD was transformed to the competent Y187 yeast strain using the same protocol from Zymo Research (CA, USA). Transformed yeast strains were confirmed by auxotroph growth on the proper synthetic defined (SD) dropout minimal media. To check if ACD6 was able to confer bait auto-activation, the transformed Y2HGold strain was grown on -Trp SD media supplemented with X-α-Gal (SDO/X). Additionally, the transformed Y2HGold strain carrying the pGBKT7-BD::ACD6 vector was mated with the Y187 strain carrying the empty pGADT7-AD vector. Mating was done overnight by mixing both transformed strains in 2X YPDA liquid media after each one reached an OD_{600} of 0.8. Afterwards, colonies were screened on microscope for the detection of zygotes. When zygotes were detected (approx. 24 hours), the culture was plated on SD/-Leu/-Trp plates for the selection of diploids and SD/-Leu/-Trp/X-α-Gal/Aureobasidin A to determine bait auto-activation.

3. Results

3.1 Impact of heterozygosity in a single growth habitat

The first part of my thesis looked at the impact heterozygosity brought to metabolism and growth within Arabidopsis individuals collected from the same growth habitat in the year 2007. We hypothesised that hybridization could act as a source of metabolic diversity within a highly-selfing local group of Arabidopsis individuals, providing thus more options for adaptation to sudden changes in the environment. In order to test our hypothesis, we monitored primary and secondary metabolism, together with growth (defined as rosette radius), in a full diallel cross experiment. The following chapters highlight the main results and conclusions.

3.1.1 Hybridization increases the overall metabolic and phenotypic variation in a local collection site of Arabidopsis

To determine the impact hybridization had on metabolism and growth, two replicates of a full diallel cross with seven parental lines collected in 2007 from one location in Altenriet, Tübingen (Southern Germany) were used. From the 42 hybrids, four could not be assessed due to technical difficulties. Genotyping through RAD sequencing (Świadek et al., 2017) revealed more than 95.61% of homozygosity, based on the 1985 informative markers from the parents. Pairwise comparison of the SNPs showed that similarity among the parents varied from 60.3 % to 97.5 %, with an average similarity of 69 % (Table S2). Both the parents and hybrids were phenotyped for their metabolism and rosette radiuses. Rosettes of at least four plants were harvested at the 10-leaf stage for each parent and hybrid to avoid changes due to different developmental stages. Sixty-six analytes from primary metabolism and thirty-four from secondary metabolism (Table S3) were identified and quantified using gas chromatography mass spectrometry (GC-MS) and liquid chromatography mass spectrometry (LC-MS) (Lisec et al., 2006; Tohge & Fernie, 2010). To quantify growth, each plant rosette radius was measured from photos taken at a 10-leaf stage.

To assess the impact of hybridization on the overall metabolic variation, the coefficient of variation (CV) for each metabolite was calculated across all hybrids and parents, and the mean CV-ratio between hybrids and parents was determined. This process was done separately for primary and secondary metabolism, and growth based on rosette radius. A positive non-significant shift from the empirical mean of a permutation test revealed that hybridization increased overall metabolic and rosette size variation (Fig. 2). Regarding metabolism, the effect was slightly more pronounced on secondary metabolism than primary metabolism (Fig. 2A-B). Interestingly, the increased metabolic diversity was accompanied by an even larger variation in rosette size (Fig. 2C); a variation that was augmented in the fourth measured timepoint, when plants were at the 8-leaf stage (Fig. 2D).

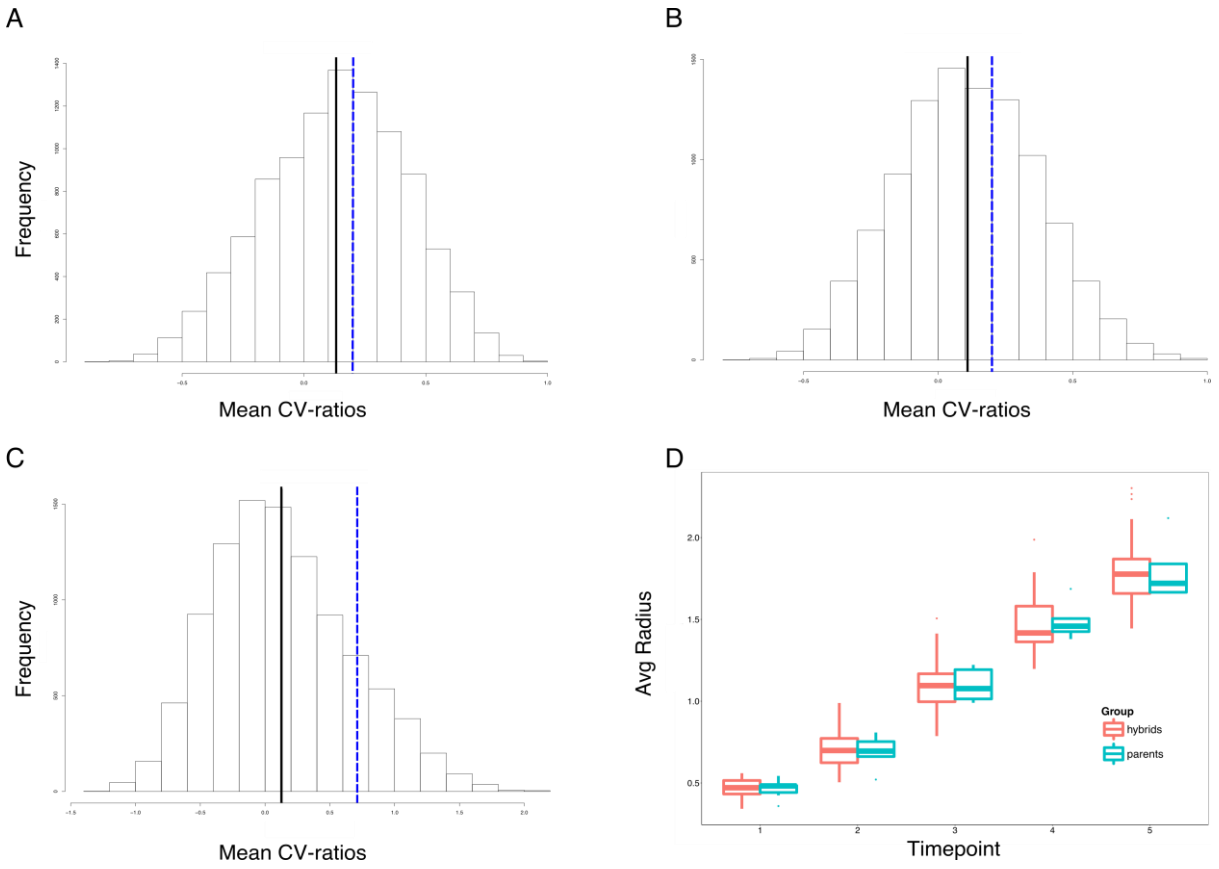

Figure 2. Hybridization increases the overall metabolic and phenotypic variation. The coefficient of variation (CV) ratio between hybrids and parents for primary metabolites (A), secondary metabolites (B), and growth based on rosette radius (C). The black line indicates the random mean and the blue line the observed CV ratio. The greater variation in hybrids, in terms of rosette radius, can be observed in (D).

3.1.2 Hybridization increases non-additive inheritance patterns in secondary metabolism

To gain further insights into the different inheritance patterns induced by hybridization, the relative midparental deviation (MPD) of each metabolite was calculated. The probability of each MPD to occur by chance was determined by contrasting against a random distribution generated by permutations with 5000 iterations. An alpha of 0.01 was used and metabolites with significant MPDs were classified as having non-additive inheritance. Overall, the distribution of deviations showed that secondary metabolites exhibited the highest degree of non-additive inheritance, with 20.6% of its metabolites showing a significant overall non-additive inheritance across all hybrids (α = 0.05) (Fig. 3A). In contrast, none of the primary metabolites exhibited a mean significant deviation from the midparent value (MPV) across all hybrids. When looking at the number of individual cases (individual metabolites per cross), secondary metabolism showed 39% cases of non-additive inheritance, while primary metabolism displayed 28% (Table S4). The secondary metabolites that showed the highest degree of variation from the midparent values were compounds involved in plant stress responses, mainly glucosinolates, phenylpropanoids, flavonoids, plus several unknown analytes (Fig. 3A). While glucosinolates showed both significantly positive and negative median deviations from the MPV, the detected phenylpropanoids exhibited only a significant negative median deviation. For the compound classes in primary metabolism, the median deviations from the MPV were negative and considerably smaller than those for the majority of secondary metabolites (Fig. 3A). We also found that the variation in the MPD was larger for compounds comprising secondary metabolism (Fig. 3, Table S4). This indicated that some of the analysed hybrids showed particularly different levels of secondary metabolites in comparison to the average of the parents, suggesting that non-additive inheritance is a strong contributor in the shaping of secondary metabolism.

When looking at the total number of significant non-additive cases, certain crosses were more likely to exhibit non-additive inheritance in metabolism. Among these, six showed non-additive inheritance in more than 50% of their primary metabolites (i.e. cross 43) and fourteen crosses showed non-additive inheritance in at least 50% of their secondary metabolism (i.e. cross 17) (Fig. 3B-C). Since only two of these crosses were reciprocal (Alt6xAlt1 and Alt6xAlt2), the direction of the cross was

important in determining the extent of non-additive inheritance (Fig. 3C). In addition, crosses with Alt2 and Alt6 parents were involved in more than 40 % of the non-additive inheritance patterns for secondary metabolites (Fig. 3C, Table S4), while seven secondary metabolites (i.e. coniferin, *trans*-sinapoyl malate, phenylpropanoid sinapoyl malate, a structurally undefined aliphatic glucosinolate, benzenoid and flavonoid, and an unknown compound) showed significant non-additive inheritance across all hybrid crosses (α = 0.05) (Table S4).

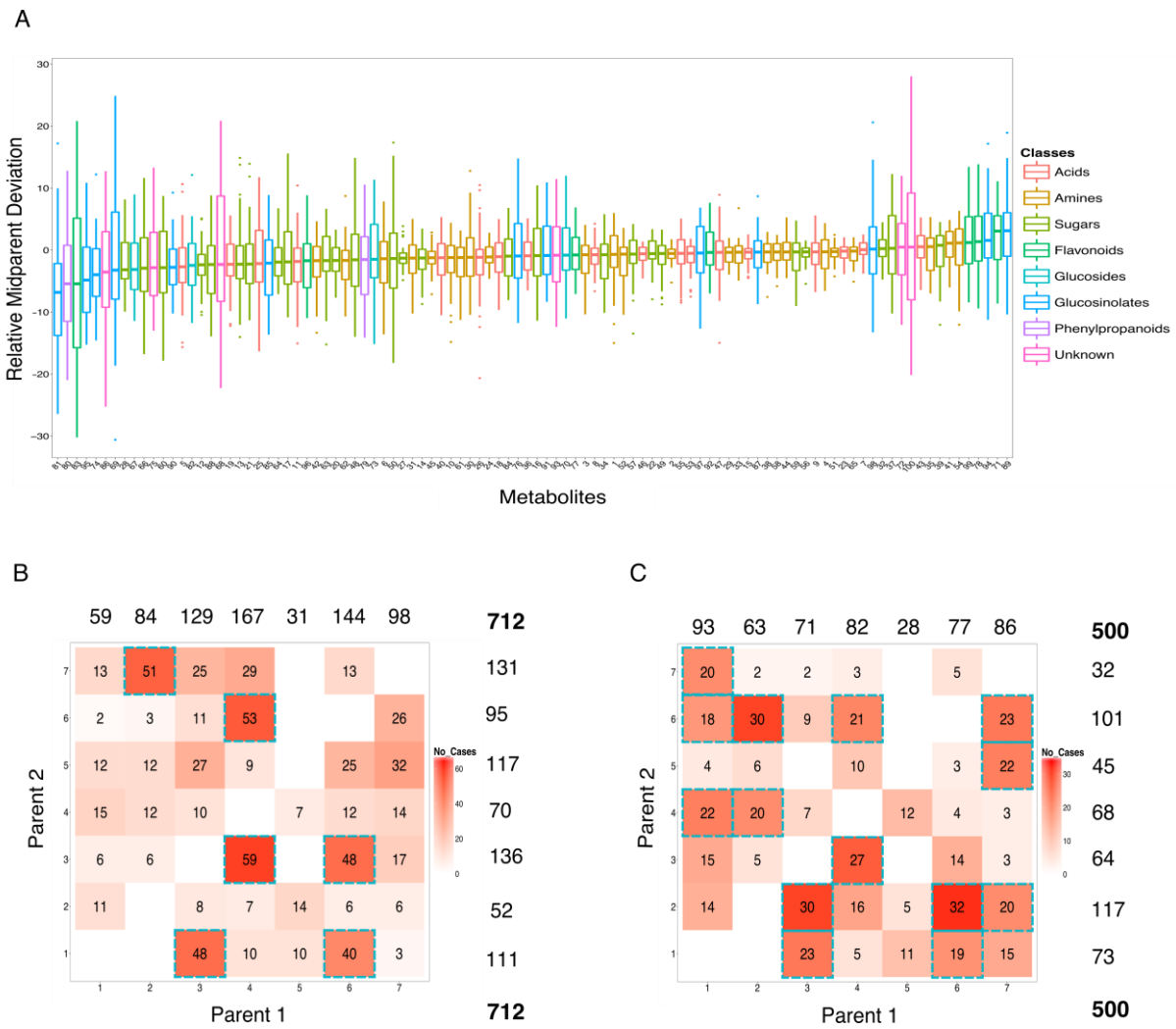

Figure 3. Secondary metabolism showed more non-additive inheritance than primary metabolism. To understand the impact hybridization brings to the natural variation of a local collection site, a metabolic profiling of a full diallel cross was analyzed. (A) Relative deviations of all measured metabolites from the midparent value. Indices correspond to primary (1-66) and secondary (67-100) metabolites ordered according to their median deviations from the midparent value. Number of (B) primary and (C) secondary metabolites inherited in a non-additive way across different hybrids. Crosses with more than 50% non-additive inheritance are marked by blue squares. Non-additive inheritance was based on significant deviations from the parental mean (α = 0.01).

Altogether, we could not identify a particular pattern for the sign of deviations from MPV for the examined compound classes. Nevertheless, the levels of compounds from secondary metabolism showed predominantly non-additive inheritance patterns in comparison to primary metabolites. Moreover, some crosses were more likely to show non-additive inheritance than others; findings that were in line with the higher variance observed in secondary metabolism when compared to primary metabolism.

3.1.3 Primary metabolism shows high resiliency during hybridization events

Parallel to the deviations from the midparent values, a principal component analysis (PCA) was done for each metabolic phenotype to further investigate the parental effects on hybrid metabolism. The first two PCs captured a smaller percentage of the total variance of primary metabolism (PC1, 48.8% and PC2, 8.9%) when compared to secondary metabolism (PC1, 59% and PC2, 13.8%). Nevertheless, the variance explained by each of the two principal components was significant in both cases, evidenced by a larger percentage of accumulated variance when compared against the broken-stick variances. PCAs did not reveal any clear separation between parents and their respective hybrids (Fig. 4). Nevertheless, based on their secondary metabolism, all parents were located in the lower half of the second PC and more than half of the hybrids were not grouped with the parents (Fig. 4B). Primary metabolism didn't show the same behaviour (Fig. 4A), with both parents and hybrids being more equally distributed throughout space. Reciprocal hybrids were usually plotted close to one another, though in secondary metabolism the difference between certain reciprocal hybrids was pronounced. Among them, reciprocal hybrids between Alt2 and Alt4 parents showed the largest distance with respect to the second PC. Additionally, the hybrid Alt2xAlt4 was separated from the rest of the hybrids by PC2 and its secondary metabolism also showed the lowest correlation values when compared to other hybrids. In this sense, parents with the most dissimilar secondary metabolism (Alt2 and Alt4) also gave rise to the most dissimilar hybrid in secondary metabolism (Alt2xAlt4), although this behaviour was not seen in its reciprocal counterpart (Alt4xAlt2). This could be explained by a strong parental effect from having Alt2 as a mother and Alt4 as a father. Furthermore, Alt2 and Alt4 were also involved in several crosses whose reciprocal hybrids yielded dissimilar metabolic phenotypes. Interestingly, the most divergent hybrid in primary metabolism was Alt4xAlt3 rather than the hybrid from the most divergent parents, suggesting a

considerable contribution from non-additivity (Fig. 4A). Further evidence would be needed to better understand the cause of this underlying parental effect.

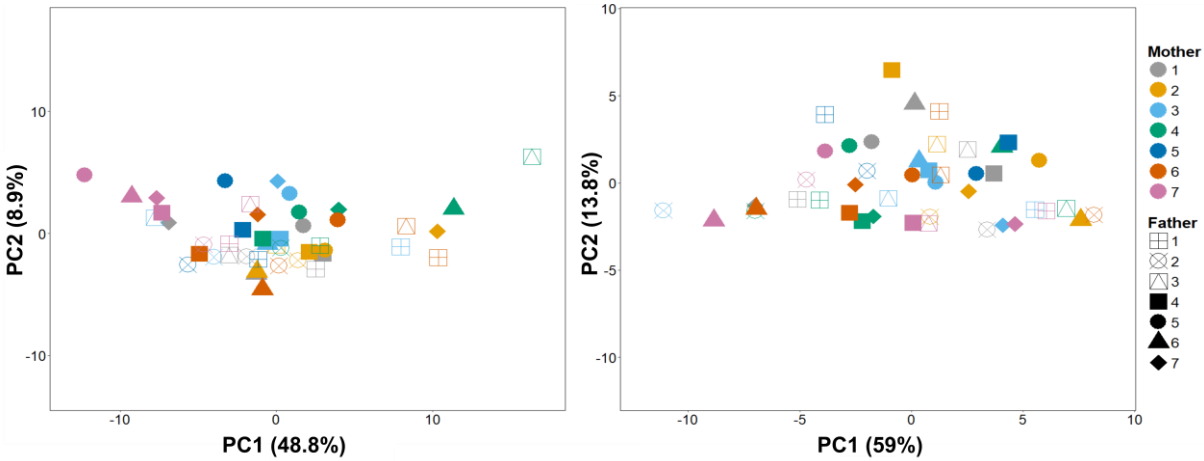

Figure 4. Principal component analysis (PCA) of the parents and hybrids. PCA was conducted based on primary metabolic profiles (A) and secondary metabolic profiles (B). Hybrids are coded based on the genotype of the parents. Colors indicate the mother while shapes indicate the father plant, indicated in the legend of panel (B).

3.1.4 Final rosette size is determined by the initial growth rate and correlates to specific metabolites

Studies on plant metabolism and growth-related traits have revealed a tight link between primary metabolism and biomass (Stitt, 2013; Sulpice et al., 2009). To find out if changes in metabolism are reflected to changes in growth-related traits, the measured rosette radius of 10-leaf stage hybrids and parents was measured and correlated against the metabolism (primary and secondary) across all individuals. The rosette size had both positive and negative non-additive inheritance in comparison to the midparent value (Fig. 5A). From the 12 hybrids with a significant deviation from the MPV, seven had larger and five smaller rosette radiuses than the midparent value indicating that parents contribute to both hybrid vigour (or heterosis) and hybrid incompatibility (Fig. 5B). From all hybrids, Alt6xAlt4 showed the highest positive deviation from the MPV and its reciprocal counterpart followed a similar behaviour with a significant positive deviation as well. Alt3xAlt1 and its reciprocal hybrid had two of the highest significant negative deviations in rosette radius (Fig. 5A-B), though many of the reciprocal hybrids did not show similar inheritance patterns. The latter indicating, again, underlying parental effects. For example, the

reciprocal hybrids of Alt3xAlt2 and Alt1xAlt-5, among the three with the largest positive deviation from the MPV, did not show significant deviations from the MPV.

When looking at the relationship between metabolism and growth by correlation analysis, twenty-four metabolites were found to be significantly correlated with the final size of hybrids using an alpha of 0.05 (Table 1). Out of these, most corresponded to positive correlations involving secondary metabolites, mainly glucosinolates, while only two primary metabolites were positively correlated with growth: 1,6-anhydrobetaglucose, a hydroxylated form of glucose which forms on the pyrolysis of cellulose and hence can be regarded as a proxy for cellulose content (Sasaki et al., 2008), and spermidine (Table 1).

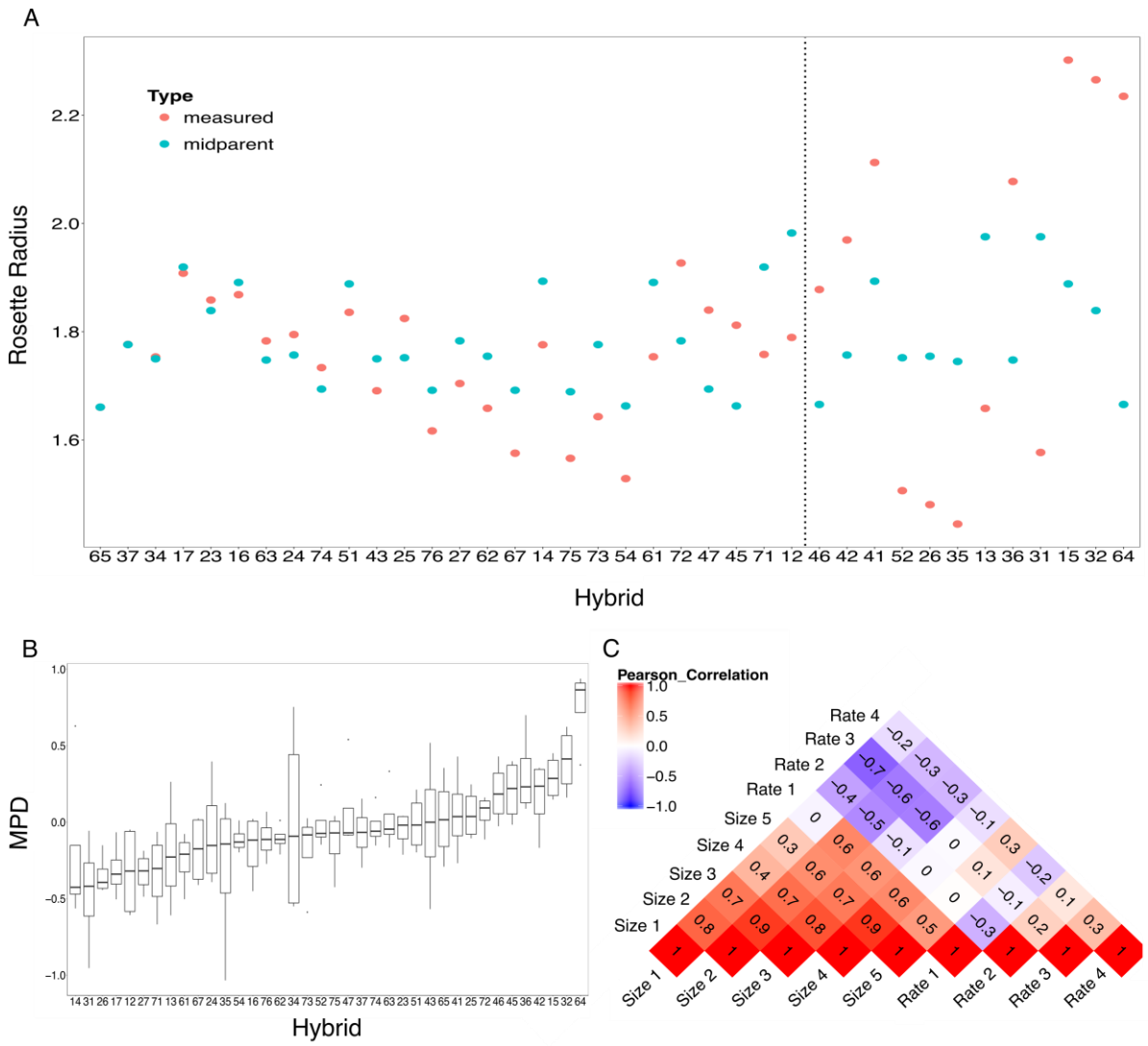

Figure 5. Non-additive inheritance patterns and correlation analysis of rosette size. Deviations of observed mean rosette radius from the midparent value in each hybrid are presented. (A) Hybrids with the highest deviations are not he right and the lowest on the left. The dashed line shows significant deviations from the midparent value (alpha = 0.05). (B) Individuals are ordered from left to right according to the median of their midparent deviation (MPD), from negative dominant to positive dominant cases. (C) Correlation analyses between rosette radius and growth rates revealed a significant positive correlation between the first growth rate (before the appearance of the second pair of leaves) and rosette size (alpha = 0.01).

Finally, to better understand the causes of an increased rosette size in hybrids, a correlation analysis between the growth rates and rosette sizes of hybrids was done. Only the initial growth rate, between the first and second time points analysed, showed a significant positive correlation with the rosette size of hybrids (Fig. 5C). Therefore, the final size of the hybrids seemed to be determined early after germination, before the appearance of the second pair of leaves; posterior growth rates didn't show any correlation with hybrid rosette size.

Table 1. Metabolites correlated with the final rosette size. Pearson correlation of all metabolites with the final rosette size (alpha = 0.05). Primary metabolites are highlighted in light blue and the mass and retention times of secondary metabolites are included, respectively, inside parenthesis.

Metabolite	Correlation	P_Value
No. 68 Unknown (463.3, 12.1)	0,51	0
No. 73 Disinapoyl glucoside-II (591.3, 19.15)	0,47	0
No. 79 Phenylprop, hydroxyferuloyl Glc (372.23, 10.4)	0,45	0
No. 84 3-Methylsulfinylpropyl gluc (358.36, 7.08)	0,43	0
No. 85 Glucosinolate (478.2, 12.8)	0,46	0
No. 76 7-Methylthioheptyl glucosinolate (462.3, 23.8)	0,36	0,01
No. 82 Sinapoyl glucoside (385.4, 13.4)	0,37	0,01
No. 94 Glucosinolate, neoglucobrassicin (477.3, 17.3)	0,37	0,01
No. 97 Glucosinolate (679.4, 17.0)	0,4	0,01
No. 22 Glucose 1-6-anhydro beta	0,35	0,02
No. 75 Unknown (585.1, 24.7)	0,34	0,02
No. 87 Glucosinolate, glucobrassicin (447.3, 15.3)	0,34	0,02
No. 91 Glucosinolate, 8-methylthiooctyl gluc (476.4, 27.7)	0,35	0,02
No. 93 Indole-3-carboxylate hex (323.30, 11.1)	0,33	0,02
No. 96 Possible flavonoid (565.19, 4.50)	0,32	0,03
No. 70 Disinapoyl glucoside-I (591.3, 18.2)	0,31	0,04
No. 71 Most likely anthocyanin (841.5, 29.3)	0,3	0,04
No. 92 Flavonoids, 3-Rha-7-Rha-Kae (577.6, 15.8)	0,31	0,04
No. 13 Fructose-6-phosphate	-0,29	0,05
No. 44 Proline	-0,29	0,05
No. 54 Spermidine	0,3	0,05
No. 77 Kaempferol 3-galactoside-7-rhamnoside (593.7, 14.9)	0,3	0,05
No. 98 Indolic glucosinolate (477.2, 20.1)	0,29	0,05
No. 100 Unknown (371.2, 11.6)	0,29	0,05

3.2 The role of ACD6 in hybrid necrosis

In the second part of my thesis I investigated hybrid incompatibilities caused by allelic interactions at the *ACD6* locus among crosses from the Tübingen collection site in Germany first identified in (Świadek et al., 2017). To further understand the possible role of ACD6 within the plant defense response pathways, physiological responses linked to senescence and flowering were measured in both the necrotic hybrids and their corresponding parents. Additionally, early metabolic and ionic changes induced by ACD6 activation were monitored in both groups, together with changes in cytoplasmic Ca^{2+} in response to cold. In parallel, different GFP-tagged constructs of ACD6 were developed with the objective of identifying candidate interacting partners through pull-down assays. The following chapters summarize the main findings of this research.

3.2.1 Necrotic hybrids senesce earlier than parents

Due to the reported link between defense and senescence regulation (Eulgem et al., 2000; Feys, 2005; Quirino et al., 1999; Robatzek & Somssich, 2002; Robatzek & Somssich, 2001), we wanted to investigate the possible role of ACD6-activated defense responses and physiological senescence on necrosis in hybrids. First, we wanted to find out if and at what stage of development where defense and senescence-associated molecular markers expressed. For this, the expression of molecular senescence markers, *SENESCENCE-ASSOCIATED GENE 12* (*SAG12*) (Weaver, Gan, Quirino, & Amasino, 1998) and *WRKY53* (Miao, Laun, Zimmermann, & Zentgraf, 2004), were screened together with the defense marker *PATHOGENESIS-RELATED PROTEIN 1* (*PR1*) in the Alt-5xBod-6 necrotic hybrid and its parents across different developmental stages.

Both molecular senescence markers were expressed earlier in hybrids than in the parents, with *SAG12* induced exclusively in hybrids at the 16-leaf stage and *WRKY53* showing higher levels of expression since the 8-leaf stage (Fig. 6). In comparison, parents only showed *SAG12* expression until the flowering stage and though expression levels of *WRKY53* were also detected in parents at the 8-leaf stage, they were significantly lower than those seen in hybrids (Fig. 6). Something interesting to note is that defense was activated before senescence in necrotic hybrids, as evidenced by a significant increase in *PR1* at the 4-leaf stage (Fig. 6A).

Even though senescence was induced earlier in necrotic hybrids than in both parents, premature flowering in hybrids was not observed. Intrigued by this, the expression of different flowering markers was assessed. Though most reported flowering markers didn't show any clear expression differences between the hybrid and both parents (Fig. S1), two *NF-YA* transcription factors involved in endoplasmic reticulum (ER) stress and drought tolerance (Nelson et al., 2007; Wenkel et al., 2006) were found to be upregulated in necrotic hybrids. Interestingly, upregulation of these transcription factors has been linked to a delayed flowering response (Wenkel et al., 2006).

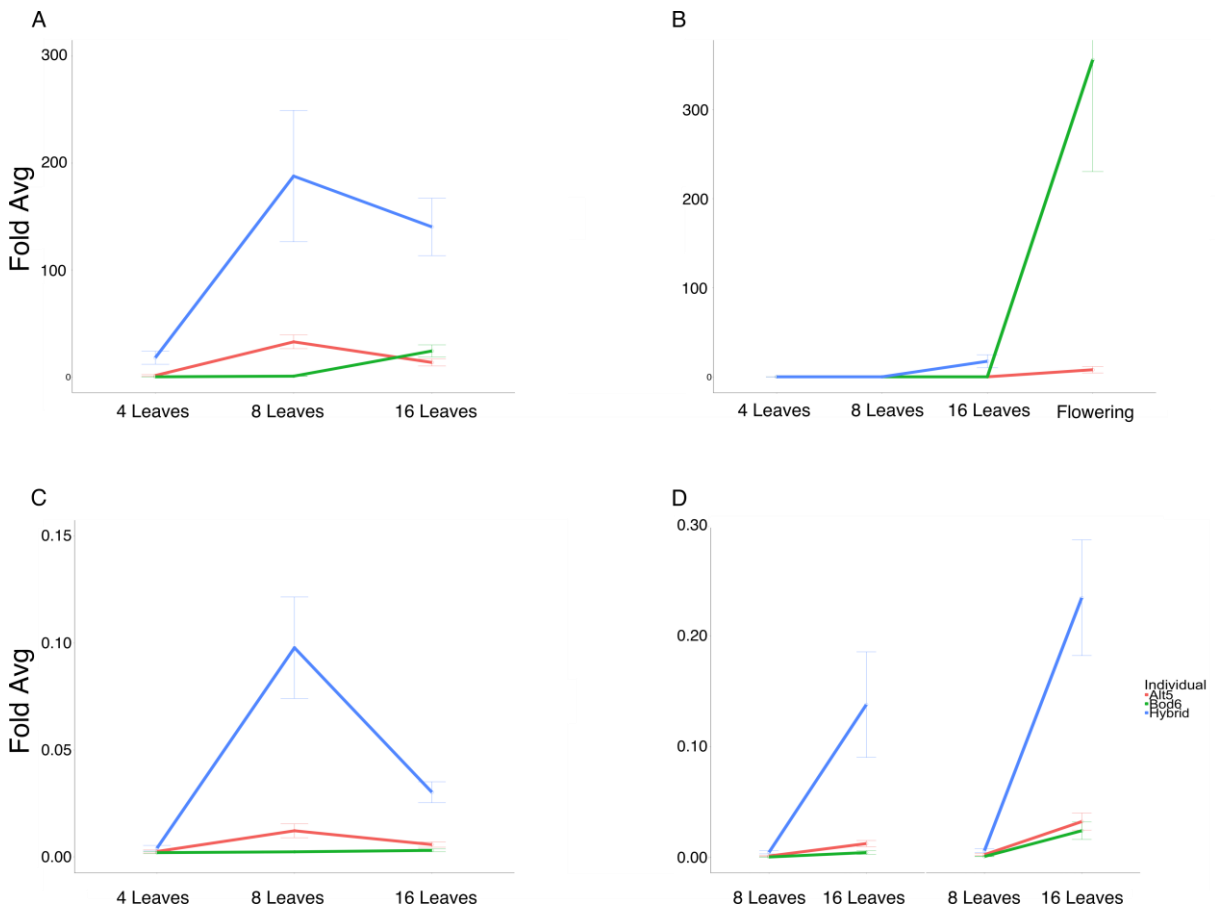

Figure 6. Senescence was induced earlier in necrotic hybrids than in parents. Analysis of the relationship between hybrid necrosis caused by ACD6 and senescence, together with flowering time, using molecular markers. (A) The defense marker *PR1* was used as a positive control for the active defense response in necrotic hybrids. (B) The senescence marker *SAG12* was expressed exclusively in hybrids at the 16-leaf stage. Parents only accumulated this transcript during the flowering stage. (C) The early-leaf senescence marker *WRKY53* was significantly higher in hybrids since the 8-leaf stage. (D) Subunits of the NF-Y/HAP transcription factor complex involved in ER stress, flowering and drought tolerance were upregulated in hybrids with respect to parents at the 16-leaf stage. Other genes involved in flowering (*FLC*, *FT* and *CBF1*) didn't show clear differences between hybrids and parents (Fig. S1). α = 0.05. Wilcoxon Test. Red line: Alt-5. Green line: Bod-6. Blue line: Hybrids.

3.2.2 Temperature induces abiotic stress compounds early during hybrid necrosis

To better understand the causes of hybrid necrosis triggered by a temperature-dependent activation of ACD6, the early metabolic changes induced by temperature were compared between hybrids and parents. For this, the Alt-5 and Bod-6 parent lines were grown with their reciprocal hybrids at constant 21ºC and subjected to a temperature switch of constant 17ºC after plants reached the 8-leaf stage. Six biological replicates were used per plant and three timepoints corresponding to 21ºC (control), 15min. and 220min. after the switch were collected. A total of 72 samples were analysed by GC-MS and ion chromatography, yielding 165 metabolites and 9 ions (5 cations and 4 anions) respectively.

A PCA of the metabolic dataset revealed that the temperature shift generated different patterns of variation between hybrids and parents 220 minutes after the switch, with PC1 separating hybrids after the temperature switch from the rest of the individuals (Fig. 7A). When plotting the metabolic dataset of hybrids and parents separately, hybrids had 83 out of 128 metabolites showing a significant contribution to the observed change due to temperature explained by PC1. In contrast, parents showed much less variation due to the temperature shift, with only 17 metabolites showing a significant contribution to the observed variation. Among these, fourteen were shared with hybrids, leaving hybrids with 69 unique metabolites showing a unique pattern of variation induced by temperature (Fig. 7B).

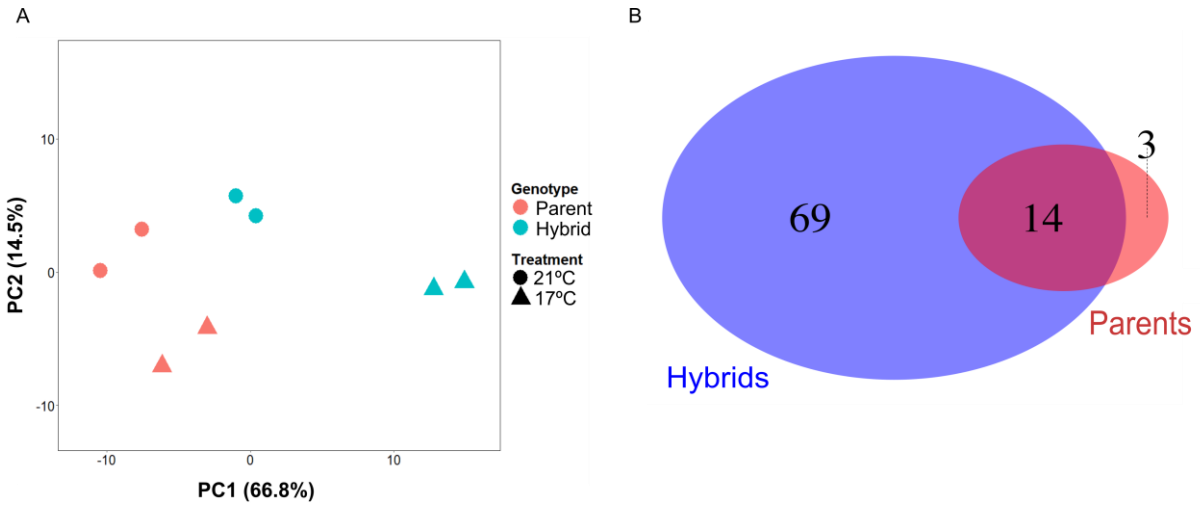

Figure 7. PCA of the metabolic changes induced by ACD6. (A) PCA of the different genotypes represented by their metabolism before and after the temperature switch. (B) Venn diagram showing the number of metabolites with a significant contribution to the two principal components, for hybrids and parents.

Although PCAs were a useful tool to compare datasets between parents and hybrids, it did not give information about metabolites whose levels were significantly different between time points and individuals. Therefore, multiple multivariate analyses of variance (MANOVA) were performed in order to find metabolites that were both significantly regulated by temperature in hybrids and with a final level different from both parents (taking the level of each parent separately). No metabolites were detected to be changing significantly 15 minutes after the temperature switch, hence all the results discussed focus on the second timepoint (220 minutes after the temperature switch). These analyses revealed a total of 60 metabolites unique for hybrids, 45 of which were shared with metabolites contributing significantly to the variation induced by temperature in hybrids (from the previous PCA results) (Fig. 7B). Among the 60 metabolites, acids and sugars were among the most abundant, comprising more than 30% of the detected compounds. Acids included intermediates of the tricarboxylic acid (TCA) cycle (Citrate, Succinate, Malate), together with compounds involved in biotic/abiotic stress tolerance (Shikimic Acid, Salicylic Acid) and glutathione metabolism (Ascorbate). Sugars included simple sugars (Glucose, Fructose) and compatible solutes (Glucose-6-phosphate, Trehalose) involved in osmoprotection (Fig. 8). Important to note is that 37% of the detected metabolites had no annotation and, therefore, their biological and molecular roles during the emergence of hybrid necrosis remain unknown for now. Overall, the biological processes that seem to be induced early by temperature in necrotic hybrids include the synthesis of ATP, compatible solutes and antioxidants, together with abiotic stress signaling molecules (Table 2).

When looking at the early ionic changes induced by temperature in hybrids, ammonium and sulfate were found to be significantly upregulated (Fig. 9A, C). However, their final levels in hybrids where not significantly different from the Alt-5 parent, casting doubt as to their biological impact on the emergence of the phenotype (Fig. 9B, Fig. S2). Growing hybrids in soil under different ammonium concentrations did not trigger the necrotic phenotype (Fig. S3).

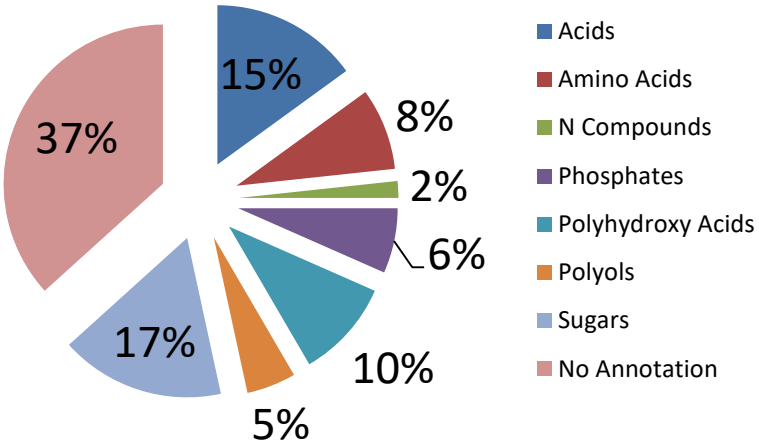

Figure 8. Metabolite classes induced early after the temperature switch in necrotic hybrids. Early metabolic changes induced by temperature in necrotic hybrids were analyzed to identify molecular causes of hybrid necrosis associated to ACD6 activation. Multiple MANOVAs revealed 60 metabolites significantly upregulated in necrotic hybrids 220 minutes after a switch from 21 to 17ºC.

Table 2. Abiotic stress compounds induced early after the temperature switch in necrotic hybrids. The physiological responses that could be affected by specific groups of metabolites induced by temperature are presented. MANOVA analyses were run with an alpha of 0.05 and all p-values were corrected according to the false discovery rate (FDR). Six biological replicates were used.

Upregulated Analytes	Involved In	Bibliography
Fructose-6-phosphate (1MEOX) (6TMS) MP, Glucose-6-phosphate (1MEOX) (6TMS) MP	Glycolysis; ATP Production	Miura et al. 2014, Sadava et al. 2017
Citrate (4TMS), Succinate (2TMS), Malate (3TMS)	TCA Cycle; ATP Production	Sadava et al. 2017
Putrescine (4TMS)	Positive Regulation TCA Cycle; Abiotic Stress	Gill & Tuteja 2010, Shu et al. 2011, Zhong et al. 2016
Maltose (1MEOX) (8TMS) MP, Glucose (1MEOX) (5TMS) BP, Fructose (1MEOX) (5TMS) BP	Gluconeogenesis; ATP Production	Kerepesi & Galiba 2000, Sadava et al. 2017
Shikimic Acid (4TMS), Salicylic Acid (2TMS)	Biotic and Abiotic Stress; Systemic Acquired Resistance (SAR); Stomata Closure	Kang et al. 2013, Khan et al. 2010, Miura & Tada 2014, Nazar et al. 2011, Noreen & Ashraf 2010, Sawada et al. 2006, Shah 2003
Pyroglutamate (2TMS), Glutamate (3TMS), Ascorbate (4TMS)	Glutathione Metabolism; Antioxidant Activity	Kang et al. 2013
Trehalose, alpha,alpha'- (8TMS)	Osmoprotection	Nuccio et al. 2015, Pilon-Smits et al. 1998

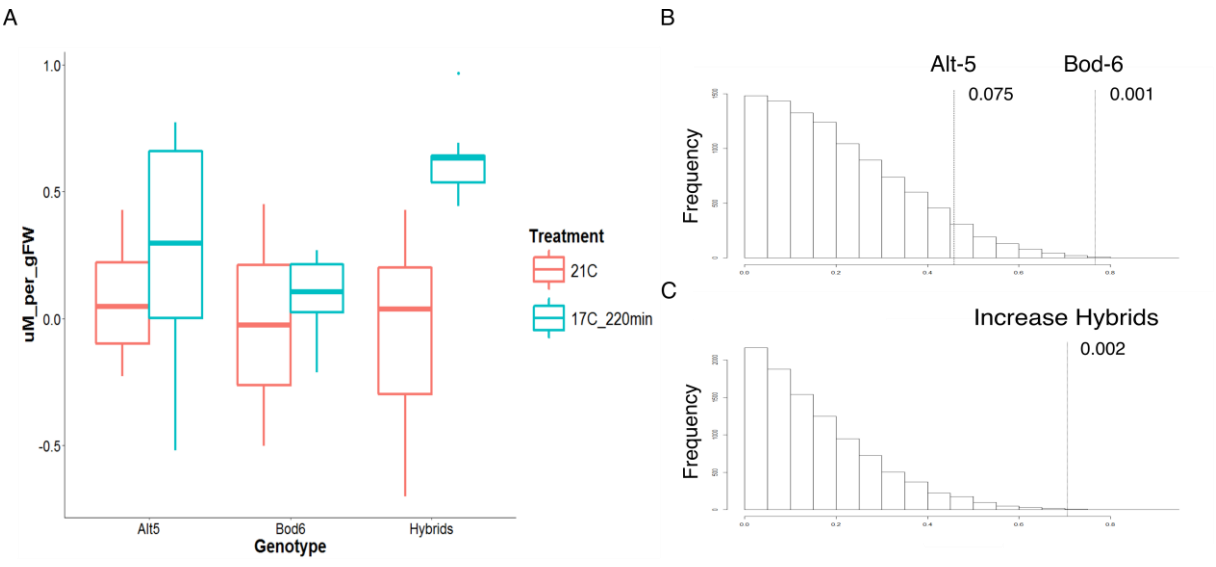

Figure 9. ACD6 activation increases intracellular ammonium in necrotic hybrids. (A) The concentration of ammonium in necrotic hybrids increased after the temperature switch. (B) A random permutation analysis revealed that the final intracellular ammonium level in hybrids was not significantly different from the Alt-5 parent. (C) Random permutations also corroborated that the increase in ammonium between the two timepoints was significant for hybrids.

3.2.3 Cytoplasmic calcium signaling and *PIF4* expression are not altered in necrotic hybrids in response to temperature fluctuations

Since calcium (Ca^{2+}) has been shown to be involved in the perception and response to different abiotic and biotic stimuli, including temperature changes (Nomura et al., 2012), we wanted to know if Ca^{2+} signaling could be altered in necrotic hybrids when compared to the parents. For this reason, we measured cytoplasmic Ca^{2+} using FRET-based yellow cameleon sensors described in (Krebs et al., 2012). Unlike the previous ionic measurements, which gave us the total ionic content of a tissue in a specific timepoint, FRET-based cameleon sensors allowed us to monitor intracellular ionic changes within organelles across time. For this, cytoplasmic Ca^{2+} sensors were transformed into necrotic hybrids and their corresponding parents, and the Ca^{2+} influxes in response to cold were assessed by confocal laser-scanning microscopy for each individual. The differences between the ranges of the FRET/CFP measurements was then calculated between the hybrid and each parent, and a random distribution of 10000 iterations was generated to establish the significance of the observed differences. Results revealed that the Ca^{2+} peak of hybrids was not significantly different from the Alt-5 parent ($\alpha = 0.05$), indicating that Ca^{2+} signaling in response to cold was not altered between parents and necrotic hybrids (Fig. 10).

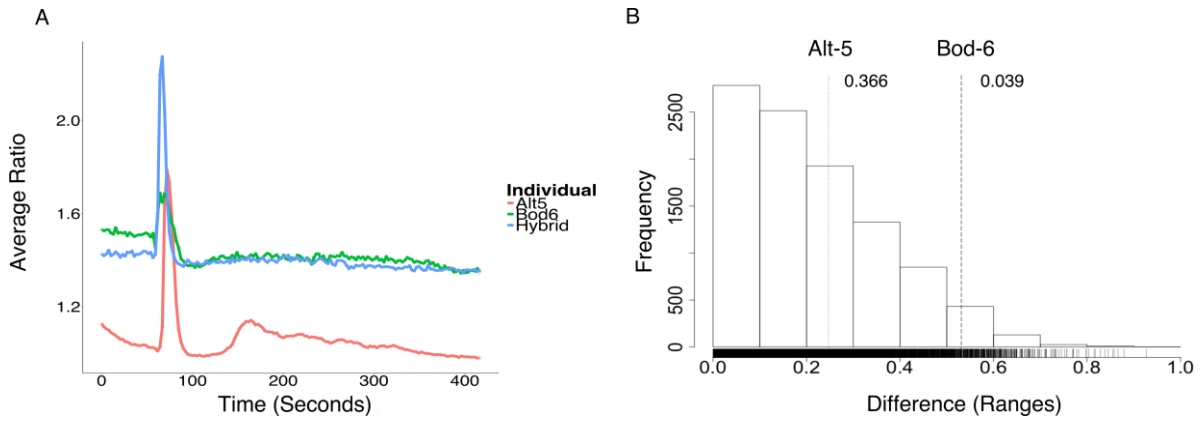

Figure 10. Intracellular calcium signaling in response to cold is not affected in necrotic hybrids. (A) The calcium spikes elicited by response to cold in Alt-5 (red), Bod-6 (green) and hybrids (blue). (B) Differences between the ranges for the FRET/CFP measurements were calculated between the hybrid and each parent and a random distribution with 10000 iterations was generated in order to establish the significance of the observed differences. The Ca peak of the hybrid was not significantly different from the Alt-5 parent. α = 0.05.

In a further attempt to understand the molecular mechanisms being triggered by ACD6 in a temperature-dependent manner, the expression of *Phytochrome Interacting Factor 4* (*PIF4*) was compared between hybrids, their corresponding parents, and the gain-of-function mutant *acd6-1*. Parental lines were screened both at 21ºC and 17ºC to corroborate the existing knowledge that *PIF4* expression decreases in a temperature-dependent manner (Gangappa et al., 2017). *PIF4* is a thermosensory negative regulator of plant defense and its decreased expression at low temperature is associated with an activation of defense responses, reduced growth and increased resistance to *P. syringae pv.* Tomato (*Pto*) DC3000 (Gangappa et al., 2017). As expected, *PIF4* accumulated in a temperature-dependent manner in both parent lines (Fig. 11). However, hybrids grown at 17ºC did not show any difference in *PIF4* expression when compared to parents grown at the same temperature (Fig. 11). Therefore, the activation of defense genes at lower temperatures in necrotic hybrids is not due to an altered expression of the thermosensory growth and immunity regulator *PIF4*.

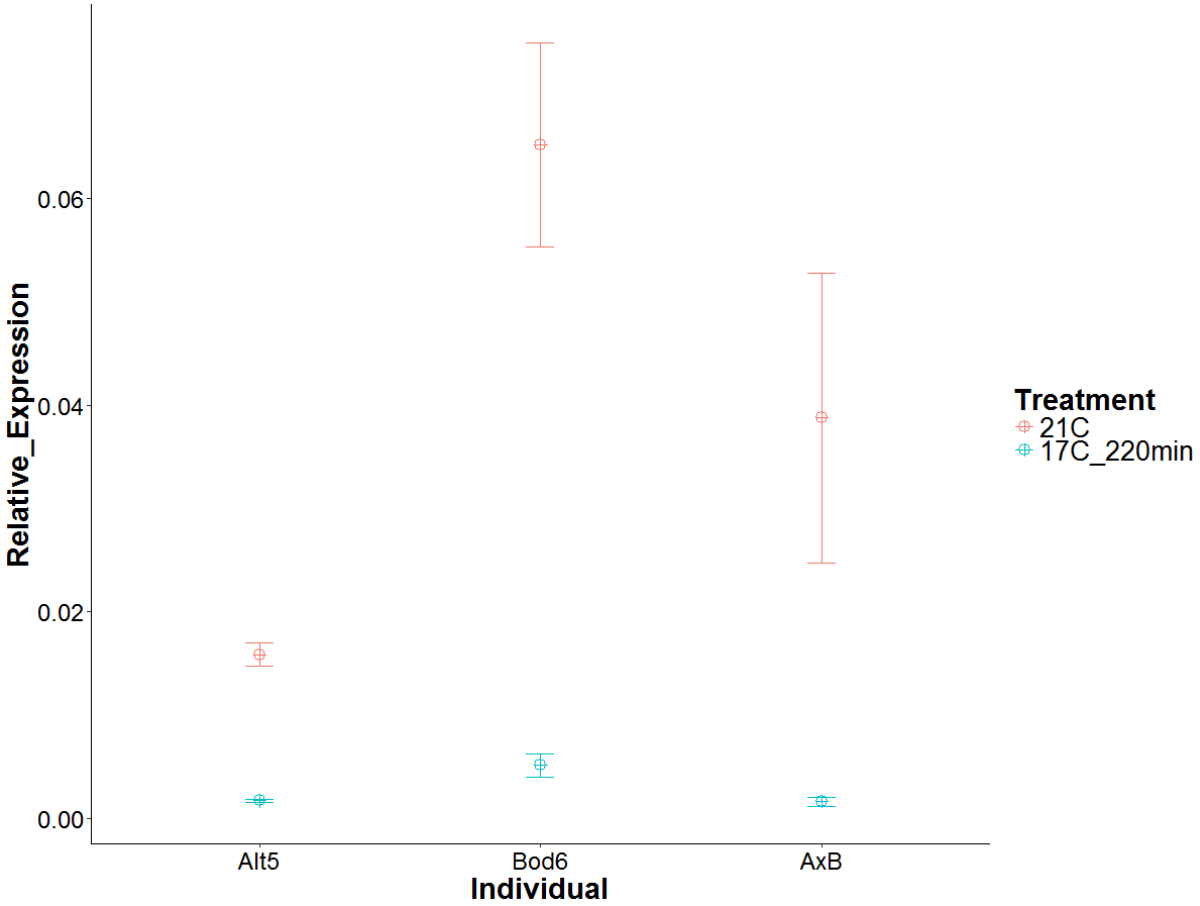

Figure 11. *PIF4* expression is not affected by ACD6 activation. *PIF4* expression was downregulated by a lower temperature as reported previously. However, necrotic hybrids at 17ºC did not show reduced levels of expression compared to the parent plants Alt-5 and Bod-6.

3.2.4 GFP-tagged ACD6 constructs localize to the nucleus and cytoplasm

Although certain interacting partners have already been described for *ACD6* in the gain-of-function mutant *acd6-1* (Zhang et al., 2014, 2017), its role in plant cell immunity remains elusive. Therefore, with the aims of characterizing novel interacting partners of ACD6, two approaches were taken. In the first approach, N-and C-terminal GFP tags were added to the coding sequence of ACD6 from the Alt-5 accession using the vectors described in (Grefen et al., 2010). These vectors were agro-transformed into the Bod-6 genetic background and seedlings were screened for fluorescent signals using confocal laser scanning microscopy. Unfortunately, very few T1 plants expressing a strong GFP signal were found (Fig. 12A).

Due to the low number of seedlings with strong GFP signal, a larger group of transgenic lines with a lower GFP signal was used for protein extraction to determine if it was already possible to pull-down the GFP-tagged ACD6. Unfortunately, after enriching GFP-bound proteins from the membrane fraction of a protein extract with the Nano-Trap®_A beads from Chromotek (Munich, Germany), blotting of the final protein extract with anti-GFP only revealed a signal in our positive control (data not shown). The second generation of the T1 lines with strong GFP signal did not produce a high proportion of seedlings with GFP expression (Fig. 12B), indicating that the transgenic T1 lines were heterozygous. Hence, screening a T3 generation from the confirmed T2 seedlings was necessary to harvest sufficient material for the pull-down of GFP-bound ACD6 proteins.

When confirming the positive transgenic lines harbouring the ACD6 constructs via confocal laser-scanning microscopy (CLSM), it was difficult to discern whether the GFP-tagged ACD6 was localizing at the plasma membrane (Fig. 12). For this reason, a cell plasmolysis experiment and staining of the plasma membrane with the endocytic marker FM4-64 was carried out (Fig. 13). In the latter experiment, it was clear that the GFP signal was not overlapping with the signal from the plasma membrane, confirming that the transgenic ACD6 proteins were only localizing to the cytoplasm. Since wild-type ACD6 is also known to be at the cytoplasm and its migration to the plasma membrane has be shown to be triggered by SA (Zhang et al., 2014), we wondered if our ACD6 constructs could still be functional. Therefore, we grew positive transgenic T3 lines confirmed by CLSM at constant 17°C to see if the necrotic phenotype could be induced. The results indicated that the positive lines, with a clear cytoplasmic ACD6 signal, did not acquire a hybrid necrotic phenotype (Fig. S8).

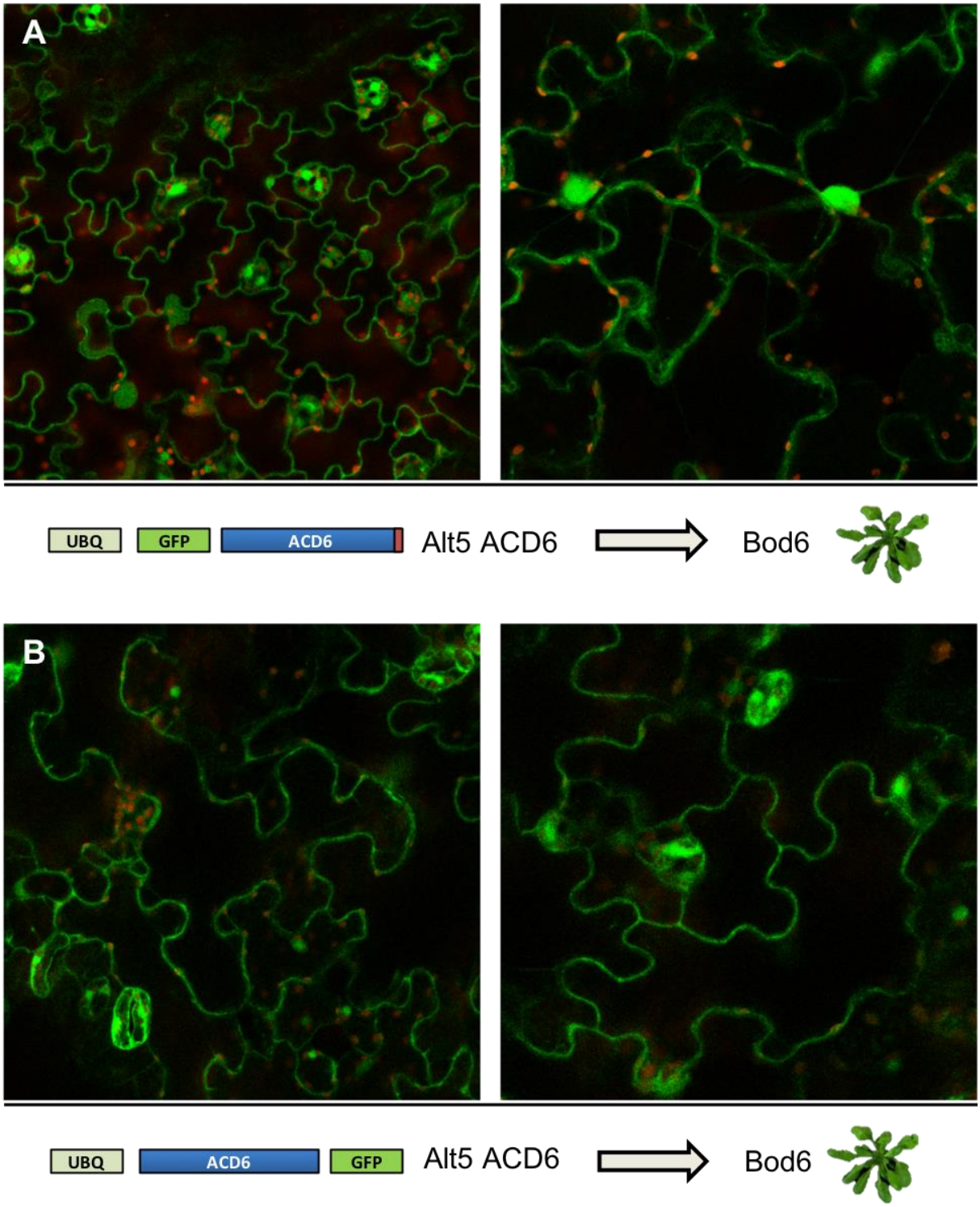

Figure 12. N and C-terminal GFP-tagged ACD6 localized to the cytoplasm and nucleus. (A) T1 transgenic lines expressing N-terminal GFP-tagged ACD6. (B) T2 transgenic lines expressing C-terminal GFP-tagged ACD6.

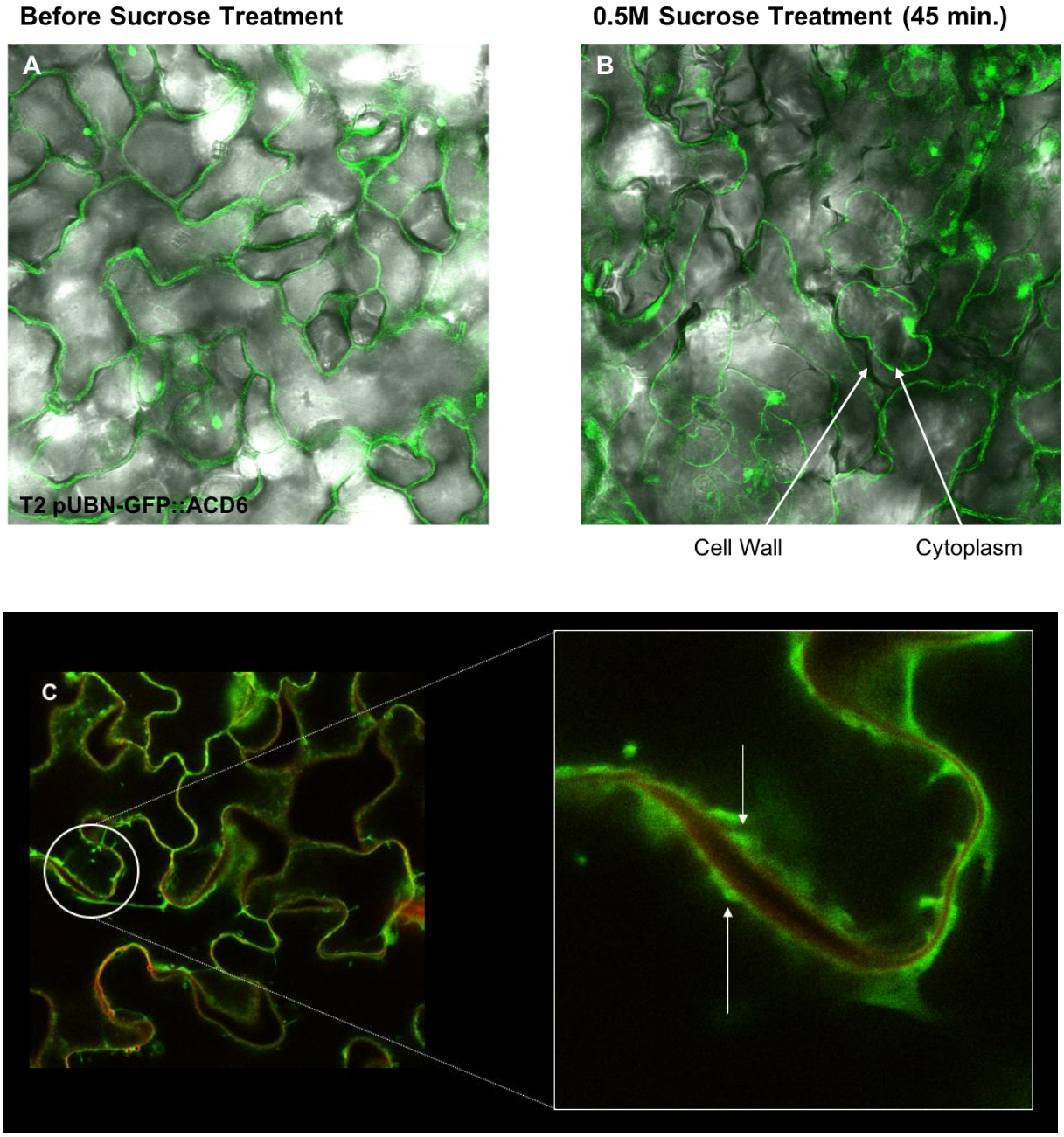

Figure 13. Cell plasmolysis and FM4-64 staining of transgenic Bod-6 plants harboring GFP-tagged ACD6 confirmed a cytoplasmic localization. Confocal laser scanning microscopy image of pUBN-GFP::ACD6 from leaf cells (A) and plasmolyzed leaf cells using 0.5 M sucrose for 45 min (B). Staining with the FM4-64 dye enabled to differentiate the cytoplasmic GFP signal (green) from the plasma membrane (red) (C).

Due to the unexpected prolongation of the GFP pull-down experiment, a yeast two-hybrid screen of ACD6 fused to the Gal4 DNA-binding domain (DNA-BD) was done using the Matchmaker® Gold Yeast Two-Hybrid System from Clontech. For this, Y2HGold yeast strains were transformed with the pGBKT7-BD construct containing the coding sequence of ACD6 from Col-0 or the *acd6-1* mutant. To confirm that ACD6 would not autonomously activate the reporter genes in Y2HGold in the absence of a prey protein, transformed colonies were plated on SD/-Trp/X-α-Gal. It was expected for the transformed colonies to grow with a white or very pale blue colour. Nevertheless, this was not the case and most of the isolated colonies turned blue (Fig. 14B). To reconfirm that ACD6 was indeed auto-activating the reporter genes in Y2HGold, the empty vector carrying the Gal4 activation domain (pGADT7-AD) was transformed to Y187 yeast cells and transformants from Y2HGold and Y187 were mated. Diploid clones were confirmed on SD/-Trp/-Leu media and SD/-Trp/-Leu/X-α-Gal/Aureobasidin A. Under the assumption that ACD6 was not autoactivating the reporter genes, no cells were expected to grow in the presence of Aureobasidin A. Additionally, colonies could only acquire a blue tone in the presence of X-α-Gal if the α-galactosidase reporter gene was activated. The presence of colonies with a slight bluish tone (Fig. 14A) indicated that identifying ACD6 interacting partners by yeast two-hybrid was not a viable approach.

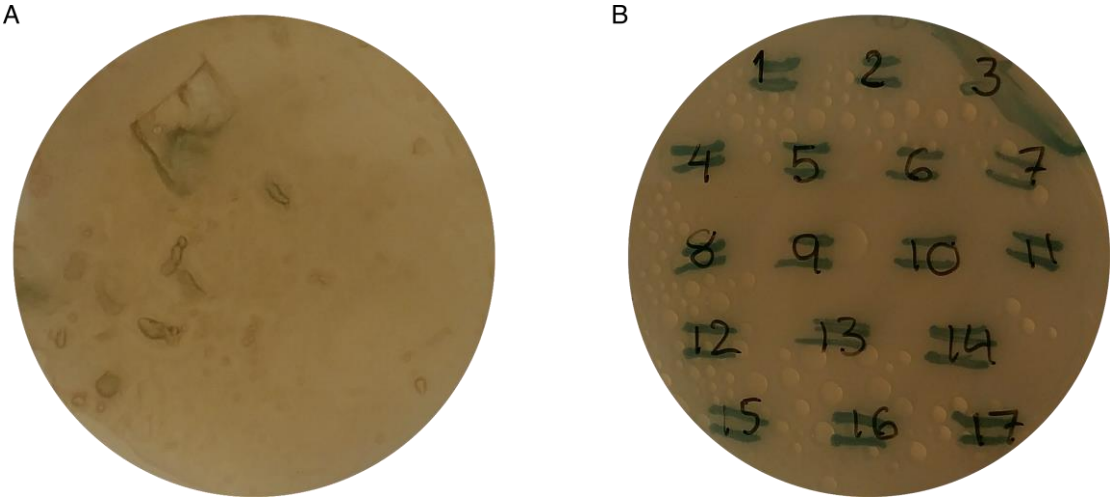

Figure 14. Autoactivation of the yeast two-hybrid reporter genes by ACD6. (A) Diploid cells of a mating between Y2HGold cells transformed with pGBKT7::ACD6 and Y187 cells transformed with the empty vector pGADT7, plated on SD/-Leu/-Trp/X-α-Gal/AbA. (B) Y2HGold cells transformed with pGBKT7::ACD6 plated on SD/-Trp/X-α-Gal.

To conclude, the different GFP-tagged ACD6 constructs developed in this work showed a similar cytoplasmic and nuclear localization. The proportion of positive transformants in the T1 generation was low, making the screening by laser scanning confocal microscopy a long process. The T2 seedlings coming from the confirmed T1 lines didn't show a high number of positive individuals either, indicating that the confirmed T1 individuals were heterozygous. The T3 generation produced a sufficient number of positive individuals.

To confirm whether the GFP-tagged ACD6 proteins are also localizing to the plasma membrane, root cells from seedlings of the T3 generation will be stained with a cytoplasmic dye and plasmolyzed with sucrose. Leaf cell plasmolysis of confirmed T2 seedlings using 0.5 M sucrose for 45 min was previously done but separation between the cytoplasm and plasma membrane was not discernable (Fig. S5).

4. Discussion

In my thesis, I presented two different studies. The first one analyzed the impact of hybridization on plant metabolism and growth within a local Arabidopsis collection site by means of a full diallel crossing scheme. In the second study, physiological and molecular changes associated to ACD6 activation were characterized in incompatible hybrids emerging from crosses between individuals within the same collection site.

4.1 Hybridization increased overall metabolic variation in Arabidopsis, impacting mostly secondary metabolites related to stress responses

Nonadditive inheritance refers to the effect of being above or below the midparent (additive) inheritance value (Falconer & Mackay, 1996). Nonadditive effects can also be referred to as epistatic interactions since epistasis helps explain how two alleles can give rise to phenotypes that challenge the expected Mendelian outcomes. In this sense, nonadditive inheritance can lead to novel phenotypes, which can impact traits desired by plant breeders or affect the adaptation of a plant to its environment. Nonadditive inheritance can therefore lead to both heterotic and disadvantageous phenotypes (Z. J. Chen, 2013) and makes prediction of hybrid phenotypes more challenging. Omic studies on hybrid vigour have identified nonadditive changes associated to transcriptomics, proteomics and metabolomics. Of special interest, it was shown that nonadditive gene expression changes in Arabidopsis hybrids correlated with an increased capacity for photosynthesis (Fujimoto, Taylor, Shirasawa, Peacock, & Dennis, 2012), and biomass heterosis of Arabidopsis intraspecific hybrids was correlated with increased levels of metabolic activity during early developmental stages (Meyer et al., 2012). Furthermore, Korn and collaborators were able to predict Arabidopsis freezing tolerance based on a limited number of metabolites (Korn et al., 2010), opening the possibility of using metabolic inheritance patterns to predict hybrid vigour. Nevertheless, a general model to explain the basis of nonadditive genetic variation is missing and hybrid phenotype prediction based on parental information remains an unsolved challenge (Seymour et al., 2016). Thus, the nonadditive effects on genetic variation remain largely unknown and should be further studied.

Previous literature has already highlighted the use of F_1 hybrids generated by diallel crossing to investigate the non-additive inheritance patterns underlying hybrid vigour in Arabidopsis inbred lines (Seymour et al., 2016). However, not much is known about the role of hybridization in the variation of plant metabolism in a single growth habitat. Even though the parent lines used in our study were mostly inbred, with heterozygosity ranging from 1 – 5.4%, hybridization among these natural local accessions was able to drastically change the metabolite abundance patterns in hybrid secondary metabolism. Hybrid secondary metabolism also varied greatly depending on the cross and direction of the cross (Fig. 3B-C), with fourteen showing non-additive inheritance in at least 50% of their secondary metabolism (i.e. 26) (Fig. 3B-C). In contrast, only six hybrids showed non-additive inheritance in more than 50% of their primary metabolism (i.e. 43). Since only two of the twenty crosses exhibiting more than 50% non-additive inheritance were reciprocal (Alt6xAlt1 and Alt6xAlt2), the direction of the cross was an important factor when determining the extent of non-additive inheritance.

Overall, hybridization increased the variation in hybrid secondary metabolism, with almost 40% of the crosses exhibiting significant deviations from the expected midparent values. The secondary metabolites that exhibited the greatest variation from the expected midparent values were related with plant stress responses (Fig. 3A), mainly glucosinolates and flavonoids. In contrast, primary metabolism was more robust, with not a single primary metabolite showing a significant non-additive inheritance pattern across all hybrids (p-value < 0.01). These observations go in hand with the notion that primary metabolism plays a central role in developmental processes. Consequently, while changes in primary metabolism exert pressure on vital processes such as growth, secondary metabolism variation is more prone to positive selection based on environmental factors (D. Kliebenstein, Kroymann, Brown, & Figuth, 2001; Kroymann, 2011; Manzaneda & Prasad, 2010; Schranz, Manzaneda, Windsor, & Clauss, 2009; Windsor, Reichelt, Figuth, & Svatoš, 2005). Therefore, an increased variation in secondary metabolism due to heterozygosity could provide mainly selfing plant populations/species such as Arabidopsis with more options to cope with rapid changes in their environments.

Although secondary metabolism showed a greater number of non-additive cases than primary metabolism, hybridization increased both primary and secondary metabolism variation (Fig. 1A-B). Even growth exhibited on average higher fluctuations in hybrids when compared to the parents (Fig. 1C). Hybrids from highly inbred maize parents, known to cause heterosis, were previously shown to display a reduced metabolic variation than their progenitors (Lisec et al., 2011). Given the hypothesis that metabolic profiles associated with better growth should be similar, the decreased variability among a heterotic hybrid population that was artificially selected for its phenotypic similarity should come as no surprise. In contrast, our study highlights that within a natural population with no prior artificial selection, hybridization increases metabolic variability, with special emphasis on secondary metabolites linked to environmental stress responses. This, in turn, increased the phenotypic diversity in hybrids as well (Fig. 1C-D).

4.2 Final rosette size was correlated with the earliest growth rate and both primary and secondary metabolites

In our study, we used growth as an indirect measurement of plant fitness and possible existing relationships between specific metabolic patterns and growth were of particular interest. Curiously, no specific inheritance patterns were shared among the biggest or smallest hybrids within our study. Yet, even though different metabolic profiles could give rise to big phenotypes, only the earliest growth rate was significantly correlated with the final rosette size (Fig. 5, Fig. S4). In contrast, smaller hybrids typically increased their growth rate at a later stage, between the development of their second and third pair of leaves (Fig. S5).

The fact that mostly secondary metabolites, particularly glucosinolates, were positively correlated with the final rosette size strengthened the notion that the trade-off between energy investment in defense compounds and growth is more complex than what we acknowledge. Several recent studies have highlighted how the trade-off between plant defense and growth has been flagrantly oversimplified, while identifying additional positive correlations between glucosinolates and growth (Joseph et al., 2013; Kliebenstein, 2016; Mauricio, 1998). In this respect, it's worth highlighting that different investigations have not been able to identify a significant association between glucosinolate-deficient genotypes and absolute growth (Joseph

et al., 2013; Paul-Victor, Züst, Rees, Kliebenstein, & Turnbull, 2010; Züst et al., 2011). On the contrary of what one would expect, it has even been shown that exogenous allyl glucosinolate increases the biomass of several Arabidopsis accessions; an effect that was modulated by the sucrose concentration in the media (Francisco et al., 2016). These observations go in line with the idea that growth-limiting factors are determined by the specific growing conditions of the plant (D. J. Kliebenstein, 2016). In this sense, defense compounds could affect plant growth either positively or negatively depending on the nutrient balance of the environment. Besides secondary metabolites, two primary metabolites were also positively associated with the final rosette radius: 1,6-anhydrobetaglucose, a by-product of cellulose degradation (Riedelsheimer et al., 2012) and spermidine, a polyamine capable of promoting plant growth under abiotic stress conditions (Paschalidis, Roubelakis-Angelakis, Perez-Amador, & Carbonell, 2005; Radhakrishnan & Lee, 2013). Hence, though it is usually expected that primary metabolites will positively correlate with plant growth, as they are involved in central metabolic pathways involved in carbohydrate assimilation, several secondary metabolites associated to plant stress responses were also found to be positively correlated to growth within the hybrid individuals of this study.

The connection between overall metabolic variation and growth is not well established yet. Though biomass has already been correlated with specific metabolite combinations in Arabidopsis (Meyer et al., 2007), the implications on how metabolic diversity can impact growth is still not understood. In our study, both positive and negative dominance in secondary metabolism was associated with big rosette sizes (Fig. 5A, Fig. S4), going in hand with the notion that different metabolic signatures can be associated with higher growth. In this sense, carrying more metabolic signatures could increase the probabilities of having a signature related to higher growth within a population under specific conditions. Although we observed more significant positive dominant cases related to rosette size, five out of twelve hybrids showed negative dominance (Fig. 5A). Whether these smaller hybrids would actually show a reduced fitness in the field is something worth to investigate in future experiments. All parental individuals used in this experiment were part of a natural wild population collected in Tübingen (southern Germany). Unlike inbred lines or induced mutation-based studies, natural populations are more suitable to understand mechanisms underlying variability and adaptation. Our study revealed that

hybridization increased the metabolic variation of a local *Arabidopsis thaliana* collection site. We also saw that the same genetic background could yield completely different metabolic phenotypes, as evidenced in certain reciprocal hybrids which showed clearly different profiles in their secondary metabolism (Fig. 4). In these cases, the hybrids involved included the top four biggest hybrids within our study. Therefore, different metabolic inheritance patterns were associated with big size within our hybrids, indicating that larger fluctuations in secondary metabolism won't always hinder growth. Additionally, if natural environments are in constant change, having more metabolic diversity might increase the probabilities of resiliency in terms of optimal growth. These results therefore add intriguing insights to our understanding of the nature of non-additive inheritance in a natural Arabidopsis population; information that may also hold in major crop species.

4.3 Characterizing the role of ACD6 by studying molecular and physiological changes associated with its activation in necrotic hybrids

Among crosses from the local individuals collected at Tübingen area (Germany), different cases of hybrid necrosis were detected. This hybrid incompatibility characterized by stunted growth and necrotic lesions was attributed to different allelic interactions of *ACD6* (Świadek et al., 2017). Previously, Todesco and collaborators identified incompatible interactions between *ACD6* alleles from different global Arabidopsis accessions (Todesco et al., 2014). The fact that *ACD6* alone is able to generate hybrid incompatibilities between local and global individuals suggests it is a central regulator of plant defense responses. Furthermore, the existence of many different *ACD6* alleles in a single population suggests this locus is under balancing selection, a pattern often seen in disease resistance (R) genes (Todesco et al., 2010; Van der Hoorn, De Wit, & Joosten, 2002). The reason to why such a high degree of sequence polymorphisms could be maintained within a locus might therefore be explained by a strong fluctuating selective pressure. Most loci involved in hybrid incompatibilities are actually well-described nucleotide-binding leucine-rich repeat (NLRs) proteins (Chae et al., 2014) in charge of detecting effectors secreted by phytopathogenic bacteria and fungi. The strong selective pressure exerted by the arms race between pathogen effectors and plant NLRs drives a surge in sequence diversity (Büttner & Bonas, 2010; Kay & Bonas, 2009; Koebnik et al., 2006); one that increases the probability of encountering genetic incompatibilities (Chae et al., 2014).

Sequence diversity in the *ACD6* locus has also been observed (Świadek et al., 2017; Todesco et al., 2014), but the role of this non-NLR protein in plant defences remains largely unknown. Therefore, to better understand the role of ACD6 within the plant stress pathways, molecular and physiological responses related to its activation were characterized in necrotic hybrids.

4.4 Senescence is induced earlier in necrotic hybrids when compared to its parents

Known to be involved in a positive feedback loop with salicylic acid (SA), ACD6 is able to induce hybrid necrosis through the activation of defense genes linked to the systemic acquired resistance (SAR) response (Świadek et al., 2017; Todesco et al., 2014). The involvement of defense genes in senescence has been reported previously, with members of the WRKY transcription factor family, brassinosteroids, and novel genes like HYS1/CPR5 promoting both disease resistance and senescence (Bartwal, Mall, Lohani, Guru, & Arora, 2013; T Eulgem et al., 2000; Yoshida, 2003; Zentgraf et al., 2001). Furthermore, it has been revealed that expression of senescence-related genes is impaired in *pad4* and *npr1* mutants unable to trigger a normal defense response through SA (Morris et al., 2000). This might be due to the fact that both defense and senescence share common molecular pathways, amongst them programmed cell death (Brodersen & Petersen, 2002; Piffanelli, Zhou, & Casais, 2002; S Robatzek & Somssich, 2002; Silke Robatzek & Somssich, 2001). Therefore, it should be more efficient to relay this activation to a common set of genes rather than having unique isolated pathways to turn on similar biological processes. To better understand the relationship between defense and senescence in necrotic hybrids with an active version of ACD6, molecular markers for both pathways were monitored in a time-course manner. Our results indicated that senescence was induced earlier in necrotic hybrids than in parental lines, but it was only after the induction of the SAR marker *PR1* (Fig. 6). Therefore, these findings suggest that the earlier onset of senescence could be a by-product of the sustained defense response in hybrids.

Fitness costs related to an early senescent phenotype can be dramatic, especially if plants don’t have enough time to produce seeds. An interesting observation in our experiments was that although hybrids displayed earlier senescence, flowering did

not occur earlier. This raised further questions around the genes controlling flowering time in hybrids. It has already been reported that plants with an active defense response show stunted growth and an earlier flowering phenotype (S Robatzek & Somssich, 2002; Steventon, Okori, & Dixelius, 2001; Veronese & Narasimhan, 2003). Nevertheless, cases were necrotic hybrids are not able to reach flowering and the involvement of stress-related genes in flowering time have also been reported (Alcazar et al., 2009; Bomblies et al., 2007; Liu & Howell, 2010; G.-F. Wang et al., 2011). However, key regulatory genes involved in flowering, among them *CBF1*, *FLC*, and *FT* were not differentially expressed in hybrids when compared to parents. Yet, *NF-YA1* and *NF-YA4*, two genes coding for the HAP2 subunit of the CCAAT-binding Heme Activator Protein (HAP) transcription factor complex were found to be significantly upregulated in hybrids when compared to parents (Fig. 6). Involved in stress responses that confer drought tolerance and trigger the unfolded protein response (UPR), the HAP complex has also been shown to delay flowering time when over-expressed in Arabidopsis (Liu & Howell, 2010; Nelson et al., 2007; Wenkel et al., 2006). Hence, it seems plausible that the upregulation of these genes linked to abiotic stress tolerance might be interfering with the flowering time in necrotic hybrids. This might be happening through the reported interaction between the HAP complex and the CCT domain-containing protein CONSTANS (CO), which promotes flowering in Arabidopsis (Wenkel et al., 2006).

4.5 Carbohydrate metabolism intermediates and sugars are upregulated in necrotic hybrids shortly after the temperature switch

As mentioned earlier, a key characteristic of hybrid necrosis is its temperature-dependency. To better understand early metabolic changes linked to the appearance of hybrid necrosis, metabolites induced in hybrids 220 minutes after a switch to 17°C were analyzed. Production of simple sugars and compatible solutes, including glucose-6-phosphate (G6P) and trehalose, together with several intermediates of the TCA cycle and glutathione metabolism seemed to indicate a very early response to abiotic stress (Miura et al. 2014, Zhong et al. 2016). The immediate increase in G6P and fructose-6-phosphate (F6P) together with several TCA intermediates indicated that ACD6 activation could be triggering glycolysis and the tricarboxylic acid (TCA) cycle. This might lead to an increase in the ATP-producing pathway of cellular respiration (Sadava, Hillis, Heller, & Hacker, 2017). The fact that the polyamine (PA)

putrescine was also significantly accumulated in necrotic hybrids shortly after the temperature switch could be linked to the upregulation of the citric acid cycle. PAs have been shown to enhance molecular protective effects in plants undergoing drought stress by adjusting the glycolytic metabolism and the TCA cycle (Zhong et al., 2016). In fact, Putrescine can be converted to γ-aminobutyric acid (GABA), a regulator of the TCA cycle (Gill & Tuteja, 2010). It has also been shown that exogenous putrescine can alleviate the inhibition of glycolysis and TCA resulting from salt stress in chickpea and cucumber plants (Shu et al., 2011; Zhong et al., 2016) by increasing the contents of TCA intermediates, specifically in citrate, succinate and malate. The early metabolic changes associated to ACD6-induced defense responses in necrotic hybrids included a significant increase in putrescine, citrate, succinate and malate, together with G6P and F6P, known intermediates of the glycolysis metabolism. However, since photosynthesis is interrupted during abiotic conditions, including drought or high salinity, new sugar sources should be available if a plant wishes to maintain the glycolysis and TCA pathways steady for ATP production. Hence, accumulation of simple sugars, including glucose and fructose, is usually observed in genotypes tolerant to drought under osmotic stress conditions (Kerepesi & Galiba, 2000). In this regard, sugars, including glucose and fructose, were also significantly upregulated in necrotic hybrids 220 minutes after the temperature switch.

Shikimic acid, a precursor of salicylic acid (SA), and SA were also upregulated exclusively in necrotic hybrids. SA regulation is widely known to be linked both to biotic and abiotic stress responses (Kang et al., 2013; Miura & Tada, 2014; Shah, 2003). Regarding abiotic stress conditions, SA has been shown to alleviate the toxic levels of hydrogen peroxide (H_2O_2) accumulated under salt or drought stress in different plant species (Khan, Syeed, Masood, Nazar, & Iqbal, 2010; Nazar, Iqbal, Syeed, & Khan, 2011; Noreen & Ashraf, 2010; Sawada, Shim, & Usui, 2006). This protective effect has been attributed to an increase in ascorbate and glutathione, two non-enzymatic antioxidants involved in the ascorbate-glutathione cycle (Kang et al., 2013). Necrotic hybrids in our experiment also showed increased levels of both ascorbate and glutathione intermediates shortly after the temperature switch (Table 2). Another role of SA during both biotic and abiotic stress responses is the closure of stomata in an ABA-independent manner. This avoids both pathogen colonization and water transpiration (Miura & Tada, 2014). In fact, it was already reported that *acd6*

gain-of-function mutants exhibited stomatal closure and drought tolerance due to SA accumulation (Miura et al., 2013; Okuma et al., 2014). Additionally, necrotic hybrids also displayed increased levels of trehalose, a known osmoprotectant, in comparison to parents after the temperature-dependent activation of ACD6. Trehalose is a disaccharide and a compatible solute that protects cells against osmotic stress, and its accumulation in plants is linked to enhanced drought tolerance (Nuccio et al., 2015; Pilon-Smits et al., 1998). Hence, taken together, our results support the findings of (Miura et al., 2013) and (Okuma et al., 2014), adding novel information as to the timing of molecular changes associated with hybrid necrosis. The amount of primary metabolites affected 220 minutes after the temperature switch, from 21ºC to 17ºC, contrast with the lack of changes observed 24 hours after the switch (Świadek et al., 2017). Hence, the metabolic changes that induce hybrid necrosis seem to be occurring very early after temperature perception. It would be interesting to consider secondary metabolism during this short time frame as well.

4.6 Low temperature did not induce any ionic changes in hybrids in comparison to parents

ACD6's migration to the membrane has been linked to its activation and is increased by SA (Zhang et al., 2014). Though it might be tempting to think that ACD6 activation is an effect of SA signaling, it has been shown that BTH, a synthetic SA analogue, is not sufficient to trigger the necrotic phenotype without an active *ACD6* allele (Rate et al., 1999). The notion that ACD6 activation is temperature-dependent raises further questions as to its possible role as a membrane protein. To further understand any possible ionic changes coupled to the activation of ACD6, ionic chromatography of the same samples used for the temperature shift experiment was done. These results did not yield any clear differences between the hybrids and both parents. Although ammonium and sulfate showed a significant increase in hybrids after the temperature switch, their final levels were not significantly different from the Alt-5 parent (Fig. 9, Fig. S2). It might be possible that the bigger biological variation observed for the Alt-5 parent could have influenced this result. Nevertheless, repeating the same experimental design using an alternate extraction protocol yielded the same results for ammonium, but not for sulfate (Fig. S7). Therefore, there seems to be a lot of biological variation in the total ionic concentrations of these samples, particularly the Alt-5 parent. Until this experiment is repeated with more than six biological replicates,

it remains difficult to estimate the significance of this ammonium rise in necrotic hybrids. Since an accumulation of intracellular ammonium has been reported to induce production of ROS, which in turn leads to SAR in rice plants (Ahn, 2007), we hypothesized whether the significant increase in intracellular ammonium could be triggering the SAR phenotype in necrotic hybrids. For this, the ACD6 gain-of-function (*acd6-1*) and loss-of-function (*acd6-2*) mutants were grown together with Columbia (Col-0) seedlings under different ammonium concentrations in soil and synthetic media. We thought *acd6-1* plants would show reduced symptoms when grown on lower ammonium concentrations. However, this was not the case and the ammonium concentration in the nutrient substrates did not correlate with the severity of the symptoms in any of the cases (Fig. S3).

The second ionic compound that was significantly increased in hybrids due to temperature was sulfate. Sulfate is the oxidized form of sulfur and is used as a sulfur carrier to generate sulfur-containing compounds (Bohrer & Takahashi, 2016). Sulfate has been previously linked with autophagy induction during senescence in mammal cells (Patel et al., 2013). Additionally, it was also shown that sulfate-reducing enzymes are usually activated after dark-induced senescence in *Phaseolus vulgaris* seedlings (Schmutz, Wyss, & Brunold, 1983). Hence, sulfur assimilation into sulfur-containing amino acids would decrease the sulfate pool in senescent tissues. Sulfur remobilization from old leaves to younger leaves has also been seen during leaf senescence, and is accompanied by decreased sulfate in senescent leaves (Dubousset et al., 2009). Since whole rosettes were harvested for the ionic measurements in our study, it was not possible to discern between senescent and non-senescent leaves. Nevertheless, an increased sulfate level within the whole rosette could be an indicator of catabolic processes that release sulfur. Whether these catabolic processes might include autophagy is not possible to determine with the current data. Hence, more experiments would need to be done to identify the source of this increased ion. Yet, taking into account that the final levels of both ammonium and sulfate were not significantly different than the Alt-5 parent, its significant rise due to temperature might not be linked to the hybrid necrotic phenotype.

4.7 Ca^{2+} signaling in response to cold was not altered in necrotic hybrids

The fact that we could not detect major ionic changes in necrotic hybrids after the temperature-dependent ACD6 induction did not meant that important ionic changes were not happening. Ion chromatography captures ionic changes at the whole cellular level. Therefore, most intracellular signaling events will be masked unless they generate substantial ionic changes. Since membrane proteins such as mechanosensory calcium (Ca^{2+}) and potassium (K^{+}) channels are known to transduce signaling events in response to temperature changes (Alcázar & Parker, 2011; Cheong et al., 2003; Finka, Cuendet, Maathuis, Saidi, & Goloubinoff, 2012; Kim, Cheong, Grant, Pandey, & Luan, 2003), we didn't discard the possibility that ACD6 could mediate intracellular calcium signaling in response to a decrease in temperature.

It has already been reported that intracellular Ca^{2+} regulates SA-mediated plant immunity in Arabidopsis (Du et al., 2009). Therefore, to monitor the changes in free cytosolic Ca^{2+} in response to temperature, fluorescence resonance energy transfer (FRET)-based yellow cameleon sensors, described in (Krebs et al., 2012), were transformed into necrotic hybrids and their corresponding parents. The differences between the ranges of the FRET/CFP measurements was calculated between the hybrid and each parent, and a random distribution with 10000 iterations was generated to establish the significance of the observed differences between the calcium peaks. Results revealed that the Ca peak of the hybrids was not significantly different from the Alt-5 parent with an $\alpha = 0.05$ (Fig. 10). Just like with ammonium, hybrids showed a significant difference only with respect to the Bod-6 parent. Among the local Tübingen collection of Arabidopsis individuals, Alt-5 displayed the largest number of crosses involved in hybrid necrosis (Świadek et al., 2017). Nevertheless, we didn't observe any particular differences in the expression of defense marker genes when compared to other Altenriet individuals from the same collection site. Particularly interesting in this expression study was that the Altenriet 7 (Alt-7) individual was the only one displaying an increased expression of *PR1*, a molecular marker of the SAR response (Fig. S6). However, this individual was not involved in any hybrid incompatibility with other plants from the same collection site (Świadek et al., 2017). Even though Alt-5 had similar intracellular ammonium and Ca^{2+} accumulation in response to cold when compared to necrotic hybrids, its phenotype at 17ºC remained healthy. This strengthens the notion that *ACD6* alleles can show

different levels of activation among different individuals. In fact, Todesco and collaborators did see that interactions between different combinations of *ACD6* alleles could elicit different levels of defense responses in hybrids, indicating that ACD6-indcued reactions are not binary by nature (Todesco et al., 2014).

4.8 *PIF4* expression did not explain the temperature-dependent activation of defense responses in necrotic hybrids

A well-described thermosensory regulator of plant defense responses is the Phytochrome Interacting Factor 4 (PIF4). Known to suppress plant immunity at elevated temperatures, *pif4* mutants show activation of SAR-related genes including *PR1* and *PR5* (Gangappa et al., 2017). The temperature-dependent negative regulation of plant defenses through PIF4 is mediated by the Phytochrome B (PHYB) photoreceptor. In this sense, PHYB promotes light-dependent degradation of the PIF4 transcription factors. It has also been shown that the immune and growth regulation exerted by PIF4 is dependent on its expression level, with bigger plants susceptible to *P. syringae pv.* Tomato (*Pto*) DC3000 showing increased *PIF4* expression (Gangappa et al., 2017). Therefore, to know whether the temperature-dependent regulation of immunity and growth was being mediated by PIF4 in necrotic hybrids, the expression of this gene was monitored in necrotic hybrids, their corresponding parents, and the ACD6 gain-of-function mutant *acd6-1*. Results indicated that *PIF4* expression was reduced after a decrease in temperature, as expected. However, levels of *PIF4* in both parents decreased to the same levels observed in necrotic hybrids. Furthermore, the ACD6 gain-of-function mutant *acd6-1* showed expression levels of PIF4 comparable to the Alt-5 parent grown at 21ºC (Fig. 11). These results indicated that the temperature-dependent upregulation of the defense response in necrotic hybrids was not caused by a downregulation of *PIF4*.

4.9 GFP-tagged ACD6 constructs showed cytoplasmic and nuclear localization

Since it is known that transcript expression levels of *ACD6* don't generate necrosis (Todesco et al., 2010), the phenotype observed in necrotic hybrids is most likely caused at the protein level. In this sense, identifying candidate interacting partners of ACD6 would yield new clues as to its role during hybrid necrosis. Zhang and collaborators already reported that ACD6 migrates to the membrane in protein

complexes with the pattern recognition receptors (PRRs) Flagellin Sensing 2 (FLS2) and BR1-Associated Receptor Kinase 1 (BAK1) upon SA induction. The active version of acd6 (*acd6-1*), however, was already present at the membrane in larger amounts prior to SA stimulation (Zhang et al., 2014). The localization of ACD6 at the membrane points to a possible role in signal perception. No ligands related to pathogen-associated molecular patterns (PAMPs) have been described to interact with ACD6 so far. However, the fact that PRRs are reduced in plants lacking ACD6 (Tateda et al., 2014), and that these plants show more susceptibility to *P. syringae* due to an attenuated flg22 response (Tateda et al., 2014) indicates that ACD6 could play an indirect role in PAMP-mediated defense signaling. Even though Zhang and collaborators were able to identify more membrane-associated proteins as candidate interactors of ACD6, among them receptor-like kinases (RLKs), the function of this protein remains unknown (Zhang et al., 2017). Important to note is that Zhang and collaborators used the hemagglutinin (HA) epitope-tagged gain-of-function ACD6-1 construct described in (Lu et al., 2005) for their immunoprecipitation assays. Several identical regions of the short HA peptide sequence can be found within the Arabidopsis proteome, incrementing the risk of pulling down false interactors with an HA-antibody. In fact, only a soluble cytoplasmic portion from a single candidate interactor described by (Zhang et al., 2017) could be confirmed by yeast two-hybrid. For this reason, we were interested in identifying novel interacting partners by creating a novel ACD6 construct fused to GFP.

N and C-terminal constructs were created and GFP signals were detected by laser scanning confocal microscopy in T1 and T2 transgenic lines (Fig. 12). Nevertheless, the GFP-fused ACD6 protein did not show a plasma membrane localization, as evidenced after FM4-64 staining (Fig. S5). Therefore, it seemed the GFP tag was altering the expected plasma membrane localization. Enriching SDS-PAGE bands during immunoprecipitation (IP) of ACD6-GFP from microsomal fractions did not reveal a GFP signal after immunoblotting with anti-GFP. Therefore, it seemed that the recombinant protein was not at the membrane.

A Y2H screen of ACD6 fused to the Gal4 DNA-binding domain was planned. Hence, ACD6 was cloned into the vector pGBKT7 DNA-BD and its ability to autoactivate the reporter genes from Clontech's Y2HGold yeast strain was assessed. Transformed yeast strains turned blue in the presence of the chromogenic substrate X-α-Gal and

grew on the toxic drug Aureobasidin A, indicating the activation of the reporter genes (Fig. 13). A second autoactivation test was done to reconfirm the results, but this time a Y187 strain carrying the empty vector pGADT7 AD was mated with the transgenic Y2HGold strain carrying the pGBKT7::ACD6 construct. Again, colonies grew, indicating the ACD6 bait could autoactivate the reporter genes; screening against a library of prey proteins was not done to avoid identification of false positives.

5. Conclusions

In conclusion, we used a full diallel crossing scheme to identify inheritance patterns induced by hybridization in a local collection site of Arabidopsis. We were able to observe that hybridization increased the overall variation in metabolism and size within hybrids when compared to parents, with several secondary metabolites showing significant non-additive inheritance patterns across most hybrids. Secondary metabolites also showed an increased non-additive mode of inheritance in hybrids when compared to primary metabolites (39% versus 28%, respectively). Interestingly, the highest midparent deviation was attributed to secondary metabolites linked to plant defense responses, mainly glucosinolates and flavonoids. Additionally, certain crosses were more likely to show non-additive inheritance in metabolism, with the direction of the cross determining the extent of non-additive inheritance. We believe therefore that an increased metabolic diversity induced by hybridization could provide hybrids with a needed source for phenotypic variation in natural changing environments, especially among inbred individuals growing at a single growth habitat.

To better characterize the role of ACD6 in plant defense responses, physiological and metabolic changes induced during hybrid necrosis were compared between necrotic hybrids and their corresponding parents. With this work, it was possible to establish that senescence markers were induced earlier in necrotic hybrids than in parents and that an active defense response preceded this early senescence induction. Additionally, the HAP2 subunit of the CCAAT-binding Heme Activator Protein (HAP) transcription factor complex was found to be significantly upregulated in necrotic hybrids; an upregulation in this transcription factor was previously linked with drought tolerance in corn and delayed flowering time in Arabidopsis.

Early metabolic changes induced in necrotic hybrids 220 minutes after a temperature switch to 17°C included accumulation of salicylic acid, trehalose, simple sugars and putrescine, together with several by-products of the TCA cycle and glutathione metabolism. Our findings therefore strengthen the notion that ACD6 could play a role in abiotic tolerance, besides its more widely discussed role in biotic stress. Strengthening this idea is the fact that ACD6 gain-of-function mutants have displayed an enhanced tolerance to drought (Miura et al., 2013; Okuma et al., 2014).

Since calcium signaling has been reported to be involved in response to temperature changes, influx of cytosolic calcium in response to cold was compared between necrotic hybrids and parents using yellow cameleon sensors. We concluded that cytoplasmic calcium signaling was not altered in necrotic hybrids in response to cold when compared to parents.

This work gave further insights into the role of hybridization within a natural local Arabidopsis collection site at the metabolic and phenotypic scale. Physiological and metabolic responses linked to the temperature-dependent induction of ACD6 were analyzed and new knowledge about the molecular processes affected by this protein was generated.

6. Supplementary Figures

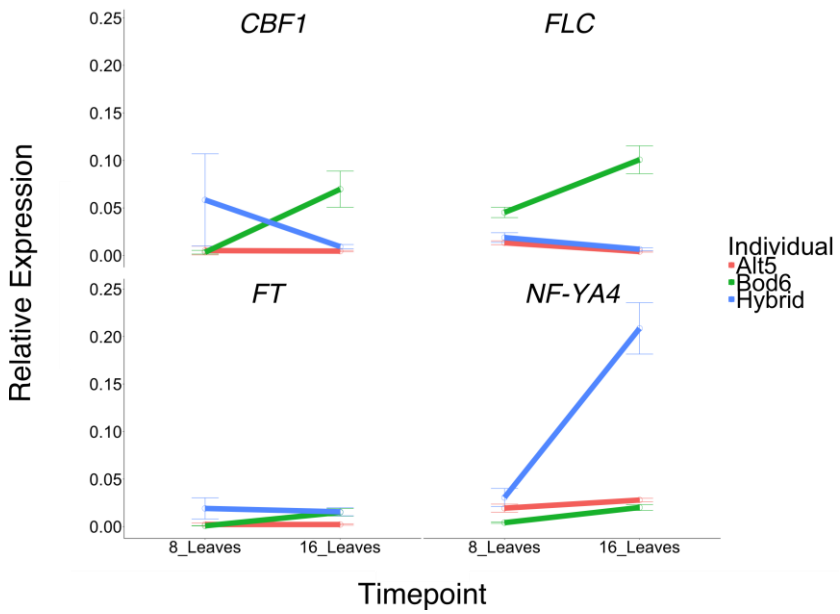

Figure S1. Known flowering regulators didn't show alterations in necrotic hybrids when compared to both parents. Only subunits of the NF-Y/HAP transcription factor complex involved in ER stress, flowering and drought tolerance were upregulated in hybrids with respect to both parents at the 16-leaf stage. Other known flowering regulators (*CBF1, FLC, FT*) didn't show differences between hybrids and parents. α = 0.05. Wilcoxon Test. Red line: Alt-5. Green line: Bod-6. Blue line: Hybrids.

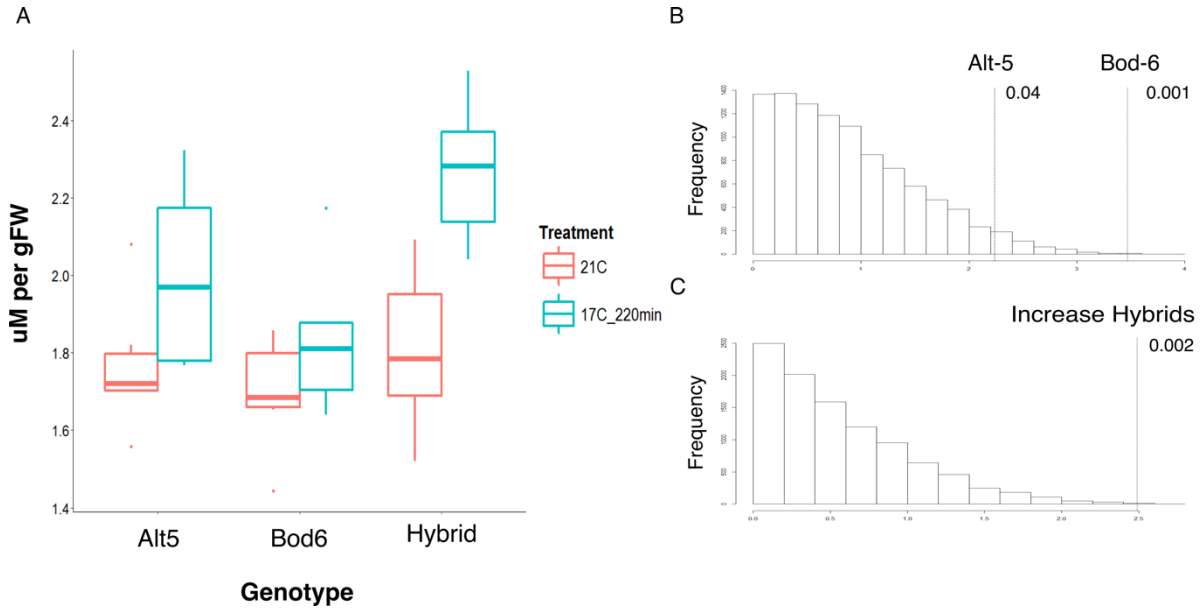

Figure S2. Sulfate increased significantly in hybrids after the temperature switch. (A) Sulfate increased significantly in hybrids after the temperature switch. Nevertheless, the accumulation pattern seen in parents could not be replicated when repeating the experiment (Fig S8). (B) A random permutation analysis revealed that the final sulfate level in hybrids was significantly different from both parents. (C) Random permutations also showed that the increase in sulfate between the two timepoints was significant in hybrids.

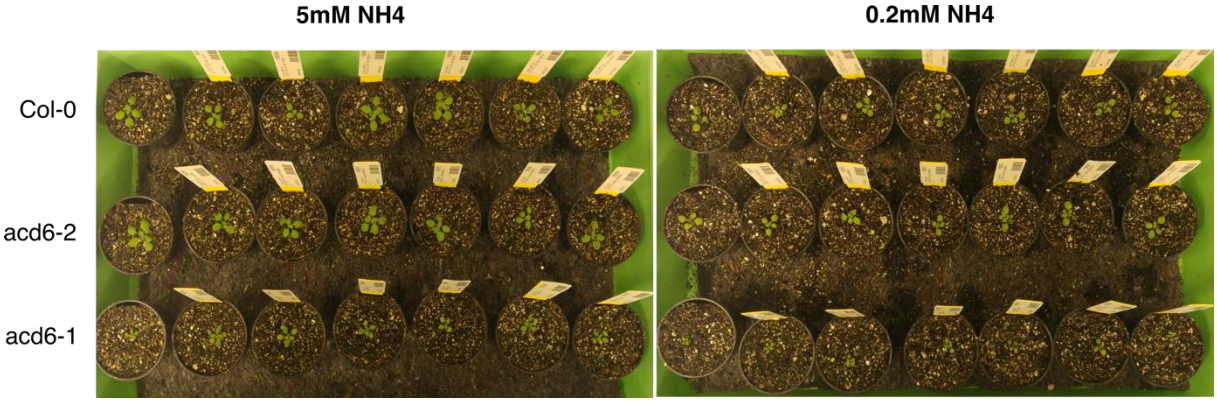

Figure S3. Ammonium (NH4) concentrations in soil did not affect the retarded growth of ACD6 gain-of-function mutants (acd6-1) in comparison to Col-0 and ACD6 loss-of-function mutants (acd6-2). The retarded growth characteristic of acd6-1 mutants is maintained both in high and low NH4 concentrations, rejecting our hypothesis that higher NH4 concentrations could aggravate the phenotype triggered by ACD6 activation.

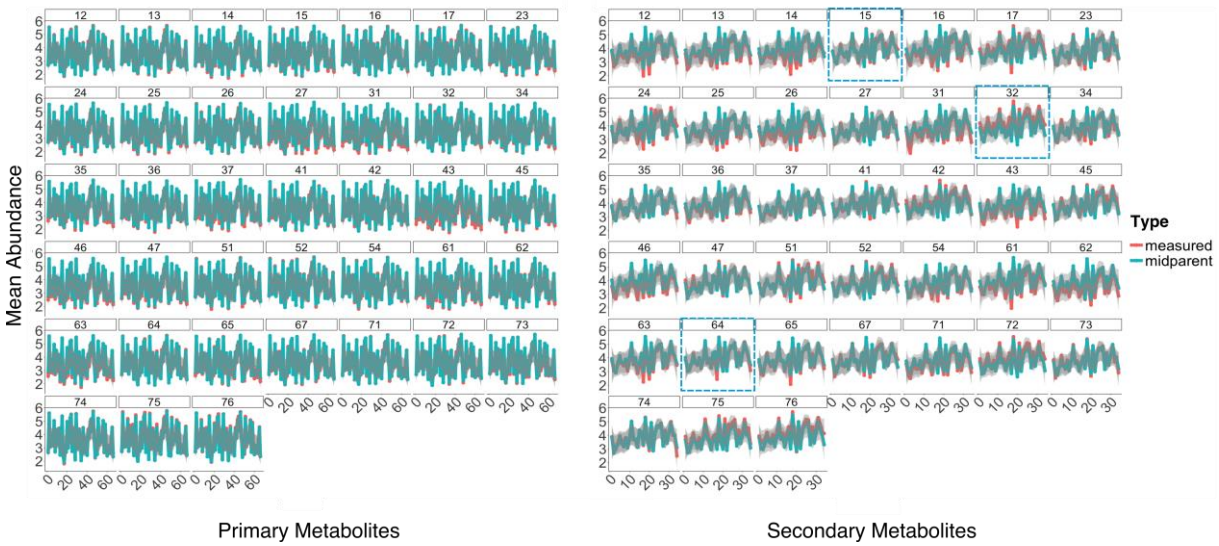

Figure S4. Secondary metabolism showed more deviations from the midparent levels than primary metabolism. Blue lines indicate the midparental level and orange lines the observed levels. Overall, secondary metabolism showed more variation from the midparent levels when compared to primary metabolism. The three biggest hybrids (inside dotted blue boxes) showed different inheritance patterns in their secondary metabolism relative to the midparent levels.

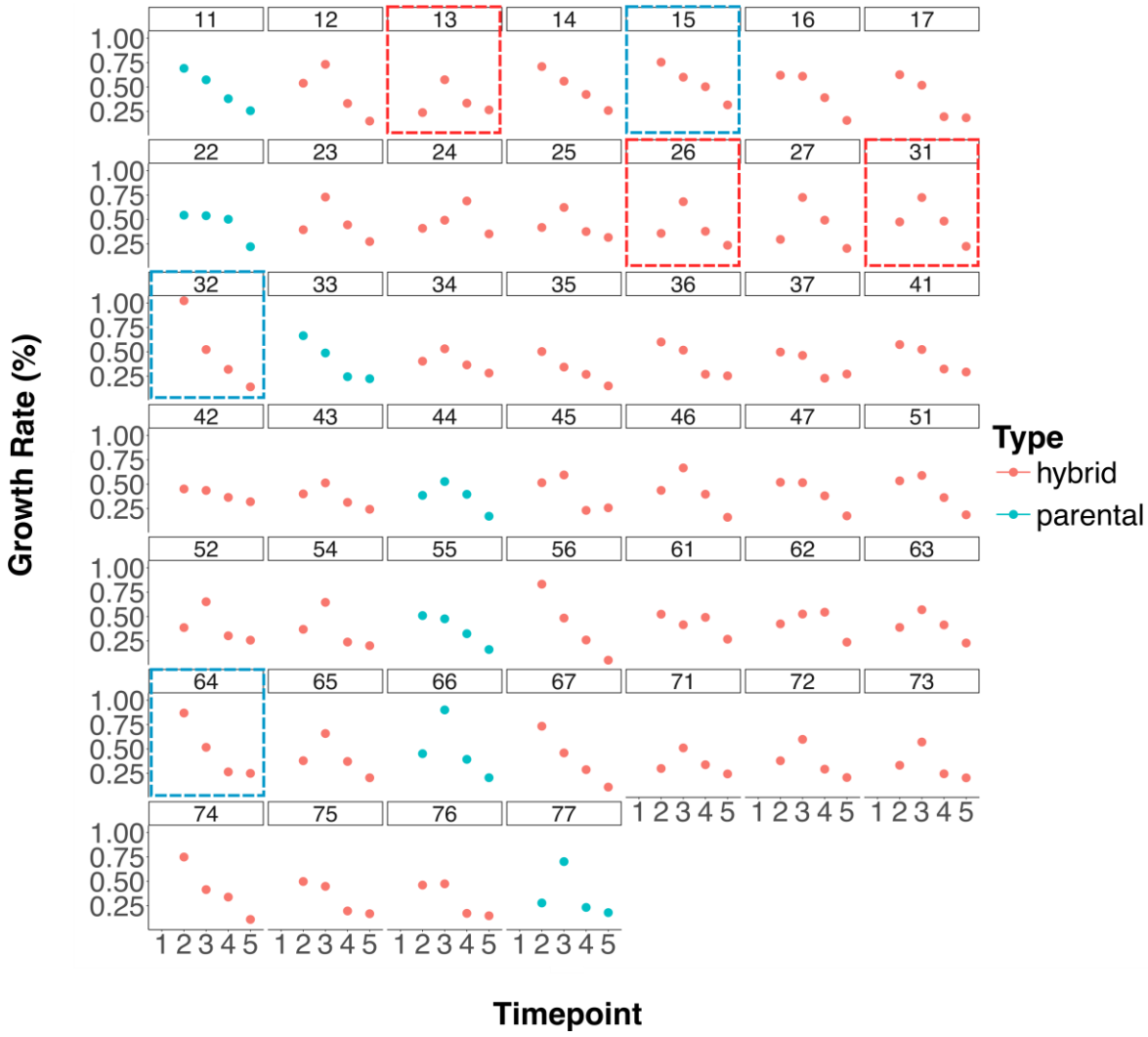

Figure S5. Biggest hybrids display similar growth rate patterns. Percent growth rate per hybrid across all timepoints revealed that the first growth rate was the highest one among larger hybrids (e.g. 15, 32, 64 enclosed in blue boxes). Small hybrids (e.g. 13, 26, 31 enclosed in red boxes) displayed a different growth rate pattern characterized by a pyramid-like arrangement, with a low initial growth rate followed by the highest one. The five timepoints reflect the following developmental stages based on the rosette-leaf number: 2-leaf, 4-leaf, 6-leaf, 8-leaf, and 10-leaf. N = 5 - 8.

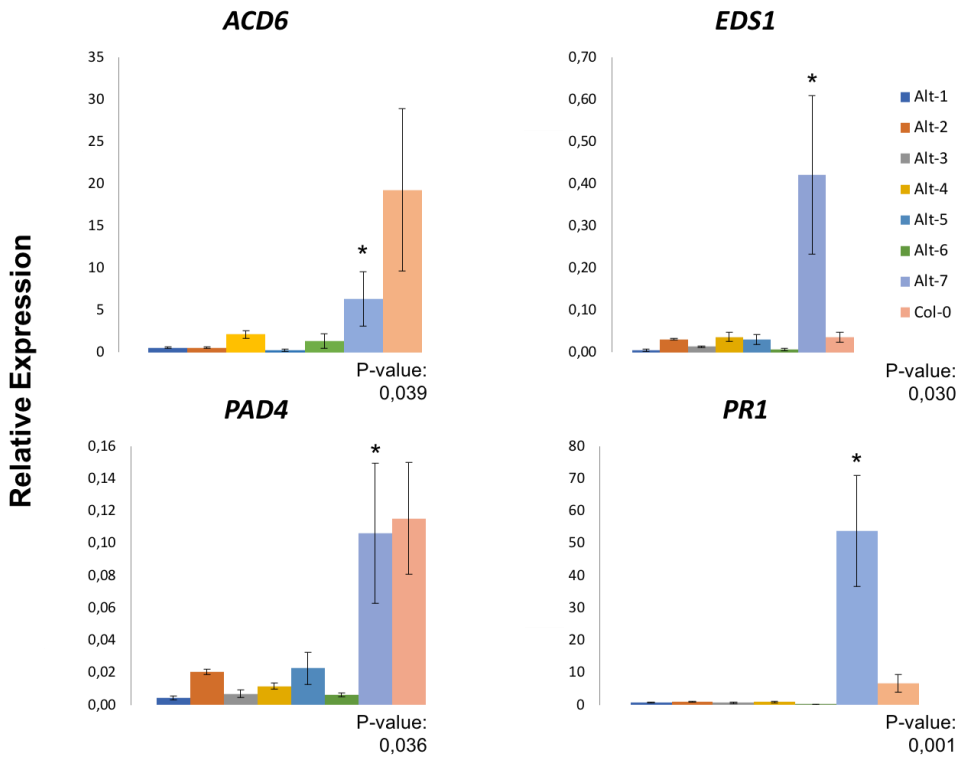

Figure S6. Expression of defense genes was altered in the Alt-7 individual. The expression levels of different defense genes involved in SAR were monitored within the Altenriet individuals collected in Tübingen, Germany. Except for Alt-7, most individuals didn't show any upregulation in any defense marker. The Col-0 accession was taken as reference. Asterisks denote a significant change was detected within the Altenriet group. Test: Kruskal-Wallis. N = 3.

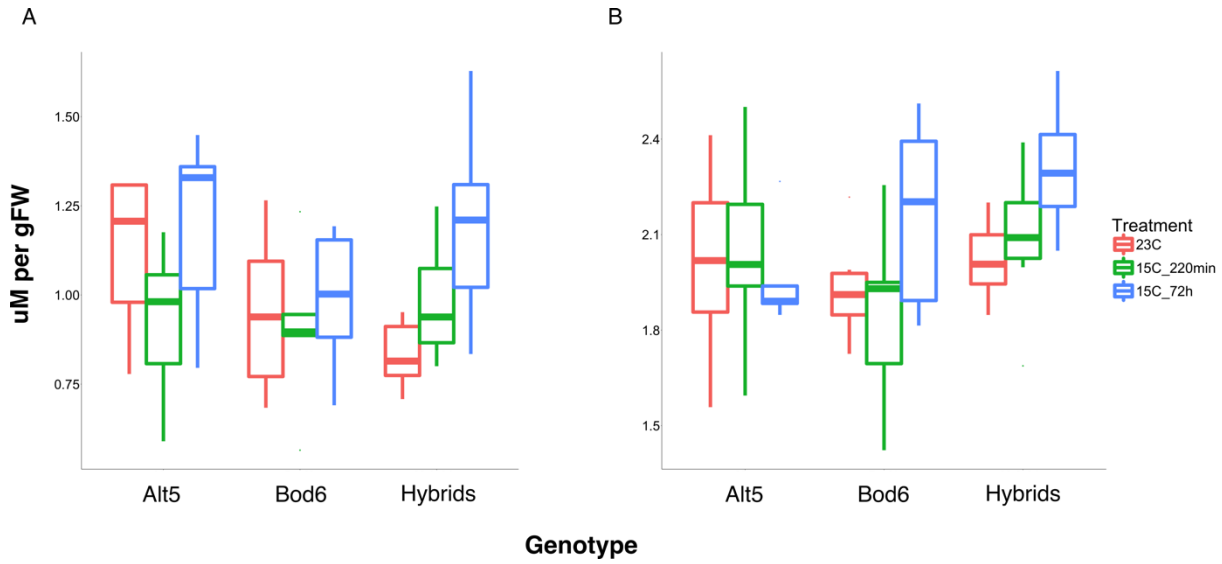

Figure S7. A second ionic measurement experiment corroborated that ammonium and sulfate were not accumulating significantly higher in hybrids than in / relative to parents. As seen before, ammonium (A) and sulfate (B) increased in hybrids due to temperature. However, even though an additional timepoint of 72 hours was added, both ammonium and sulfate failed to reach a significant difference with respect to both parents. A random permutation analysis with 10000 iterations and an alpha of 0.05 was used to identify significance. N = 6.

Figure S8. T3 lines confirmed by microscopy and grown at 17°C. After confirming T3 transgenic lines with GFP-tagged ACD6 constructs by CLSM, three different lines from each construct were grown at constant 17°C. The ACD6 allele used to generate these constructs came from the Alt-5 individual and it was transformed in the Bod-6 genetic background. Therefore, if the GFP-tagged ACD6 was functional, hybrid necrosis should be visible at 17°C. Yet, none of the transgenic plants displayed stunted growth.

7. Bibliography

Abbott, R. J., & Gomes, M. F. (1989). Population genetic structure and outcrossing rate of Arabidopsis thaliana (L) Heynh. *Heredity*, *62*(3), 411–418. https://doi.org/10.1038/hdy.1989.56

Ahn, I.-P. (2007). Glufosinate Ammonium-Induced Pathogen Inhibition and Defense Responses Culminate in Disease Protection in bar-Transgenic Rice. *Plant Physiology*, *146*(1), 213–227. https://doi.org/10.1104/pp.107.105890

Alcazar, R., Garcia, A. V., Parker, J. E., Reymond, M., Alcázar, R., García, A. V, … Reymond, M. (2009). Incremental steps toward incompatibility revealed by Arabidopsis epistatic interactions modulating salicylic acid pathway activation. *Proceedings of the National Academy of Sciences*, *106*(1), 334–339. https://doi.org/10.1073/pnas.0811734106

Alcázar, R., & Parker, J. E. (2011). The impact of temperature on balancing immune responsiveness and growth in Arabidopsis. *Trends in Plant Science*, *16*(12), 666–675. https://doi.org/10.1016/j.tplants.2011.09.001

Alcázar, R., von Reth, M., Bautor, J., Chae, E., Weigel, D., Koornneef, M., & Parker, J. E. (2014). Analysis of a plant complex resistance gene locus underlying immune-related hybrid incompatibility and its occurrence in nature. *PLoS Genetics*, *10*(12), 1–14. https://doi.org/10.1371/journal.pgen.1004848

Allwood, J. W., Erban, A., de Koning, S., Dunn, W. B., Luedemann, A., Lommen, A., … Goodacre, R. (2009). Inter-laboratory reproducibility of fast gas chromatography-electron impact-time of flight mass spectrometry (GC-EI-TOF/MS) based plant metabolomics. *Metabolomics*, *5*(4), 479–496. https://doi.org/10.1007/s11306-009-0169-z

Bakker, E. G., Toomajian, C., Kreitman, M., & Bergelson, J. (2006). A genome-wide survey of R gene polymorphisms in Arabidopsis. *The Plant Cell*, *18*(8), 1803–1818. https://doi.org/10.1105/tpc.106.042614

Bartwal, A., Mall, R., Lohani, P., Guru, S. K., & Arora, S. (2013). Role of Secondary Metabolites and Brassinosteroids in Plant Defense Against Environmental Stresses. *Journal of Plant Growth Regulation*, *32*(1), 216–232. https://doi.org/10.1007/s00344-012-9272-x

Bent, A. F., & Clough, S. J. (1998). Agrobacterium Germ-Line Transformation: Transformation of Arabidopsis without Tissue Culture. In *Plant Molecular Biology Manual* (pp. 17–30). Dordrecht: Springer Netherlands. https://doi.org/10.1007/978-94-011-5242-6_2

Bohrer, A.-S., & Takahashi, H. (2016). Compartmentalization and Regulation of Sulfate Assimilation Pathways in Plants. *International Review of Cell and Molecular Biology*, *326*, 1–31. https://doi.org/10.1016/BS.IRCMB.2016.03.001

Bomblies, K., Lempe, J., Epple, P., Warthmann, N., Lanz, C., Dangl, J. L., & Weigel, D. (2007).

Autoimmune Response as a Mechanism for a Dobzhansky-Muller-Type Incompatibility Syndrome in Plants. *PLoS Biology*, *5*(9), e236. https://doi.org/10.1371/journal.pbio.0050236

Bomblies, K., & Weigel, D. (2007). Hybrid necrosis: Autoimmunity as a potential gene-flow barrier in plant species. *Nature Reviews Genetics*, *8*(5), 382–393. https://doi.org/10.1038/nrg2082

Bomblies, K., Yant, L., Laitinen, R. A., Kim, S.-T., Hollister, J. D., Warthmann, N., … Weigel, D. (2010). Local-Scale Patterns of Genetic Variability, Outcrossing, and Spatial Structure in Natural Stands of Arabidopsis thaliana. *PLoS Genetics*, *6*(3), e1000890. https://doi.org/10.1371/journal.pgen.1000890

Box, M. S., Huang, B. E., Domijan, M., Jaeger, K. E., Khattak, A. K., Yoo, S. J., … Wigge, P. A. (2015). ELF3 controls thermoresponsive growth in Arabidopsis. *Current Biology*, *25*(2), 194–199. https://doi.org/10.1016/j.cub.2014.10.076

Breeze, E., Harrison, E., McHattie, S., Hughes, L., Hickman, R., Hill, C., … Buchanan-Wollaston, V. (2011). High-Resolution Temporal Profiling of Transcripts during Arabidopsis Leaf Senescence Reveals a Distinct Chronology of Processes and Regulation. *The Plant Cell*, *23*(3), 873–894. https://doi.org/10.1105/tpc.111.083345

Brodersen, P., & Petersen, M. (2002). Knockout of Arabidopsis accelerated-cell-death11 encoding a sphingosine transfer protein causes activation of programmed cell death and defense. *Genes & …*. Retrieved from http://genesdev.cshlp.org/content/16/4/490.short

Büttner, D., & Bonas, U. (2010). Regulation and secretion of Xanthomonas virulence factors. *FEMS Microbiology Reviews*, *34*(2), 107–133. https://doi.org/10.1111/j.1574-6976.2009.00192.x

Caldana, C., Li, Y., Leisse, A., Zhang, Y., Bartholomaeus, L., Fernie, A. R., … Giavalisco, P. (2013). Systemic analysis of inducible target of rapamycin mutants reveal a general metabolic switch controlling growth in Arabidopsis thaliana. *Plant Journal*, *73*(6), 897–909. https://doi.org/10.1111/tpj.12080

Chae, E., Bomblies, K., Kim, S.-T., Karelina, D., Zaidem, M., Ossowski, S., … Weigel, D. (2014). Species-wide Genetic Incompatibility Analysis Identifies Immune Genes as Hot Spots of Deleterious Epistasis. *Cell*, *159*(6), 1341–1351. https://doi.org/10.1016/j.cell.2014.10.049

Chae, E., Tran, D. T. N., & Weigel, D. (2016). Cooperation and Conflict in the Plant Immune System. *PLOS Pathogens*, *12*(3), e1005452. https://doi.org/10.1371/journal.ppat.1005452

Chakravarthy, S., Velásquez, A. C., Ekengren, S. K., Collmer, A., & Martin, G. B. (2010). Identification of *Nicotiana benthamiana* Genes Involved in Pathogen-Associated Molecular Pattern–Triggered Immunity. *Molecular Plant-Microbe Interactions*, *23*(6), 715–726. https://doi.org/10.1094/MPMI-23-6-0715

Charlesworth, D., & Willis, J. H. (2009). The genetics of inbreeding depression. *Nature Reviews Genetics*, *10*(11), 783–796. https://doi.org/10.1038/nrg2664

Chen, C., Chen, H., Lin, Y.-S. S., Shen, J.-B. B., Shan, J.-X. X., Qi, P., … Lin, H.-X. X. (2014). A two-locus interaction causes interspecific hybrid weakness in rice. *Nature Communications*, *5*, 3357. https://doi.org/10.1038/ncomms4357

Chen, Z. J. (2013). Genomic and epigenetic insights into the molecular bases of heterosis. *Nature Reviews Genetics*, *14*(7), 471–482. https://doi.org/10.1038/nrg3503

Cheng, D., Vrieling, K., & Klinkhamer, P. G. L. (2011). The effect of hybridization on secondary metabolites and herbivore resistance: Implications for the evolution of chemical diversity in plants. *Phytochemistry Reviews*, *10*(1), 107–117. https://doi.org/10.1007/s11101-010-9194-9

Cheong, Y. H., Kim, K.-N., Pandey, G. K., Gupta, R., Grant, J. J., & Luan, S. (2003). CBL1, a calcium sensor that differentially regulates salt, drought, and cold responses in Arabidopsis. *The Plant Cell*, *15*(8), 1833–1845. https://doi.org/10.1105/tpc.012393

Clark, R. M., Schweikert, G., Toomajian, C., Ossowski, S., Zeller, G., Shinn, P., … Weigel, D. (2007). Common sequence polymorphisms shaping genetic diversity in Arabidopsis thaliana. *Science (New York, N.Y.)*, *317*(5836), 338–342. https://doi.org/10.1126/science.1138632

Corbett-Detig, R. B., Zhou, J., Clark, A. G., Hartl, D. L., & Ayroles, J. F. (2013). Genetic incompatibilities are widespread within species. *Nature*, *504*(7478), 135–137. https://doi.org/10.1038/nature12678

Coyne, J. A., & Orr, H. A. (2004). *Speciation*. Sunderland, MA: Sinauer Associates.

Crespi, B., & Nosil, P. (2013). Conflictual speciation: species formation via genomic conflict. *Trends in Ecology & Evolution*, *28*(1), 48–57. https://doi.org/10.1016/J.TREE.2012.08.015

Cutter, A. D. (2012). The polymorphic prelude to Bateson–Dobzhansky–Muller incompatibilities. *Trends in Ecology & Evolution*, *27*(4), 209–218. https://doi.org/10.1016/J.TREE.2011.11.004

Davenport, C. (1908). Determination of dominance in Mendelian inheritance. *Proceedings of the American Philosophical Society*. Retrieved from http://www.jstor.org/stable/983798

Davenport, C. B. (1908). DEGENERATION, ALBINISM AND INBREEDING. *Science (New York, N.Y.)*, *28*(718), 454–455. https://doi.org/10.1126/science.28.718.454-b

Davila Olivas, N. H., Frago, E., Thoen, M. P. M., Kloth, K. J., Becker, F. F. M., van Loon, J. J. A., … Dicke, M. (2017). Natural variation in life history strategy of *Arabidopsis thaliana* determines stress responses to drought and insects of different feeding guilds. *Molecular Ecology*, *26*(11), 2959–2977. https://doi.org/10.1111/mec.14100

Dethloff, F., Erban, A., Orf, I., Alpers, J., Fehrle, I., Beine-Golovchuk, O., … Kopka, J. (2014). Profiling Methods to Identify Cold-Regulated Primary Metabolites Using Gas Chromatography Coupled to Mass Spectrometry (pp. 171–197). Humana Press, New York, NY. https://doi.org/10.1007/978-1-4939-0844-8_14

Dobzhansky, T. (1937). *Genetics and the Origin of Species*. New York, NY: Columbia Univ Press.

Du, L., Ali, G. S., Simons, K. A., Hou, J., Yang, T., Reddy, A. S. N., & Poovaiah, B. W. (2009). Ca2+/calmodulin regulates salicylic-acid-mediated plant immunity. *Nature*, *457*(7233), 1154–1158. https://doi.org/10.1038/nature07612

Dubousset, L., Abdallah, M., Desfeux, A. S., Etienne, P., Meuriot, F., Hawkesford, M. J., … Avice, J. C. (2009). Remobilization of leaf S compounds and senescence in response to restricted sulphate supply during the vegetative stage of oilseed rape are affected by mineral N availability. *Journal of Experimental Botany*, *60*(11), 3239–3253. https://doi.org/10.1093/jxb/erp172

Eulgem, T. (2005). Regulation of the Arabidopsis defense transcriptome. *Trends in Plant Science*, *10*(2), 71–78. https://doi.org/10.1016/j.tplants.2004.12.006

Eulgem, T., Rushton, P., Robatzek, S., & Somssich, I. (2000). The WRKY superfamily of plant transcription factors. *Trends in Plant Science*. Retrieved from http://www.sciencedirect.com/science/article/pii/S1360138500016009

Eulgem, T., & Somssich, I. E. (2007). Networks of WRKY transcription factors in defense signaling. *Current Opinion in Plant Biology*, *10*(4), 366–371. https://doi.org/10.1016/J.PBI.2007.04.020

Falconer, D. S., & Mackay, T. F. (1996). Introduction to quantitative genetics (4th edn). *Trends in Genetics*, *12*(7), 280.

Feys, B. J. (2005). Arabidopsis SENESCENCE-ASSOCIATED GENE101 Stabilizes and Signals within an ENHANCED DISEASE SUSCEPTIBILITY1 Complex in Plant Innate Immunity. *The Plant Cell Online*, *17*(9), 2601–2613. https://doi.org/10.1105/tpc.105.033910

Finka, A., Cuendet, A. F. H., Maathuis, F. J. M., Saidi, Y., & Goloubinoff, P. (2012). Plasma Membrane Cyclic Nucleotide Gated Calcium Channels Control Land Plant Thermal Sensing and Acquired Thermotolerance. *The Plant Cell*, *24*(8), 3333–3348. https://doi.org/10.1105/tpc.112.095844

Fishman, L., & Sweigart, A. L. (2018). When Two Rights Make a Wrong: The Evolutionary Genetics of Plant Hybrid Incompatibilities. *Https://Doi.Org/10.1146/Annurev-Arplant-042817-040113*, *69*(1), annurev-arplant-042817-040113. https://doi.org/10.1146/annurev-arplant-042817-040113

Fournier-Level, A., Korte, A., Cooper, M. D., Nordborg, M., Schmitt, J., & Wilczek, A. M. (2011). A Map of Local Adaptation in Arabidopsis thaliana. *Science*, *334*(October), 86–89. https://doi.org/10.1126/science.1209271

Francisco, M., Joseph, B., Caligagan, H., Li, B., Corwin, J. A., Lin, C., … Kliebenstein, D. J. (2016). The Defense Metabolite, Allyl Glucosinolate, Modulates Arabidopsis thaliana Biomass Dependent upon the Endogenous Glucosinolate Pathway. *Frontiers in Plant Science*, *7*(June), 1–14. https://doi.org/10.3389/fpls.2016.00774

Fujimoto, R., Taylor, J. M., Shirasawa, S., Peacock, W. J., & Dennis, E. S. (2012). Heterosis of

Arabidopsis hybrids between C24 and Col is associated with increased photosynthesis capacity. *Proceedings of the National Academy of Sciences of the United States of America*, *109*(18), 7109–7114. https://doi.org/10.1073/pnas.1204464109

Fukuda, Y. (1997). Interaction of tobacco nuclear protein with an elicitor-responsive element in the promoter of a basic class I chitinase gene. *Plant Molecular Biology*, *34*(1), 81–87. https://doi.org/10.1023/A:1005737128339

Fukuda, Y., & Shinshi, H. (1994). Characterization of a novel cis-acting element that is responsive to a fungal elicitor in the promoter of a tobacco class I chitinase gene. *Plant Molecular Biology*, *24*(3), 485–493. https://doi.org/10.1007/BF00024116

Gangappa, S. N., Berriri, S., & Kumar, S. V. (2017). PIF4 Coordinates Thermosensory Growth and Immunity in Arabidopsis. *Current Biology*, *27*(2), 243–249. https://doi.org/10.1016/j.cub.2016.11.012

Genoud, T., Buchala, A. J., Chua, N.-H., & Métraux, J.-P. (2002). Phytochrome signalling modulates the SA-perceptive pathway in *Arabidopsis*. *The Plant Journal*, *31*(1), 87–95. https://doi.org/10.1046/j.1365-313X.2002.01338.x

Gill, S. S., & Tuteja, N. (2010). Polyamines and abiotic stress tolerance in plants. *Plant Signaling & Behavior*, *5*(1), 26–33. https://doi.org/10.4161/psb.5.1.10291

Göhre, V., & Robatzek, S. (2008). Breaking the Barriers: Microbial Effector Molecules Subvert Plant Immunity. *Annual Review of Phytopathology*, *46*(1), 189–215. https://doi.org/10.1146/annurev.phyto.46.120407.110050

Grefen, C., Donald, N., Hashimoto, K., Kudla, J., Schumacher, K., & Blatt, M. R. (2010). A ubiquitin-10 promoter-based vector set for fluorescent protein tagging facilitates temporal stability and native protein distribution in transient and stable expression studies. *Plant Journal*, *64*(2), 355–365. https://doi.org/10.1111/j.1365-313X.2010.04322.x

Guiboileau, A., Sormani, R., Meyer, C., & Masclaux-Daubresse, C. (2010). Senescence and death of plant organs: Nutrient recycling and developmental regulation. *Comptes Rendus Biologies*, *333*(4), 382–391. https://doi.org/10.1016/j.crvi.2010.01.016

Hara, K., Yagi, M., Kusano, T., & Sano, H. (2000). Rapid systemic accumulation of transcripts encoding a tobacco WRKY transcription factor upon wounding. *MGG - Molecular and General Genetics*, *263*(1), 30–37. https://doi.org/10.1007/PL00008673

Hedrick, P. W. (2006). Genetic Polymorphism in Heterogeneous Environments: The Age of Genomics. *Annual Review of Ecology, Evolution, and Systematics*, *37*(1), 67–93. https://doi.org/10.1146/annurev.ecolsys.37.091305.110132

Hereford, J. (2009). A Quantitative Survey of Local Adaptation and Fitness Trade-Offs. *The American Naturalist*, *173*(5), 579–588. https://doi.org/10.1086/597611

Hoffmann, M. H. (2002). Biogeography of Arabidopsis thaliana (L.) Heynh. (Brassicaceae). *Journal of Biogeography*, *29*(1), 125–134. https://doi.org/10.1046/j.1365-2699.2002.00647.x

Hou, J., Friedrich, A., de Montigny, J., & Schacherer, J. (2014). Chromosomal Rearrangements as a Major Mechanism in the Onset of Reproductive Isolation in Saccharomyces cerevisiae. *Current Biology*, *24*(10), 1153–1159. https://doi.org/10.1016/J.CUB.2014.03.063

Hull, F. H. (1945). Recurrent Selection for Specific Combining Ability in Corn1. *Agronomy Journal*, *37*(2), 134. https://doi.org/10.2134/agronj1945.00021962003700020006x

Joseph, B., Corwin, J. A., Züst, T., Li, B., Iravani, M., Schaepman-Strub, G., … Kliebenstein, D. J. (2013). Hierarchical Nuclear and Cytoplasmic Genetic Architectures for Plant Growth and Defense within Arabidopsis. *The Plant Cell*, *25*(6), 1929–1945. https://doi.org/10.1105/tpc.113.112615

Kang, G. Z., Li, G. Z., Liu, G. Q., Xu, W., Peng, X. Q., Wang, C. Y., … Guo, T. C. (2013). Exogenous salicylic acid enhances wheat drought tolerance by influence on the expression of genes related to ascorbate-glutathione cycle. *Biologia Plantarum*, *57*(4), 718–724. https://doi.org/10.1007/s10535-013-0335-z

Kay, S., & Bonas, U. (2009). How Xanthomonas type III effectors manipulate the host plant. *Current Opinion in Microbiology*, *12*(1), 37–43. https://doi.org/10.1016/j.mib.2008.12.006

Kerepesi, I., & Galiba, G. (2000). Osmotic and Salt Stress-Induced Alteration in Soluble Carbohydrate Content in Wheat Seedlings. *Crop Science*, *40*(2), 482. https://doi.org/10.2135/cropsci2000.402482x

Khan, N., Syeed, S., Masood, A., Nazar, R., & Iqbal, N. (2010). Application of salicylic acid increases contents of nutrients and antioxidative metabolism in mungbean and alleviates adverse effects of salinity stress. *International Journal of Plant Biology*, *1*(1), 1. https://doi.org/10.4081/pb.2010.e1

Kim, K.-N., Cheong, Y. H., Grant, J. J., Pandey, G. K., & Luan, S. (2003). CIPK3 , a calcium sensor – associated protein kinase that regulates abscisic acid and cold signal transduction in Arabidopsis. *The Plant Cell*, *15*(February), 411–423. https://doi.org/10.1105/tpc.006858.2

Kliebenstein, D. J. (2016). False idolatry of the mythical growth versus immunity tradeoff in molecular systems plant pathology. *Physiological and Molecular Plant Pathology*, *95*, 55–59. https://doi.org/10.1016/j.pmpp.2016.02.004

Kliebenstein, D., Kroymann, J., Brown, P., & Figuth, A. (2001). Genetic control of natural variation in Arabidopsis glucosinolate accumulation. *Plant*. Retrieved from http://www.plantphysiol.org/content/126/2/811.short

Koebnik, R., Krüger, A., Thieme, F., Urban, A., & Bonas, U. (2006). Specific binding of the Xanthomonas campestris pv. vesicatoria AraC-type transcriptional activator HrpX to plant-inducible promoter boxes. *Journal of Bacteriology*, *188*(21), 7652–7660.

https://doi.org/10.1128/JB.00795-06

Koornneef, M., Alonso-Blanco, C., & Vreugdenhil, D. (2004). NATURALLY OCCURRING GENETIC VARIATION IN *ARABIDOPSIS THALIANA*. *Annual Review of Plant Biology*, *55*(1), 141–172. https://doi.org/10.1146/annurev.arplant.55.031903.141605

Korn, M., Gärtner, T., Erban, A., Kopka, J., Selbig, J., & Hincha, D. K. (2010). Predicting arabidopsis freezing tolerance and heterosis in freezing tolerance from metabolite composition. *Molecular Plant*, *3*(1), 224–235. https://doi.org/10.1093/mp/ssp105

Krebs, M., Held, K., Binder, A., Hashimoto, K., Den Herder, G., Parniske, M., … Schumacher, K. (2012). FRET-based genetically encoded sensors allow high-resolution live cell imaging of Ca2+ dynamics. *Plant Journal*, *69*(1), 181–192. https://doi.org/10.1111/j.1365-313X.2011.04780.x

Kroymann, J. (2011). Natural diversity and adaptation in plant secondary metabolism. *Current Opinion in Plant Biology*, *14*(3), 246–251. https://doi.org/10.1016/j.pbi.2011.03.021

Lachance, J., & True, J. R. (2010). X-AUTOSOME INCOMPATIBILITIES IN DROSOPHILA MELANOGASTER: TESTS OF HALDANE'S RULE AND GEOGRAPHIC PATTERNS WITHIN SPECIES. *Evolution*, *64*(10), no-no. https://doi.org/10.1111/j.1558-5646.2010.01028.x

Leonelli, S. (2007). Arabidopsis, the botanical Drosophila: from mouse cress to model organism. *Endeavour*, *31*(1), 34–38. https://doi.org/10.1016/j.endeavour.2007.01.003

Li, R.-F., Lu, G.-T., Li, L., Su, H.-Z., Feng, G.-F., Chen, Y., … Tang, J.-L. (2013). Identification of a putative cognate sensor kinase for the two-component response regulator HrpG, a key regulator controlling the expression of the hrp genes in Xanthomonas campestris pv. campestris. *Environmental Microbiology*. https://doi.org/10.1111/1462-2920.12207

Lisec, J., Römisch-Margl, L., Nikoloski, Z., Piepho, H. P., Giavalisco, P., Selbig, J., … Willmitzer, L. (2011). Corn hybrids display lower metabolite variability and complex metabolite inheritance patterns. *Plant Journal*, *68*(2), 326–336. https://doi.org/10.1111/j.1365-313X.2011.04689.x

Lisec, J., Schauer, N., Kopka, J., Willmitzer, L., & Fernie, A. R. (2006). Gas chromatography mass spectrometry–based metabolite profiling in plants. *Nature Protocols*, *1*(1), 387–396. https://doi.org/10.1038/nprot.2006.59

Liu, J. X., & Howell, S. H. (2010). bZIP28 and NF-Y Transcription Factors Are Activated by ER Stress and Assemble into a Transcriptional Complex to Regulate Stress Response Genes in Arabidopsis. *The Plant Cell*, *22*(3), 782–796. https://doi.org/10.1105/tpc.109.072173

Lodha, T. D., & Basak, J. (2012). Plant–Pathogen Interactions: What Microarray Tells About It? *Molecular Biotechnology*, *50*(1), 87–97. https://doi.org/10.1007/s12033-011-9418-2

Lu, H., Liu, Y., & Greenberg, J. T. (2005). Structure-function analysis of the plasma membrane-localized Arabidopsis defense component ACD6. *Plant Journal*, *44*(5), 798–809.

https://doi.org/10.1111/j.1365-313X.2005.02567.x

Lu, H., Rate, D. N., Song, J. T., & Greenberg, J. T. (2003). ACD6, a Novel Ankyrin Protein, Is a Regulator and an Effector of Salicylic Acid Signaling in the Arabidopsis Defense Response. *The Plant Cell Online*, *15*(10), 2408–2420. https://doi.org/10.1105/tpc.015412

Lu, H., Salimian, S., Gamelin, E., Wang, G., Fedorowski, J., LaCourse, W., & Greenberg, J. T. (2009). Genetic analysis of acd6-1 reveals complex defense networks and leads to identification of novel defense genes in Arabidopsis. *The Plant Journal : For Cell and Molecular Biology*, *58*(3), 401–412. https://doi.org/10.1111/j.1365-313X.2009.03791.x

Luedemann, A., Strassburg, K., Erban, A., & Kopka, J. (2008). TagFinder for the quantitative analysis of gas chromatography - Mass spectrometry (GC-MS)-based metabolite profiling experiments. *Bioinformatics*, *24*(5), 732–737. https://doi.org/10.1093/bioinformatics/btn023

Mable, B. K., & Adam, A. (2007). Patterns of genetic diversity in outcrossing and selfing populations of Arabidopsis lyrata. *Molecular Ecology*, *16*(17), 3565–3580. https://doi.org/10.1111/j.1365-294X.2007.03416.x

Maheshwari, S., & Barbash, D. A. (2011). The Genetics of Hybrid Incompatibilities. *Annual Review of Genetics*, *45*(1), 331–355. https://doi.org/10.1146/annurev-genet-110410-132514

Maiti, S., Basak, J., & Pal, A. (2014). Current Understanding on Plant R-Genes/Proteins and Mechanisms of Defense Responses Against Biotic Stresses, *6*.

Manzaneda, A., & Prasad, K. (2010). Variation and fitness costs for tolerance to different types of herbivore damage in Boechera stricta genotypes with contrasting glucosinolate structures. *New Phytologist*. Retrieved from http://onlinelibrary.wiley.com/doi/10.1111/j.1469-8137.2010.03385.x/full

Mauricio, R. (1998). Costs of resistance to natural enemies in field populations of the annual plant Arabidopsis thaliana. *The American Naturalist*, *151*(1), 20–28. https://doi.org/10.1086/286099

Meyer, R. C., Steinfath, M., Lisec, J., Becher, M., Witucka-Wall, H., Torjek, O., … Altmann, T. (2007). The metabolic signature related to high plant growth rate in Arabidopsis thaliana. *Proceedings of the National Academy of Sciences*, *104*(11), 4759–4764. https://doi.org/10.1073/pnas.0609709104

Meyer, R. C., Witucka-Wall, H., Becher, M., Blacha, A., Boudichevskaia, A., Dörmann, P., … Altmann, T. (2012). Heterosis manifestation during early Arabidopsis seedling development is characterized by intermediate gene expression and enhanced metabolic activity in the hybrids. *The Plant Journal*, *71*(4), 669–683. https://doi.org/10.1111/j.1365-313X.2012.05021.x

Miao, Y., Laun, T., Zimmermann, P., & Zentgraf, U. (2004). Targets of the WRKY53 transcription factor and its role during leaf senescence in Arabidopsis. *Plant Molecular Biology*, *55*(6), 853–867. https://doi.org/10.1007/s11103-005-2142-1

Miura, K., Okamoto, H., Okuma, E., Shiba, H., Kamada, H., Hasegawa, P. M., & Murata, Y. (2013). SIZ1 deficiency causes reduced stomatal aperture and enhanced drought tolerance via controlling salicylic acid-induced accumulation of reactive oxygen species in Arabidopsis. *Plant Journal*, *73*(1), 91–104. https://doi.org/10.1111/tpj.12014

Miura, K., & Tada, Y. (2014). Regulation of water, salinity, and cold stress responses by salicylic acid. *Frontiers in Plant Science*, *5*(January), 1–12. https://doi.org/10.3389/fpls.2014.00004

Morris, K., MacKerness, S. a, Page, T., John, C. F., Murphy, a M., Carr, J. P., & Buchanan-Wollaston, V. (2000). Salicylic acid has a role in regulating gene expression during leaf senescence. *The Plant Journal : For Cell and Molecular Biology*, *23*(5), 677–685. https://doi.org/10.1046/j.1365-313x.2000.00836.x

Morrison, J. W. (1957). Dwarfs, semi-lethals and lethals in wheat. *Euphytica*, *6*(3), 213–223. https://doi.org/10.1007/BF00042303

Muller, H. (1942). Isolating mechanisms, evolution, and temperature. *Biol Symp*, *6*, 71–124.

Nazar, R., Iqbal, N., Syeed, S., & Khan, N. A. (2011). Salicylic acid alleviates decreases in photosynthesis under salt stress by enhancing nitrogen and sulfur assimilation and antioxidant metabolism differentially in two mungbean cultivars. *Journal of Plant Physiology*, *168*(8), 807–815. https://doi.org/10.1016/J.JPLPH.2010.11.001

Nelson, D. E., Repetti, P. P., Adams, T. R., Creelman, R. A., Wu, J., Warner, D. C., … Heard, J. E. (2007). Plant nuclear factor Y (NF-Y) B subunits confer drought tolerance and lead to improved corn yields on water-limited acres. *Proceedings of the National Academy of Sciences of the United States of America*, *104*(42), 16450–16455. https://doi.org/10.1073/pnas.0707193104

Ng, D. W.-K., Lu, J., & Chen, Z. J. (2012). Big roles for small RNAs in polyploidy, hybrid vigor, and hybrid incompatibility. *Current Opinion in Plant Biology*, *15*(2), 154–161. https://doi.org/10.1016/J.PBI.2012.01.007

Noel, L. (1999). Pronounced intraspecific haplotype divergence at the RPP8 complex disease resistance locus of Arabidopsis. *Plant Cell*, *11*(November), 2099–2111.

Nomura, H., Komori, T., Uemura, S., Kanda, Y., Shimotani, K., Nakai, K., … Shiina, T. (2012). Chloroplast-mediated activation of plant immune signalling in Arabidopsis. *Nature Communications*, *3*(May), 910–926. https://doi.org/10.1038/ncomms1926

Noreen, S., & Ashraf, M. (2010). Modulation of salt (NaCl)-induced effects on oil composition and fatty acid profile of sunflower (Helianthus annuus L.) by exogenous application of salicylic acid. *Journal of the Science of Food and Agriculture*, *90*(15), 2608–2616. https://doi.org/10.1002/jsfa.4129

Nuccio, M. L., Wu, J., Mowers, R., Zhou, H. P., Meghji, M., Primavesi, L. F., … Lagrimini, L. M. (2015). Expression of trehalose-6-phosphate phosphatase in maize ears improves yield in well-watered

and drought conditions. *Nature Biotechnology*, *33*(8), 862–869. https://doi.org/10.1038/nbt.3277

Okuma, E., Nozawa, R., Murata, Y., & Miura, K. (2014). Accumulation of endogenous salicylic acid confers drought tolerance to Arabidopsis. *Plant Signaling and Behavior*, *9*(MAR). https://doi.org/10.4161/psb.28085

Paschalidis, K. A., Roubelakis-Angelakis, K. A., Perez-Amador, M. A., & Carbonell, J. (2005). Spatial and temporal distribution of polyamine levels and polyamine anabolism in different organs/tissues of the tobacco plant. Correlations with age, cell division/expansion, and differentiation. *Plant Physiology*, *138*(1), 142–152. https://doi.org/10.1104/pp.104.055483

Patel, K. R., Andreadi, C., Britton, R. G., Horner-Glister, E., Karmokar, A., Sale, S., … Brown, K. (2013). Sulfate metabolites provide an intracellular pool for resveratrol generation and induce autophagy with senescence. *Science Translational Medicine*, *5*(205), 205ra133. https://doi.org/10.1126/scitranslmed.3005870

Paul-Victor, C., Züst, T., Rees, M., Kliebenstein, D. J., & Turnbull, L. A. (2010). A new method for measuring relative growth rate can uncover the costs of defensive compounds in Arabidopsis thaliana. *New Phytologist*, *187*(4), 1102–1111. https://doi.org/10.1111/j.1469-8137.2010.03325.x

Piffanelli, P., Zhou, F., & Casais, C. (2002). The barley MLO modulator of defense and cell death is responsive to biotic and abiotic stress stimuli. *Plant* …. Retrieved from http://www.plantphysiol.org/content/129/3/1076.short

Pilon-Smits, E. A. H., Terry, N., Sears, T., Kim, H., Zayed, A., Hwang, S., … Goddijn, O. J. M. (1998). Trehalose-producing transgenic tobacco plants show improved growth performance under drought stress. *Journal of Plant Physiology*, *152*(4–5), 525–532. https://doi.org/10.1016/S0176-1617(98)80273-3

Platt, A., Horton, M., Huang, Y. S., Li, Y., Anastasio, A. E., Mulyati, N. W., … Borevitz, J. O. (2010). The scale of population structure in Arabidopsis thaliana. *PLoS Genetics*, *6*(2). https://doi.org/10.1371/journal.pgen.1000843

Pombo, M. A., Zheng, Y., Fernandez-Pozo, N., Dunham, D. M., Fei, Z., & Martin, G. B. (2014). Transcriptomic analysis reveals tomato genes whose expression is induced specifically during effector-triggered immunity and identifies the Epk1 protein kinase which is required for the host response to three bacterial effector proteins. *Genome Biology*, *15*(10), 492. https://doi.org/10.1186/s13059-014-0492-1

Presgraves, D. C. (2010). The molecular evolutionary basis of species formation. *Nature Reviews Genetics*, *11*(3), 175–180. https://doi.org/10.1038/nrg2718

Pukhalskiy, V. A., Martynov, S. P., & Dobrotvorskaya, T. V. (2000). Analysis of geographical and breeding-related distribution of hybrid necrosis genes in bread wheat (Triticum aestivum L.). *Euphytica*, *114*(3), 233–240. https://doi.org/10.1023/A:1003915708448

Quirino, B. F., Normanly, J., & Amasino, R. M. (1999). Diverse range of gene activity during Arabidopsis thaliana leaf senescence includes pathogen-independent induction of defense-related genes. *Plant Molecular Biology*, *40*(2), 267–278. https://doi.org/10.1023/A:1006199932265

Radhakrishnan, R., & Lee, I.-J. (2013). Regulation of salicylic acid, jasmonic acid and fatty acids in cucumber (Cucumis sativus L.) by spermidine promotes plant growth against salt stress. *Acta Physiologiae Plantarum*, *35*(12), 3315–3322. https://doi.org/10.1007/s11738-013-1364-0

Rate, D. N., Cuenca, J. V, Bowman, G. R., Guttman, D. S., & Greenberg, J. T. (1999). The Gain-of-Function Arabidopsis acd6 Mutant Reveals Novel Regulation and Function of the Salicylic Acid Signaling Pathway in Controlling Cell Death, Defenses, and Cell Growth. *The Plant Cell Online*, *11*(9), 1695–1708. https://doi.org/10.1105/tpc.11.9.1695

Riedelsheimer, C., Czedik-Eysenberg, A., Grieder, C., Lisec, J., Technow, F., Sulpice, R., … Melchinger, A. E. (2012). Genomic and metabolic prediction of complex heterotic traits in hybrid maize. *Nature Genetics*, *44*(2), 217–220. https://doi.org/10.1038/ng.1033

Rieseberg, L. H., & Blackman, B. K. (2010). Speciation genes in plants. *Annals of Botany*, *106*(3), 439–455. https://doi.org/10.1093/aob/mcq126

Robatzek, S., & Somssich, I. (2002). Targets of AtWRKY6 regulation during plant senescence and pathogen defense. *Genes & Development*, 1139–1149. Retrieved from http://genesdev.cshlp.org/content/16/9/1139.short

Robatzek, S., & Somssich, I. E. (2001). A new member of the Arabidopsis WRKY transcription factor family, AtWRKY6, is associated with both senescence-and defence-related processes. *Plant Journal*, *28*(2), 123–133. https://doi.org/10.1046/j.1365-313X.2001.01131.x

Rushton, P. J., & Somssich, I. E. (1998). Transcriptional control of plant genes responsive to pathogens. *Current Opinion in Plant Biology*, *1*(4), 311–315. https://doi.org/10.1016/1369-5266(88)80052-9

Rushton, P. J., Torres, J. T., Parniske, M., Wernert, P., Hahlbrock, K., & Somssich, I. E. (1996). Interaction of elicitor-induced DNA-binding proteins with elicitor response elements in the promoters of parsley PR1 genes. *The EMBO Journal*, *15*(20), 5690–5700. https://doi.org/10.1002/J.1460-2075.1996.TB00953.X

Sadava, D., Hillis, D., Heller, C., & Hacker, S. (2017). *Life: The Science of Biology (11th Edition)*. *WH Freeman and Company* (11th ed.). Sinauer Associates & Macmillan Learning. Retrieved from https://scholar.google.de/scholar?as_q=Life+Science+Biology&as_epq=&as_oq=&as_eq=&as_occt=title&as_sauthors=Sadava&as_publication=&as_ylo=2015&as_yhi=2018&hl=en&as_sdt=0%2C5

Santoni, V. (2007). Plant Plasma Membrane Protein Extraction and Solubilization for Proteomic

Analysis. In *Plant Proteomics* (pp. 93–110). New Jersey: Humana Press. https://doi.org/10.1385/1-59745-227-0:93

Sasaki, M., Takahashi, K., Haneda, Y., Satoh, H., Sasaki, A., Narumi, A., … Kaga, H. (2008). Thermochemical transformation of glucose to 1,6-anhydroglucose in high-temperature steam. *Carbohydrate Research*, *343*(5), 848–854. https://doi.org/10.1016/J.CARRES.2008.02.005

Sawada, H., Shim, I.-S., & Usui, K. (2006). Induction of benzoic acid 2-hydroxylase and salicylic acid biosynthesis—Modulation by salt stress in rice seedlings. *Plant Science*, *171*(2), 263–270. https://doi.org/10.1016/J.PLANTSCI.2006.03.020

Schauer, N., Steinhauser, D., Strelkov, S., Schomburg, D., Allison, G., Moritz, T., … Kopka, J. (2005). GC-MS libraries for the rapid identification of metabolites in complex biological samples. *FEBS Letters*, *579*(6), 1332–1337. https://doi.org/10.1016/j.febslet.2005.01.029

Schmutz, D., Wyss, H.-R., & Brunold, C. (1983). Activity of Sulfate-assimilating Enzymes in Primary Leaves of Phaseolus vulgaris L. During Dark-induced Senescence. *Zeitschrift Für Pflanzenphysiologie*, *110*(3), 211–219. https://doi.org/10.1016/S0044-328X(83)80103-2

Schranz, M., Manzaneda, A., Windsor, A., & Clauss, M. (2009). Ecological genomics of Boechera stricta: identification of a QTL controlling the allocation of methionine-vs branched-chain amino acid-derived glucosinolates and. *Heredity*. Retrieved from http://www.nature.com/hdy/journal/v102/n5/abs/hdy200912a.html

Schwartz, D., & Laughner, W. J. (1969). A molecular basis for heterosis. *Science (New York, N.Y.)*, *166*(3905), 626–627. https://doi.org/10.1126/science.166.3905.626

Seidel, H. S., Rockman, M. V, & Kruglyak, L. (2008). Widespread genetic incompatibility in C. elegans maintained by balancing selection. *Science (New York, N.Y.)*, *319*(5863), 589–594. https://doi.org/10.1126/science.1151107

Seymour, D., Chae, E., & Grimm, D. (2016). Genetic architecture of nonadditive inheritance in Arabidopsis thaliana hybrids. *Proceedings of The*. Retrieved from http://www.pnas.org/content/113/46/E7317.short

Shah, J. (2003). The salicylic acid loop in plant defense. *Current Opinion in Plant Biology*, *6*(4), 365–371. https://doi.org/10.1016/S1369-5266(03)00058-X

Sharp, N. P., & Agrawal, A. F. (2016). The decline in fitness with inbreeding: evidence for negative dominance-by-dominance epistasis in *Drosophila melanogaster*. *Journal of Evolutionary Biology*, *29*(4), 857–864. https://doi.org/10.1111/jeb.12815

Shu, L., Lou, Q., Ma, C., Ding, W., Zhou, J., Wu, J., … Mei, H. (2011). Genetic, proteomic and metabolic analysis of the regulation of energy storage in rice seedlings in response to drought. *PROTEOMICS*, *11*(21), 4122–4138. https://doi.org/10.1002/pmic.201000485

Steventon, L., Okori, P., & Dixelius, C. (2001). An investigation of the susceptibility of Arabidopsis thaliana to isolates of two species of Verticillium. *Journal of Phytopathology*. Retrieved from http://onlinelibrary.wiley.com/doi/10.1111/j.1439-0434.2001.tb03869.x/abstract

Stitt, M. (2013). Systems-integration of plant metabolism: means, motive and opportunity. *Current Opinion in Plant Biology*, *16*(3), 381–388. https://doi.org/10.1016/J.PBI.2013.02.012

Sulpice, R., Pyl, E.-T. T., Ishihara, H., Trenkamp, S., Steinfath, M., Witucka-Wall, H., … Stitt, M. (2009). Starch as a major integrator in the regulation of plant growth. *Proceedings of the National Academy of Sciences*, *106*(25), 10348–10353. https://doi.org/10.1073/pnas.0903478106

Świadek, M., Proost, S., Sieh, D., Yu, J., Todesco, M., Jorzig, C., … Laitinen, R. A. E. E. (2017). Novel allelic variants in ACD6 cause hybrid necrosis in local collection of Arabidopsis thaliana. *New Phytologist*, *213*(2), 900–915. https://doi.org/10.1111/nph.14155

Tateda, C., Zhang, Z., Shrestha, J., Jelenska, J., Chinchilla, D., & Greenberg, J. T. (2014). Salicylic Acid Regulates Arabidopsis Microbial Pattern Receptor Kinase Levels and Signaling. *The Plant Cell*, *26*(10), 4171–4187. https://doi.org/10.1105/tpc.114.131938

The 1001 Genomes Consortium, Alonso-Blanco, C., Andrade, J., Becker, C., Bemm, F., Bergelson, J., … Zhou, X. (2016). 1,135 Genomes Reveal the Global Pattern of Polymorphism in Arabidopsis thaliana. *Cell*, *166*(2), 481–491. https://doi.org/10.1016/j.cell.2016.05.063

Todesco, M., Balasubramanian, S., Hu, T. T., Traw, M. B., Horton, M., Epple, P., … Weigel, D. (2010). Natural allelic variation underlying a major fitness trade-off in Arabidopsis thaliana. *Nature*, *465*(7298), 632–636. https://doi.org/10.1038/nature09083

Todesco, M., Kim, S.-T. T., Chae, E., Bomblies, K., Zaidem, M., Smith, L. M., … Laitinen, R. A. E. E. (2014). Activation of the Arabidopsis thaliana Immune System by Combinations of Common ACD6 Alleles. *PLoS Genetics*, *10*(7), e1004459. https://doi.org/10.1371/journal.pgen.1004459

Tohge, T., & Fernie, A. R. (2010). Combining genetic diversity, informatics and metabolomics to facilitate annotation of plant gene function. *Nature Protocols*, *5*(6), 1210–1227. https://doi.org/10.1038/nprot.2010.82

Trontin, C., Tisné, S., Bach, L., & Loudet, O. (2011). What does Arabidopsis natural variation teach us (and does not teach us) about adaptation in plants? *Current Opinion in Plant Biology*, *14*(3), 225–231. https://doi.org/10.1016/j.pbi.2011.03.024

Ülker, B., & Somssich, I. E. (2004). WRKY transcription factors: from DNA binding towards biological function. *Current Opinion in Plant Biology*, *7*(5), 491–498. https://doi.org/10.1016/J.PBI.2004.07.012

Van der Hoorn, R. A. ., De Wit, P. J. G. ., & Joosten, M. H. A. . (2002). Balancing selection favors guarding resistance proteins. *Trends in Plant Science*, *7*(2), 67–71. https://doi.org/10.1016/S1360-1385(01)02188-4

Veronese, P., & Narasimhan, M. (2003). Identification of a locus controlling Verticillium disease symptom response in Arabidopsis thaliana. *The Plant* …. Retrieved from http://onlinelibrary.wiley.com/doi/10.1046/j.1365-313X.2003.01830.x/pdf

Vogelmann, K., Drechsel, G., Bergler, J., Subert, C., Philippar, K., Soll, J., … Hoth, S. (2012). Early Senescence and Cell Death in Arabidopsis saul1 Mutants Involves the PAD4-Dependent Salicylic Acid Pathway. *Plant Physiology*, *159*(4), 1477–1487. https://doi.org/10.1104/pp.112.196220

Wang, G.-F., Seabolt, S., Hamdoun, S., Ng, G., Park, J., & Lu, H. (2011). Multiple Roles of WIN3 in Regulating Disease Resistance, Cell Death, and Flowering Time in Arabidopsis. *Plant Physiology*, *156*(3), 1508–1519. https://doi.org/10.1104/pp.111.176776

Wang, Y., Bao, Z., Zhu, Y., & Hua, J. (2009). Analysis of Temperature Modulation of Plant Defense Against Biotrophic Microbes. *Molecular Plant-Microbe Interactions*, *22*(5), 498–506. https://doi.org/10.1094/MPMI-22-5-0498

Wang, Z., Yang, P., Fan, B., & Chen, Z. (1998). An oligo selection procedure for identification of sequence-specific DNA-binding activities associated with the plant defence response. *The Plant Journal*, *16*(4), 515–522. https://doi.org/10.1046/j.1365-313x.1998.00311.x

Weaver, L. M., Gan, S., Quirino, B., & Amasino, R. M. (1998). A comparison of the expression patterns of several senescence-associated genes in response to stress and hormone treatment. *Plant Molecular Biology*, *37*(3), 455–469. https://doi.org/10.1023/A:1005934428906

Weigel, D. (2012). Natural Variation in Arabidopsis: From Molecular Genetics to Ecological Genomics. *Plant Physiology*, *158*(1), 2–22. https://doi.org/10.1104/pp.111.189845

Wengelnik, K. A. I., & Bonas, U. (1996). HrpXv , an AraC-type regulator, activates expression of five of the six loci in the hrp cluster of Xanthomonas campestris pv. vesicatoria. *Journal of Bacteriology*, *178*(12).

Wengelnik, K., Van den Ackerveken, G., & Bonas, U. (1996). HrpG, a key hrp regulatory protein of Xanthomonas campestris pv. vesicatoria is homologous to two-component response regulators. *Molecular Plant-Microbe Interactions : MPMI*, *9*(8), 704–712.

Wenkel, S., Turck, F., Singer, K., Gissot, L., Le Gourrierec, J., Samach, A., & Coupland, G. (2006). CONSTANS and the CCAAT Box Binding Complex Share a Functionally Important Domain and Interact to Regulate Flowering of Arabidopsis. *The Plant Cell Online*, *18*(11), 2971–2984. https://doi.org/10.1105/tpc.106.043299

Windsor, A., Reichelt, M., Figuth, A., & Svatoš, A. (2005). Geographic and evolutionary diversification of glucosinolates among near relatives of Arabidopsis thaliana (Brassicaceae). *Phytochemistry*. Retrieved from http://www.sciencedirect.com/science/article/pii/S0031942205001718

Xu, S., Xu, Y., Gong, L., & Zhang, Q. (2016). Metabolomic Prediction of Yield in Hybrid Rice. *The*

Plant Journal. https://doi.org/10.1111/tpj.13242

Yoshida, S. (2003). Molecular regulation of leaf senescence, 79–84. https://doi.org/10.1016/S1369-5266(02)00009-2

Zeier, J. J., Pink, B., Mueller, M. J., & Berger, S. (2004). Light conditions influence specific defence responses in incompatible plant-pathogen interactions: uncoupling systemic resistance from salicylic acid and PR-1 accumulation. *Planta*, *219*(4), 673–683. https://doi.org/10.1007/s00425-004-1272-z

Zentgraf, U., Hinderhofer, K., & Zentgraf, U. (2001). Identification of a transcription factor specifically expressed at the onset of leaf senescence. *Planta*, *213*(3), 469–473. https://doi.org/10.1007/s004250000512

Zhang, Z., Shrestha, J., Tateda, C., & Greenberg, J. T. (2014). Salicylic acid signaling controls the maturation and localization of the arabidopsis defense protein ACCELERATED CELL DEATH6. *Molecular Plant*, *7*(8), 1365–1383. https://doi.org/10.1093/mp/ssu072

Zhang, Z., Tateda, C., Jiang, S.-C., Shrestha, J., Jelenska, J., Speed, D. J., & Greenberg, J. T. (2017). A Suite of Receptor-Like Kinases and a Putative Mechano-Sensitive Channel Are Involved in Autoimmunity and Plasma Membrane–Based Defenses in *Arabidopsis*. *Molecular Plant-Microbe Interactions*, *30*(2), 150–160. https://doi.org/10.1094/MPMI-09-16-0184-R

Zhong, M., Yuan, Y., Shu, S., Sun, J., Guo, S., Yuan, R., & Tang, Y. (2016). Effects of exogenous putrescine on glycolysis and Krebs cycle metabolism in cucumber leaves subjected to salt stress. *Plant Growth Regulation*, *79*(3), 319–330. https://doi.org/10.1007/s10725-015-0136-9

Zhu, Y., Qian, W., & Hua, J. (2010). Temperature Modulates Plant Defense Responses through NB-LRR Proteins. *PLoS Pathogens*, *6*(4), e1000844. https://doi.org/10.1371/journal.ppat.1000844

Züst, T., Joseph, B., Shimizu, K. K., Kliebenstein, D. J., Turnbull, L. A., Zust, T., … Turnbull, L. A. (2011). Using knockout mutants to reveal the growth costs of defensive traits. *Proceedings of the Royal Society B: Biological Sciences*, *278*(1718), 2598–2603. https://doi.org/10.1098/rspb.2010.2475

8. Supplementary Tables

Table S1. Primers used throughout the study for the different target and housekeeping genes.

Name	Sequence	Description
18S_rRNA_F	GCGACGCATCATTCAAATTTC	Housekeeping
18S_rRNA_R	TCCGGAATCGAACCCTAATTC	Housekeeping
GAPDH3'_F	TTGGTGACAACAGGTCAAGCA	Housekeeping
GAPDH3'_R	AAACTTGTCGCTCAATGCAATC	Housekeeping
GAPDH5'_F	TCTCGATCTCAATTTCGCAAAA	Housekeeping
GAPDH5'_R	CGAAACCGTTGATTCCGATTC	Housekeeping
ACT2-155_F	AACTCTCCCGCTATGTATGTCGC	Housekeeping
ACT2-155_R	CAATACCGGTTGTACGACCACTG	Housekeeping
ACT2-633_F	ACTTTCATCAGCCGTTTTGA	Housekeeping
ACT2-633_R	ACGATTGGTTGAATATCATCAG	Housekeeping
SAND_50_F	TCGCCGATCCAAATCCTAGC	Housekeeping
SAND_50_R	TTGCTAACTCCGCCTTCGTT	Housekeeping
SAND_862_F	ATGACACCCTTGCTTGGAGG	Housekeeping
SAND_862_R	ATAAGACACCAGACGCGCAA	Housekeeping
UBQ-5_F	CCAAGCCGAAGAAGATCAAG	Housekeeping
UBQ-5_R	ATGACTCGCCATGAAAGTCC	Housekeeping
EF_F	TGAGCACGCTCTTCTTGCTTTCA	Housekeeping
EF_R	GGTGGTGGCATCCATCTTGTTACA	Housekeeping
TUB2_F	CAACGCTACTCTGTCTGTCC	Housekeeping
TUB2_R	TCTGTGAATTCCATCTCGTC	Housekeeping
CDS(ACD6)-pJL_F	AAATTCTCGAGTTATGGACAGTTCTGGAGCAGA	ACD6 CDS for insertion in pJL-Blue
CDS(ACD6)-pJL_R	AATATGCGGCCGCTTATTCGGAACACGCCACAC	ACD6 CDS for insertion in pJL-Blue
Ct-CDS(ACD6)pJL_R	AATATGCGGCCGCTTCGGAACACGCCACAC	ACD6 CDS for insertion in pJL-Blue (no stop codon)

ACD6Prom_F	AAATTCTCGAGGAGTTTGTAGCCTATTCAAAGGC	ACD6 promoter for GUS constructs
ACD6Prom_R	AATATGCGGCCGCCGCAAACCTAAAATAATCACAC	ACD6 promoter for GUS constructs
FT_F	AGTCCTAGCAACCCTCACCT	Flowering marker
FT_R	CCTGCAGTGGGACTTGGATT	Flowering marker
FLC_F	GGCTAGCCAGATGGAGAATAATCA	Flowering marker
FLC_R	AGTCACCGGAAGATTGTCGG	Flowering marker
CBF_F	TGTGATACGACGACCACGAA	Flowering marker
CBF_R	AAACGCACCTTCGCTCTGTT	Flowering marker
NF-YA1_F	GGAAAGTCATCCGGGACAGAAAGC	Late-flowering marker
NF-YA1_R	TTTCTTCGCAAACCGGCCTCCA	Late-flowering marker
NF-YA4_F	CAGATTCCCAAACCCGACCA	Late-flowering marker
NF-YA4_R	CTGCAATTGGACCCCAGGAT	Late-flowering marker
GSR2_F	CACATCAGTGCCTACGGTGA	Ammonium assimilation
GSR2_R	ACGTCCCACACGAATAGAGC	Ammonium assimilation
PAL1_F	ACACTGTCTCTCAAGTGGCG	Ammonium assimilation
PAL1_R	ACGTTGCGCTACAAGGATCA	Ammonium assimilation
CSY4_F	TGACGACCCTCTTTTCCAGC	Ammonium assimilation
CSY4_R	CAAGACCCCACTGTGAGCAT	Ammonium assimilation
ACO3_F	GACTGGTCACGAACGCTACA	Ammonium assimilation
ACO3_R	GCGGACTGTGCAAGTGAAAG	Ammonium assimilation
AOX2_F	CGCGGTTAGCTCATAGGGTC	Ammonium assimilation
AOX2_R	AATCAATAGCAATCGCGGGC	Ammonium assimilation
GLU1_F	GTTCGTGCCGTTATCGACCT	Ammonium assimilation
GLU1_R	GAAACTTTGCACGTTGGGTGT	Ammonium assimilation
GDH1_F	GGTGGATCGCTAGGGAGAGA	Ammonium assimilation
GDH1_R	GATGACAAAACGCTGCCCTG	Ammonium assimilation

IDH1_F	ACCATGCGGTATTCGAGCAA	Ammonium assimilation
IDH1_R	TTTCGTCCGGCACTTTCCTT	Ammonium assimilation
CICDH_F	AAGTGTGCCACCATCACTCC	Ammonium assimilation
CICDH_R	ATGCAGATGGGCTTTGTCCA	Ammonium assimilation
EDS1_F	TCC TGA GGA ATG TCC TGT GA	Defense marker
EDS1_R	GAA CCG TGT TCA GTT TCC TTG	Defense marker
NPR1_F	CGT TTC TCA GCA GTG TCG TC	Defense marker
NPR1_R	CCG TCT CAC TGG TAC GAA GA	Defense marker
PAD4_F	GGC GGT ATC GAT GAT TCA GT	Defense marker
PAD4_R	GGT TGA ATG GCC GGT TAT C	Defense marker
PR1_F	CGT TCA CAT AAT TCC CAC GA	Defense marker
PR1_R	AAG AGG CAA CTG CAG ACT CA	Defense marker
PDF1.2_F	CTG CTC TTG TTC TCT TTG CT	Defense marker
PDF1.2_R	GTG TGC TGG GAA GAC ATA	Defense marker
PR5_F	CGG AAA CGG TAG ATG TGT AAC	Defense marker
PR5_R	GTT GAG GTC AGA GAC ACA GCC	Defense marker
SAG12_F	CGA AGG CGG TTT AAT GGA TAC TGC	Senescence marker
SAG12_R	TTA ACC GGG ACA TCC TCA TAA CCT G	Senescence marker
WRKY53_F	AGCCGCAGACTTCTTGTTGT	Senescence marker
WRKY53_R	GCGAATACGTCTTTGCAGGA	Senescence marker
PIF4_F	ACAGAGCCCGGTACAGTTAC	Thermosensory immunity regulator
PIF4_R	CCATCGGCTGCATCTGAGTC	Thermosensory immunity regulator

Table S2. Pairwise comparison of genetic similarity among Altenriet individuals. The amount of heterozygosity for each Altenriet parent is indicated in the first row. A total of 1985 SNPs were used.

	Alt1	Alt2	Alt3	Alt4	Alt5	Alt6	Alt7
Heterozygosity	1.66%	1.21%	2.37%	1.01%	1.21%	2.67%	5.39%
Alt2	66.5%						
Alt3	65.5%	68.8%					
Alt4	72.7%	66.4%	64.3%				
Alt5	73.6%	67.0%	67.5%	79.7%			
Alt6	97.5%	65.6%	65.2%	72.6%	73.2%		
Alt7	60.3%	68.8%	67.5%	65.0%	69.5%	60.3%	

Table S3. Metabolites identified in the first project. Sixty-six analytes from primary metabolism and thirty-four from secondary metabolism were identified and quantified using gas chromatography mass spectrometry (GC-MS) and liquid chromatography mass spectrometry (LC-MS). Mass and retention times of secondary metabolites (Met_ID 67-100) are included respectively inside parenthesis.

Met_ID	Metabolite	Class
1	Adenine	Amines
2	Alanine	Amines
3	Alanine_beta	Amines
4	Arginine	Amines
5	Ascorbic_acid	Acids
6	Asparagine	Amines
7	Aspartic_acid	Acids
8	Benzoic_acid	Acids
9	Citric_acid	Acids
10	Cysteine	Amines
11	Dehydroascorbic_acid_dimer	Acids
12	Fructose	Sugars
13	Fructose_6_phosphate	Sugars
14	Fucose	Sugars
15	Fumaric_acid	Acids
16	GABA	Sugars
17	Galactinol	Sugars
18	Galactonic_acid	Acids
19	Gluconic_acid	Acids
20	Glucose	Sugars
21	Glucose_6_phosphate	Sugars
22	Glucose_1_6_anhydro_beta	Sugars
23	Glutamic_acid	Acids
24	Glutamine	Amines
25	Glutaric_acid_2_oxo	Acids
26	Glyceric_acid	Acids

27	Glycerol	Sugars
28	Glycerol_3_phosphate	Sugars
29	Glycine	Amines
30	Guanidine	Amines
31	Homoserine	Amines
32	Inositol_myo	Sugars
33	Isoleucine	Amines
34	Isomaltose	Sugars
35	Lysine	Amines
36	Malic_acid	Acids
37	Maltose	Sugars
38	Methionine	Amines
39	Nicotinamide	Sugars
40	Nicotinic_acid	Acids
41	Ornithine	Amines
42	Phenylalanine	Amines
43	Phosphoric_acid	Acids
44	Proline	Amines
45	Putrescine	Amines
46	Pyroglutamic_acid	Acids
47	Pyruvic_acid	Acids
48	Raffinose	Sugars
49	Rhamnose	Sugars
50	Ribose_5_phosphate	Sugars
51	Serine	Amines
52	Serine_O_acetyl	Amines
53	Shikimic_acid	Acids
54	Spermidine	Amines
55	Succinic_acid	Acids

56	Sucrose	Sugars
57	Threitol	Sugars
58	Threonine	Amines
59	Trehalose_alpha.alpha	Sugars
60	Tryptophan	Sugars
61	Tyramine	Amines
62	Tyrosine	Amines
63	Uracil	Sugars
64	Urea	Sugars
65	Valine	Amines
66	Xylose	Sugars
67	Coniferin; Coniferoside (333.31, 2.48)	Glucosides
68	Unknown (463.3, 12.1)	Unknown
69	L-Glutathione (306.23, 3.22)	Glucosinolates
70	Disinapoyl.glucoside-I (591.3, 18.2)	Glucosides
71	Most likely Anthocyanin (841.5, 29.3)	Flavonoids
72	Unknown (721.3, 26.3)	Unknown
73	Disinapoyl.glucoside-II (591.3, 19.15)	Glucosides
74	Trans-sinapoyl malate (341, 2.16)	Glucosinolates
75	Unknown (585.1, 24.7)	Unknown
76	7-Methylthioheptyl glucosinolate (462.3, 23.8)	Glucosinolates
77	Kaempferol 3-galactoside-7-rhamnoside (593.7, 14.9)	Flavonoids
78	Quercetin.Glc.Rha (609.3, 14.2)	Flavonoids
79	Phenylpropanoid, hydroxyferuloyl Glc (372.23, 10.4)	Phenylpropanoids
80	Phenylpropanoid, cis or trans, sinapoyl malate (339.3, 21.5)	Phenylpropanoids
81	Glucosinolate.SO (422.29, 4.6)	Glucosinolates
82	Sinapoyl.glucoside (385.4, 13.4)	Glucosides
83	Anthocyanin (1685.4, 24.8)	Flavonoids
84	3-methylsulfinylpropyl Gluc (358.36, 7.08)	Sugars

85	Glucosinolate (478.2, 12.8)	Glucosinolates
86	Unknown (406.2, 11.81)	Unknown
87	Glucosinolates, glucobrassicin (447.3, 15.3)	Glucosinolates
88	Sinapoyl + sugar (289.1, 3.74)	Sugars
89	Glucosinolates, methylsulfinyloctyl Gluc (492.5, 14.5)	Glucosinolates
90	Glucosinolates, 3-methylbutyl Gluc (387.53, 2.16)	Glucosinolates
91	Glucosinolates, 8-methylthiooctyl Gluc (476.4, 27.7)	Glucosinolates
92	Flavonoids, 3-Rha-7-Rha-Kae (577.6, 15.8)	Flavonoids
93	indole-3-carboxylate hex (323.30, 11.1)	Unknown
94	Glucosinolates, neoglucobrassicin or 4-methoxyglucobrassicin (477.3, 17.3)	Glucosinolates
95	Benzenoids, protocatechoyl Xyl (285.2, 7.6)	Glucosinolates
96	Possible flavonoid (565.19, 4.50)	Flavonoids
97	Glucosinolate (679.4, 17.0)	Glucosinolates
98	Indolic.glucosinolate (477.2, 20.1)	Glucosinolates
99	Kaempferol.Glc.Rha.Rha (739.5, 13.5)	Flavonoids
100	Unknown (371.2, 11.6)	Unknown

Table S4. Individual modes of inheritance per metabolite for each hybrid analyzed. Metabolites with significant midparental deviations (MPDs), based on random permutation analyses, were classified as having additive or non-additive inheritance; the latter classified as positive or negative. Alpha = 0.01.

Metabolite	Classification	12	13	14	15	16	17	23	24	25	26	27	31	32	34	35	36	37	41	42	43	45	46	47	51	52	54	61	62	63	64	65	67	71	72	73	74	75	76
Adenine	Primary	Additive	Additive	Additive	Additive	Additive	Positive	Additive	Additive	Additive	Additive	Negative	Negative	Additive	Additive	Negative	Additive	Additive	Additive	Additive	Negative	Additive	Negative	Additive	Additive	Additive	Additive	Additive	Additive	Negative	Additive	Negative	Additive	Positive	Additive	Additive	Positive	Additive	Additive
Alanine	Primary	Additive	Additive	Additive	Additive	Positive	Additive	Additive	Additive	Additive	Additive	Negative	Negative	Additive	Negative	Additive	Negative	Negative	Additive	Additive	Negative	Additive	Additive	Negative	Additive	Additive	Additive	Negative	Additive	Negative	Additive	Negative	Negative	Additive	Additive	Additive	Additive	Positive	Additive
Alanine_beta	Primary	Additive	Additive	Additive	Additive	Additive	Positive	Additive	Additive	Additive	Additive	Negative	Negative	Additive	Additive	Negative	Additive	Negative	Negative	Additive	Negative	Additive	Negative	Additive	Additive	Additive	Additive	Additive	Additive	Negative	Additive	Negative	Additive	Additive	Additive	Negative	Additive	Additive	Positive
Arginine	Primary	Positive	Additive	Additive	Negative	Additive	Positive	Additive	Negative	Additive	Additive	Negative	Negative	Additive	Additive	Additive	Additive	Negative	Additive	Additive	Negative	Additive	Negative	Negative	Additive	Additive	Additive	Negative	Additive	Additive	Additive	Additive	Additive	Additive	Additive	Additive	Positive	Positive	Positive
Ascorbic_acid	Primary	Additive	Negative	Additive	Additive	Additive	Additive	Additive	Negative	Additive	Additive	Negative	Negative	Additive	Additive	Additive	Additive	Additive	Additive	Negative	Negative	Additive	Negative	Additive	Additive	Positive	Positive	Additive	Additive	Negative	Additive	Additive	Additive	Additive	Additive	Additive	Additive	Positive	Additive
Asparagine	Primary	Additive	Additive	Additive	Additive	Additive	Additive	Additive	Additive	Additive	Additive	Negative	Negative	Additive	Additive	Additive	Negative	Negative	Additive	Additive	Negative	Additive	Negative	Negative	Additive	Additive	Additive	Additive	Additive	Negative	Additive	Additive	Additive	Additive	Additive	Negative	Additive	Positive	Additive
Aspartic_acid	Primary	Additive	Additive	Additive	Additive	Additive	Additive	Additive	Additive	Additive	Additive	Negative	Negative	Negative	Additive	Additive	Additive	Additive	Additive	Additive	Negative	Additive	Additive	Additive	Additive	Additive	Additive	Additive	Additive	Additive	Additive	Additive	Additive	Additive	Additive	Additive	Additive	Positive	Positive
Benzoic_acid	Primary	Additive	Additive	Negative	Negative	Additive	Additive	Additive	Additive	Negative	Additive	Additive	Additive	Additive	Additive	Additive	Additive	Additive	Additive	Additive	Negative	Additive	Negative	Negative	Additive	Positive	Additive	Negative	Additive	Negative	Additive	Negative	Additive	Additive	Additive	Additive	Positive	Additive	Negative
Citric_acid	Primary	Additive	Additive	Additive	Additive	Additive	Additive	Additive	Additive	Additive	Additive	Additive	Negative	Negative	Additive	Additive	Additive	Additive	Additive	Additive	Negative	Additive	Negative	Additive	Additive	Additive	Additive	Additive	Additive	Negative	Additive	Negative	Additive	Additive	Additive	Additive	Additive	Positive	Additive
Cysteine	Primary	Additive	Additive	Additive	Additive	Additive	Additive	Additive	Additive	Additive	Additive	Negative	Negative	Additive	Additive	Negative	Additive	Additive	Additive	Additive	Negative	Additive	Negative	Additive	Positive	Additive	Additive	Negative	Additive	Negative	Additive	Negative	Additive	Additive	Additive	Additive	Positive	Additive	Additive
Dehydroascorbic_acid_dimer	Primary	Additive	Negative	Negative	Additive	Additive	Additive	Negative	Negative	Additive	Additive	Additive	Negative	Positive	Additive	Additive	Additive	Additive	Additive	Additive	Negative	Additive	Negative	Additive	Additive	Positive	Additive	Negative	Additive	Negative	Additive	Additive	Additive	Additive	Additive	Additive	Additive	Additive	Negative
Fructose	Primary	Additive	Additive	Additive	Additive	Additive	Additive	Additive	Additive	Additive	Additive	Negative	Negative	Additive	Negative	Additive	Additive	Additive	Additive	Additive	Negative	Additive	Negative	Additive	Additive	Additive	Additive	Additive	Additive	Additive	Additive	Additive	Additive	Additive	Additive	Additive	Additive	Additive	Additive
Fructose_6_phosphate	Primary	Positive	Additive	Negative	Additive	Additive	Additive	Additive	Additive	Negative	Additive	Additive	Additive	Additive	Additive	Additive	Additive	Additive	Additive	Negative	Negative	Additive	Negative	Negative	Additive	Positive	Additive	Negative	Additive	Negative	Additive	Additive	Additive	Additive	Additive	Additive	Additive	Positive	Positive
Fucose	Primary	Additive	Additive	Additive	Additive	Additive	Additive	Negative	Additive	Negative	Additive	Negative	Negative	Positive	Negative	Negative	Additive	Additive	Additive	Additive	Negative	Additive	Negative	Additive	Additive	Additive	Additive	Negative	Additive	Negative	Positive	Additive	Additive	Additive	Additive	Additive	Additive	Additive	Additive
Fumaric_acid	Primary	Additive	Additive	Negative	Additive	Additive	Additive	Additive	Additive	Additive	Additive	Negative	Negative	Additive	Additive	Additive	Additive	Additive	Additive	Additive	Negative	Additive	Negative	Additive	Additive	Additive	Additive	Negative	Additive	Negative	Additive	Additive	Additive	Additive	Additive	Additive	Additive	Positive	Additive
GABA	Primary	Positive	Additive	Additive	Additive	Additive	Positive	Additive	Additive	Negative	Additive	Negative	Negative	Additive	Negative	Negative	Additive	Additive	Additive	Additive	Negative	Additive	Additive	Additive	Additive	Additive	Additive	Additive	Additive	Negative	Additive	Additive	Additive	Additive	Additive	Additive	Positive	Additive	Positive
Galactinol	Primary	Additive	Additive	Negative	Additive	Additive	Additive	Additive	Additive	Additive	Additive	Additive	Negative	Additive	Additive	Additive	Additive	Negative	Additive	Positive	Additive	Negative	Positive	Additive	Negative	Additive	Negative	Additive	Additive	Negative	Additive	Positive	Additive	Additive	Additive	Additive	Additive	Additive	Additive
Galactonic_acid	Primary	Additive	Additive	Additive	Additive	Additive	Additive	Additive	Additive	Additive	Additive	Negative	Negative	Additive	Additive	Additive	Additive	Negative	Additive	Additive	Negative	Additive	Negative	Negative	Additive	Additive	Additive	Negative	Additive	Negative	Additive	Additive	Additive	Additive	Additive	Additive	Additive	Positive	Additive
Gluconic_acid	Primary	Additive	Additive	Additive	Additive	Additive	Additive	Additive	Additive	Additive	Additive	Negative	Negative	Additive	Additive	Negative	Additive	Negative	Additive	Additive	Negative	Additive	Negative	Additive	Additive	Additive	Additive	Negative	Additive	Negative	Positive	Additive	Negative	Additive	Additive	Additive	Additive	Additive	Positive
Glucose	Primary	Additive	Additive	Additive	Additive	Additive	Additive	Additive	Additive	Additive	Additive	Negative	Negative	Additive	Negative	Additive	Additive	Additive	Additive	Additive	Negative	Negative	Negative	Additive	Additive	Additive	Additive	Additive	Additive	Negative	Additive	Additive	Additive	Additive	Additive	Additive	Additive	Additive	Additive
Glucose_6_phosphate	Primary	Positive	Additive	Negative	Additive	Additive	Additive	Additive	Additive	Negative	Additive	Additive	Additive	Additive	Additive	Additive	Additive	Negative	Additive	Additive	Negative	Additive	Negative	Negative	Additive	Positive	Negative	Negative	Additive	Negative	Additive	Additive	Additive	Additive	Additive	Negative	Additive	Positive	Positive
Glucose_1_6_anhydro_beta	Primary	Additive	Additive	Additive	Additive	Additive	Additive	Additive	Additive	Additive	Additive	Negative	Negative	Additive	Additive	Additive	Additive	Additive	Additive	Additive	Negative	Additive	Negative	Additive	Additive	Positive	Additive	Negative	Additive	Negative	Additive	Additive	Negative	Additive	Additive	Additive	Additive	Additive	Additive
Glutamic_acid	Primary	Additive	Additive	Negative	Additive	Additive	Additive	Additive	Additive	Additive	Additive	Negative	Negative	Additive	Additive	Additive	Negative	Additive	Additive	Additive	Negative	Additive	Additive	Negative	Additive	Additive	Additive	Negative	Positive	Negative	Additive	Additive	Negative	Additive	Additive	Additive	Additive	Positive	Positive
Glutamine	Primary	Additive	Additive	Additive	Additive	Additive	Additive	Additive	Additive	Additive	Additive	Negative	Additive	Additive	Negative	Additive	Negative	Negative	Additive	Additive	Negative	Additive	Additive	Negative	Additive	Additive	Additive	Additive	Additive	Additive	Additive	Additive	Additive	Additive	Additive	Additive	Additive	Positive	Positive
Glutaric_acid_2_oxo	Primary	Positive	Additive	Additive	Additive	Additive	Additive	Additive	Negative	Additive	Additive	Additive	Negative	Additive	Additive	Additive	Negative	Negative	Additive	Additive	Negative	Additive	Additive	Negative	Additive	Positive	Additive	Negative	Additive	Negative	Additive	Additive	Additive	Additive	Additive	Additive	Additive	Positive	Positive
Glyceric_acid	Primary	Positive	Additive	Additive	Additive	Additive	Additive	Additive	Additive	Additive	Additive	Additive	Additive	Additive	Additive	Additive	Additive	Negative	Negative	Additive	Negative	Additive	Negative	Negative	Positive	Positive	Additive	Negative	Additive	Negative	Additive	Additive	Additive	Additive	Additive	Negative	Additive	Positive	Additive
Glycerol	Primary	Positive	Additive	Positive	Negative	Additive	Additive	Negative	Additive	Negative	Additive	Additive	Positive	Additive	Additive	Additive	Additive	Additive	Negative	Additive	Negative	Additive	Negative	Additive	Additive	Additive	Negative	Negative	Additive	Additive	Additive	Negative	Additive	Additive	Additive	Additive	Positive	Negative	Negative
Glycerol_3_phosphate	Primary	Additive	Additive	Positive	Additive	Additive	Positive	Additive	Additive	Additive	Additive	Negative	Negative	Additive	Additive	Negative	Additive	Negative	Additive	Additive	Additive	Negative	Negative	Additive	Positive	Additive	Additive	Negative	Negative	Additive	Additive	Additive	Additive	Additive	Additive	Negative	Positive	Positive	Positive
Glycine	Primary	Additive	Additive	Negative	Additive	Additive	Additive	Additive	Additive	Additive	Additive	Negative	Additive	Additive	Additive	Negative	Negative	Negative	Additive	Additive	Negative	Negative	Negative	Negative	Additive	Additive	Additive	Negative	Additive	Negative	Additive	Additive	Negative	Additive	Additive	Additive	Additive	Positive	Additive
Guanidine	Primary	Additive	Positive	Additive	Additive	Additive	Positive	Additive	Additive	Negative	Additive	Negative	Positive	Additive	Additive	Additive	Additive	Negative	Additive	Additive	Positive	Additive	Negative	Negative	Additive	Additive	Additive	Negative	Additive	Additive	Positive	Negative	Additive	Additive	Negative	Additive	Additive	Negative	Additive
Homoserine	Primary	Positive	Positive	Additive	Additive	Additive	Additive	Additive	Negative	Additive	Additive	Negative	Additive	Additive	Additive	Additive	Additive	Negative	Negative	Additive	Negative	Additive	Negative	Negative	Additive	Positive	Additive	Negative	Additive	Negative	Additive	Additive	Negative	Additive	Positive	Additive	Additive	Positive	Additive
Inositol_myo	Primary	Additive	Additive	Additive	Additive	Additive	Additive	Additive	Additive	Additive	Additive	Negative	Negative	Additive	Additive	Additive	Additive	Additive	Additive	Positive	Negative	Additive	Additive	Additive	Additive	Additive	Additive	Additive	Additive	Negative	Additive	Additive	Additive	Additive	Additive	Additive	Additive	Additive	Positive
Isoleucine	Primary	Additive	Additive	Additive	Additive	Additive	Additive	Additive	Additive	Negative	Additive	Negative	Negative	Additive	Additive	Negative	Additive	Additive	Additive	Additive	Negative	Additive	Additive	Additive	Additive	Additive	Additive	Negative	Additive	Negative	Positive	Negative	Additive	Additive	Additive	Negative	Additive	Additive	Additive
Isomaltose	Primary	Additive	Additive	Negative	Additive	Additive	Positive	Additive	Negative	Additive	Additive	Negative	Additive	Additive	Additive	Additive	Negative	Negative	Additive	Additive	Negative	Additive	Additive	Negative	Additive	Additive	Additive	Additive	Additive	Negative	Additive	Additive	Additive	Additive	Additive	Additive	Additive	Positive	Additive
Lysine	Primary	Additive	Additive	Additive	Additive	Additive	Positive	Negative	Additive	Additive	Additive	Negative	Negative	Additive	Additive	Negative	Additive	Additive	Positive	Additive	Negative	Additive	Negative	Additive	Additive	Additive	Additive	Additive	Additive	Negative	Positive	Negative	Additive	Additive	Additive	Negative	Additive	Additive	Positive
Malic_acid	Primary	Additive	Additive	Additive	Additive	Additive	Additive	Additive	Negative	Additive	Additive	Negative	Negative	Negative	Additive	Additive	Additive	Additive	Additive	Additive	Negative	Additive	Additive	Negative	Additive	Additive	Additive	Additive	Additive	Additive	Additive	Additive	Additive	Additive	Additive	Additive	Additive	Positive	Additive
Maltose	Primary	Additive	Additive	Additive	Positive	Additive	Additive	Additive	Additive	Negative	Additive	Negative	Negative	Additive	Additive	Additive	Additive	Additive	Positive	Additive	Positive	Negative	Additive	Positive	Negative	Additive	Additive	Additive	Positive	Additive	Additive	Additive	Additive	Additive	Additive	Additive	Positive	Positive	Positive
Methionine	Primary	Additive	Additive	Additive	Additive	Additive	Additive	Additive	Additive	Additive	Additive	Negative	Negative	Additive	Additive	Negative	Additive	Negative	Additive	Additive	Negative	Additive	Negative	Negative	Additive	Positive	Additive	Negative	Additive	Negative	Additive	Negative	Additive	Additive	Additive	Additive	Positive	Additive	Additive
Nicotinamide	Primary	Additive	Additive	Additive	Additive	Additive	Additive	Additive	Additive	Additive	Positive	Negative	Negative	Additive	Additive	Additive	Additive	Additive	Negative	Positive	Negative	Additive	Negative	Additive	Positive	Positive	Additive	Negative	Additive	Negative	Positive	Negative	Additive	Additive	Additive	Additive	Additive	Additive	Additive
Nicotinic_acid	Primary	Additive	Additive	Additive	Additive	Additive	Additive	Additive	Additive	Additive	Additive	Negative	Negative	Additive	Additive	Negative	Additive	Additive	Additive	Additive	Negative	Additive	Negative	Additive	Additive	Additive	Additive	Additive	Additive	Negative	Additive	Additive	Additive	Additive	Additive	Additive	Additive	Additive	Additive
Ornithine	Primary	Additive	Additive	Additive	Additive	Additive	Additive	Additive	Additive	Additive	Additive	Additive	Additive	Additive	Additive	Additive	Additive	Additive	Additive	Additive	Additive	Additive	Negative	Additive	Additive	Additive	Additive	Additive	Additive	Additive	Additive	Additive	Additive	Additive	Additive	Additive	Additive	Additive	Additive
Phenylalanine	Primary	Positive	Additive	Additive	Negative	Additive	Additive	Additive	Negative	Additive	Additive	Negative	Additive	Additive	Additive	Additive	Negative	Negative	Negative	Additive	Negative	Additive	Negative	Negative	Additive	Additive	Additive	Negative	Additive	Negative	Additive	Additive	Additive	Additive	Additive	Additive	Additive	Positive	Additive
Phosphoric_acid	Primary	Additive	Additive	Additive	Additive	Additive	Additive	Additive	Positive	Additive	Additive	Additive	Negative	Additive	Additive	Negative	Additive	Additive	Additive	Additive	Additive	Additive	Additive	Additive	Additive	Additive	Additive	Additive	Additive	Additive	Additive	Additive	Additive	Positive	Positive	Additive	Positive	Positive	Positive
Proline	Primary	Additive	Positive	Negative	Additive	Additive	Additive	Additive	Additive	Additive	Positive	Additive	Additive	Additive	Additive	Additive	Additive	Negative	Additive	Positive	Additive	Additive	Negative	Negative	Additive	Additive	Additive	Additive	Additive	Additive	Additive	Additive	Additive	Additive	Additive	Additive	Additive	Positive	Positive
Putrescine	Primary	Additive	Additive	Additive	Additive	Additive	Additive	Additive	Additive	Additive	Additive	Negative	Negative	Additive	Additive	Additive	Negative	Additive	Additive	Additive	Negative	Negative	Negative	Negative	Additive	Additive	Additive	Negative	Additive	Negative	Additive	Negative	Additive	Additive	Positive	Additive	Positive	Additive	Additive
Pyroglutamic_acid	Primary	Additive	Additive	Additive	Negative	Additive	Additive	Additive	Additive	Additive	Additive	Negative	Negative	Additive	Negative	Negative	Additive	Additive	Additive	Additive	Negative	Additive	Negative	Negative	Additive	Additive	Additive	Negative	Additive	Negative	Additive	Additive	Additive	Additive	Additive	Additive	Additive	Additive	Additive
Pyruvic_acid	Primary	Positive	Additive	Negative	Additive	Additive	Additive	Additive	Negative	Additive	Additive	Additive	Additive	Additive	Additive	Additive	Additive	Additive	Additive	Additive	Negative	Additive	Negative	Negative	Additive	Positive	Additive	Negative	Additive	Negative	Additive	Additive	Additive	Additive	Positive	Additive	Additive	Positive	Positive
Raffinose	Primary	Additive	Additive	Negative	Additive	Additive	Additive	Additive	Additive	Negative	Additive	Negative	Additive	Positive	Additive	Additive	Additive	Additive	Additive	Positive	Additive	Additive	Positive	Additive	Negative	Additive	Additive	Additive	Additive	Additive	Positive	Additive	Additive	Additive	Additive	Additive	Additive	Additive	Additive
Rhamnose	Primary	Additive	Additive	Additive	Additive	Additive	Positive	Additive	Additive	Additive	Additive	Negative	Negative	Additive	Additive	Negative	Additive	Negative	Additive	Additive	Negative	Additive	Negative	Additive	Additive	Additive	Additive	Negative	Additive	Negative	Positive	Additive	Additive	Additive	Additive	Negative	Positive	Additive	Additive
Ribose_5_phosphate	Primary	Additive	Negative	Additive	Additive	Additive	Additive	Additive	Additive	Additive	Additive	Negative	Additive	Positive	Additive	Additive	Negative	Negative	Additive	Additive	Negative	Additive	Negative	Additive	Additive	Positive	Positive	Negative	Additive	Additive	Positive	Negative	Negative	Additive	Additive	Additive	Additive	Additive	Additive
Serine	Primary	Additive	Additive	Additive	Additive	Additive	Positive	Additive	Additive	Additive	Additive	Negative	Negative	Additive	Additive	Negative	Additive	Additive	Additive	Additive	Negative	Additive	Negative	Negative	Additive	Additive	Additive	Negative	Additive	Additive	Additive	Additive	Additive	Additive	Additive	Additive	Additive	Positive	Positive
Serine_O_acetyl	Primary	Negative	Additive	Additive	Additive	Positive	Additive	Additive	Additive	Additive	Additive	Negative	Negative	Additive	Negative	Negative	Additive	Negative	Additive	Additive	Negative	Additive	Additive	Additive	Additive	Additive	Additive	Negative	Additive	Negative	Additive	Negative	Negative	Additive	Additive	Negative	Additive	Additive	Negative
Shikimic_acid	Primary	Additive	Additive	Additive	Additive	Additive	Additive	Additive	Additive	Additive	Additive	Negative	Negative	Additive	Additive	Negative	Additive	Additive	Additive	Additive	Negative	Additive	Negative	Additive	Additive	Additive	Additive	Negative	Additive	Negative	Additive	Additive	Additive	Additive	Additive	Negative	Additive	Additive	Additive
Spermidine	Primary	Additive	Additive	Additive	Positive	Additive	Positive	Additive	Positive	Additive	Positive	Negative	Negative	Additive	Additive	Negative	Additive	Additive	Positive	Additive	Negative	Additive	Negative	Additive	Additive	Positive	Additive	Additive	Additive	Negative	Additive	Additive	Additive	Additive	Additive	Negative	Additive	Additive	Additive
Succinic_acid	Primary	Additive	Additive	Additive	Additive	Additive	Additive	Additive	Additive	Additive	Additive	Negative	Negative	Additive	Negative	Additive	Additive	Additive	Additive	Additive	Negative	Additive	Negative	Additive	Additive	Additive	Additive	Additive	Positive	Negative	Additive	Negative	Additive	Additive	Negative	Negative	Additive	Positive	Additive
Sucrose	Primary	Additive	Additive	Negative	Additive	Additive	Additive	Additive	Additive	Additive	Additive	Negative	Negative	Additive	Additive	Additive	Negative	Additive	Additive	Additive	Negative	Additive	Negative	Negative	Additive	Additive	Additive	Negative	Additive	Negative	Negative	Additive	Additive	Additive	Additive	Additive	Additive	Positive	Positive
Threitol	Primary	Additive	Additive	Additive	Positive	Additive	Additive	Additive	Positive	Additive	Additive	Negative	Negative	Positive	Additive	Negative	Additive	Additive	Additive	Additive	Negative	Additive	Negative	Negative	Additive	Additive	Additive	Negative	Additive	Additive	Additive	Additive	Additive	Additive	Additive	Negative	Additive	Positive	Additive
Threonine	Primary	Additive	Additive	Additive	Additive	Additive	Positive	Additive	Additive	Additive	Additive	Negative	Negative	Additive	Additive	Negative	Additive	Additive	Additive	Additive	Negative	Additive	Negative	Negative	Additive	Additive	Additive	Negative	Additive	Negative	Additive	Negative	Additive	Additive	Additive	Negative	Additive	Additive	Positive
Trehalose_alpha.alpha	Primary	Additive	Additive	Additive	Additive	Additive	Additive	Additive	Additive	Additive	Additive	Additive	Additive	Additive	Additive	Additive	Additive	Negative	Additive	Additive	Negative	Additive	Negative	Additive	Positive	Additive	Additive	Negative	Additive	Negative	Additive	Additive	Negative	Additive	Additive	Negative	Additive	Additive	Additive
Tryptophan	Primary	Additive	Additive	Additive	Negative	Additive	Positive	Negative	Additive	Additive	Additive	Negative	Additive	Additive	Additive	Negative	Additive	Additive	Additive	Additive	Negative	Additive	Negative	Additive	Additive	Additive	Additive	Additive	Negative	Negative	Additive	Negative	Positive	Additive	Additive	Additive	Additive	Positive	Positive
Tyramine	Primary	Additive	Additive	Additive	Additive	Additive	Additive	Additive	Additive	Additive	Additive	Negative	Additive	Additive	Additive	Negative	Additive	Negative	Additive	Additive	Negative	Negative	Negative	Additive	Additive	Additive	Additive	Negative	Additive	Negative	Additive	Negative	Negative	Additive	Additive	Additive	Additive	Additive	Negative
Tyrosine	Primary	Additive	Additive	Additive	Negative	Additive	Additive	Additive	Additive	Negative	Additive	Negative	Additive	Additive	Negative	Negative	Additive	Additive	Additive	Additive	Negative	Negative	Negative	Additive	Additive	Additive	Negative	Additive	Additive	Negative	Positive	Negative	Additive	Additive	Additive	Negative	Additive	Additive	Additive
Uracil	Primary	Additive	Additive	Additive	Additive	Additive	Additive	Additive	Additive	Additive	Additive	Negative	Negative	Additive	Additive	Negative	Additive	Additive	Additive	Additive	Negative	Additive	Negative	Additive	Positive	Additive	Additive	Additive	Additive	Negative	Additive	Negative	Positive	Positive	Additive	Additive	Positive	Additive	Additive
Urea	Primary	Additive	Additive	Additive	Negative	Additive	Additive	Additive	Additive	Negative	Additive	Additive	Positive	Additive	Additive	Additive	Additive	Additive	Negative	Additive	Additive	Negative	Negative	Additive	Negative	Additive	Negative	Negative	Additive	Additive	Additive	Negative	Additive	Additive	Additive	Additive	Additive	Negative	Additive
Valine	Primary	Additive	Additive	Additive	Additive	Additive	Additive	Additive	Additive	Additive	Additive	Negative	Negative	Additive	Additive	Negative	Additive	Negative	Additive	Additive	Negative	Additive	Negative	Negative	Additive	Additive	Additive	Negative	Additive	Negative	Positive	Negative	Negative	Additive	Additive	Negative	Additive	Additive	Additive
Xylose	Primary	Additive	Additive	Additive	Negative	Additive	Additive	Negative	Additive	Additive	Additive	Negative	Negative	Additive	Additive	Negative	Additive	Additive	Additive	Additive	Negative	Additive	Negative	Negative	Additive	Additive	Additive	Negative	Negative	Additive	Additive	Negative	Additive	Additive	Additive	Additive	Positive	Additive	Additive
Coniferin; Coniferoside (333.31, 2.48)	Secondary	Additive	Negative	Negative	Additive	Negative	Positive	Additive	Negative	Additive	Negative	Additive	Negative	Positive	Additive	Additive	Negative	Additive	Additive	Positive	Negative	Additive	Negative	Additive	Additive	Additive	Negative	Negative	Negative	Additive	Additive	Additive	Additive	Negative	Positive	Additive	Additive	Positive	Additive
Unknown (463.3, 12.1)	Secondary	Negative	Negative	Additive	Additive	Additive	Positive	Additive	Additive	Additive	Additive	Additive	Negative	Positive	Additive	Additive	Additive	Additive	Positive	Positive	Additive	Positive	Additive	Positive	Additive	Additive	Additive	Negative	Negative	Additive	Additive	Additive	Negative	Additive	Positive	Negative	Positive	Additive	Positive
L-Glutathione (306.23, 3.22)	Secondary	Additive	Additive	Additive	Additive	Negative	Additive	Additive	Negative	Additive	Negative	Additive	Negative	Positive	Additive	Additive	Negative	Additive	Positive	Additive	Negative	Additive	Negative	Additive	Additive	Positive	Additive	Additive	Negative	Additive	Additive	Additive	Positive	Negative	Positive	Positive	Additive	Additive	Positive
Disinapoyl.glucoside-I (591.3, 18.2)	Secondary	Negative	Additive	Additive	Additive	Additive	Additive	Additive	Positive	Additive	Negative	Additive	Negative	Positive	Additive	Additive	Additive	Additive	Additive	Positive	Negative	Additive	Additive	Additive	Positive	Additive	Additive	Additive	Negative	Additive	Additive	Additive	Additive	Additive	Positive	Additive	Additive	Positive	Positive
Most likely Anthocyanin (841.5, 29.3)	Secondary	Additive	Additive	Negative	Additive	Additive	Positive	Additive	Additive	Negative	Negative	Additive	Additive	Positive	Positive	Additive	Additive	Additive	Additive	Positive	Additive	Positive	Additive	Positive	Additive	Additive	Additive	Additive	Negative	Additive	Additive	Additive	Additive	Additive	Positive	Positive	Additive	Positive	Additive
Unknown (721.3, 26.3)	Secondary	Additive	Additive	Additive	Additive	Negative	Additive	Additive	Additive	Negative	Negative	Positive	Additive	Positive	Additive	Additive	Additive	Negative	Additive	Positive	Additive	Positive	Additive	Additive	Additive	Additive	Additive	Negative	Negative	Additive	Additive	Additive	Additive	Negative	Additive	Additive	Positive	Additive	Additive
Disinapoyl.glucoside-II (591.3, 19.15)	Secondary	Negative	Additive	Additive	Additive	Additive	Positive	Additive	Additive	Additive	Negative	Additive	Negative	Positive	Additive	Additive	Additive	Additive	Additive	Additive	Negative	Additive	Negative	Additive	Additive	Additive	Additive	Negative	Negative	Additive	Additive	Additive	Additive	Additive	Positive	Additive	Additive	Positive	Positive
Trans-sinapoyl malate (341, 2.16)	Secondary	Additive	Negative	Negative	Additive	Negative	Additive	Additive	Negative	Additive	Negative	Additive	Additive	Positive	Negative	Additive	Negative	Additive	Additive	Additive	Negative	Additive	Negative	Additive	Additive	Additive	Negative	Negative	Negative	Negative	Additive	Additive	Additive	Additive	Additive	Additive	Additive	Additive	Additive
Unknown (585.1, 24.7)	Secondary	Negative	Negative	Negative	Additive	Negative	Positive	Negative	Additive	Negative	Negative	Additive	Negative	Positive	Additive	Additive	Negative	Additive	Additive	Positive	Negative	Additive	Negative	Additive	Additive	Additive	Negative	Negative	Negative	Negative	Additive	Additive	Additive	Negative	Positive	Additive	Additive	Positive	Positive
7-Methylthioheptyl glucosinolate (462.3, 23.8)	Secondary	Negative	Negative	Additive	Additive	Additive	Additive	Additive	Positive	Additive	Negative	Additive	Negative	Positive	Additive	Additive	Additive	Additive	Additive	Positive	Additive	Additive	Negative	Additive	Additive	Positive	Additive	Additive	Negative	Negative	Additive	Additive	Additive	Negative	Positive	Additive	Additive	Positive	Positive
Kaempferol 3-galactoside-7-rhamnoside (593.7, 14.9)	Secondary	Additive	Additive	Negative	Additive	Additive	Positive	Additive	Additive	Additive	Negative	Additive	Negative	Positive	Additive	Additive	Additive	Additive	Additive	Additive	Negative	Additive	Negative	Additive	Positive	Additive	Additive	Additive	Negative	Additive	Additive	Additive	Additive	Additive	Positive	Additive	Additive	Positive	Positive
Quercetin.Glc.Rha (609.3, 14.2)	Secondary	Additive	Additive	Additive	Positive	Additive	Positive	Additive	Positive	Additive	Negative	Additive	Negative	Positive	Additive	Additive	Additive	Negative	Additive	Additive	Additive	Positive	Additive	Additive	Positive	Additive	Additive	Additive	Negative	Additive	Additive	Additive	Additive	Additive	Positive	Additive	Additive	Positive	Additive
Phenylpropanoid, hydroxyferuloyl Glc (372.23, 10.4)	Secondary	Negative	Negative	Negative	Additive	Negative	Positive	Additive	Additive	Additive	Negative	Additive	Negative	Positive	Additive	Additive	Negative	Additive	Additive	Positive	Negative	Additive	Negative	Additive	Additive	Additive	Additive	Negative	Negative	Negative	Additive	Additive	Additive	Additive	Additive	Additive	Additive	Additive	Positive
Phenylpropanoid, cis or trans, sinapoyl malate (339.3, 21.5)	Secondary	Additive	Negative	Negative	Additive	Negative	Positive	Negative	Negative	Negative	Negative	Additive	Negative	Positive	Additive	Additive	Negative	Additive	Additive	Additive	Negative	Additive	Negative	Additive	Additive	Additive	Negative	Negative	Negative	Negative	Additive	Additive	Additive	Negative	Additive	Additive	Additive	Additive	Positive
Glucosinolate.SO (422.29, 4.6)	Secondary	Additive	Additive	Negative	Additive	Negative	Additive	Additive	Negative	Additive	Negative	Additive	Additive	Positive	Negative	Additive	Additive	Additive	Negative	Additive	Negative	Negative	Negative	Additive	Additive	Additive	Negative	Additive	Negative	Additive	Negative	Additive	Additive	Additive	Additive	Additive	Additive	Additive	Additive
Sinapoyl.glucoside (385.4, 13.4)	Secondary	Additive	Additive	Negative	Additive	Negative	Additive	Additive	Additive	Additive	Negative	Additive	Additive	Positive	Additive	Additive	Additive	Additive	Additive	Additive	Negative	Additive	Negative	Additive	Additive	Additive	Additive	Negative	Negative	Additive	Negative	Additive	Additive	Additive	Additive	Additive	Additive	Additive	Additive
Anthocyanin (1685.4, 24.8)	Secondary	Negative	Additive	Negative	Additive	Additive	Negative	Additive	Negative	Additive	Additive	Additive	Additive	Positive	Additive	Additive	Additive	Additive	Additive	Additive	Additive	Additive	Additive	Additive	Additive	Additive	Additive	Negative	Negative	Additive	Negative	Negative	Negative	Additive	Additive	Additive	Additive	Additive	Positive
3-methylsulfinylpropyl Gluc (358.36, 7.08)	Secondary	Negative	Negative	Negative	Additive	Negative	Positive	Additive	Additive	Additive	Negative	Additive	Negative	Positive	Additive	Additive	Additive	Additive	Additive	Positive	Negative	Additive	Negative	Additive	Additive	Additive	Additive	Negative	Negative	Negative	Additive	Additive	Additive	Additive	Additive	Additive	Additive	Positive	Positive
Glucosinolate (478.2, 12.8)	Secondary	Negative	Negative	Negative	Additive	Negative	Positive	Additive	Additive	Additive	Negative	Additive	Negative	Positive	Additive	Additive	Additive	Additive	Additive	Additive	Negative	Additive	Negative	Additive	Additive	Additive	Negative	Negative	Negative	Negative	Additive	Additive	Additive	Negative	Additive	Additive	Additive	Positive	Positive
Unknown (406.2, 11.81)	Secondary	Negative	Additive	Negative	Additive	Additive	Additive	Additive	Additive	Additive	Negative	Additive	Additive	Additive	Negative	Additive	Additive	Additive	Negative	Additive	Negative	Additive	Additive	Additive	Additive	Additive	Additive	Negative	Negative	Additive	Additive	Additive	Additive	Additive	Additive	Additive	Additive	Positive	Additive
Glucosinolates, glucobrassicin (447.3, 15.3)	Secondary	Negative	Additive	Negative	Additive	Additive	Additive	Additive	Positive	Additive	Negative	Additive	Additive	Positive	Additive	Additive	Additive	Additive	Additive	Positive	Negative	Additive	Negative	Additive	Positive	Additive	Additive	Additive	Negative	Negative	Negative	Additive	Additive	Negative	Positive	Additive	Additive	Positive	Additive
Sinapoyl + sugar (289.1, 3.74)	Secondary	Additive	Negative	Negative	Additive	Negative	Positive	Additive	Negative	Negative	Negative	Additive	Additive	Additive	Additive	Additive	Negative	Additive	Additive	Positive	Additive	Additive	Additive	Positive	Negative	Additive	Negative	Negative	Negative	Negative	Additive	Negative	Additive	Negative	Additive	Additive	Additive	Additive	Positive
Glucosinolates, methylsulfinyloctyl Gluc (492.5, 14.5)	Secondary	Additive	Additive	Additive	Positive	Positive	Additive	Positive	Positive	Additive	Negative	Additive	Negative	Additive	Additive	Additive	Additive	Additive	Additive	Additive	Negative	Positive	Additive	Additive	Positive	Additive	Additive	Positive	Negative	Additive	Additive	Additive	Positive	Additive	Positive	Additive	Additive	Positive	Additive
Glucosinolates, 3-methylbutyl Gluc (387.53, 2.16)	Secondary	Additive	Negative	Negative	Additive	Negative	Additive	Additive	Negative	Additive	Negative	Additive	Additive	Positive	Negative	Additive	Negative	Additive	Additive	Additive	Negative	Additive	Negative	Additive	Additive	Additive	Negative	Negative	Negative	Negative	Additive	Additive	Additive	Additive	Additive	Additive	Additive	Positive	Additive
Glucosinolates, 8-methylthiooctyl Gluc (476.4, 27.7)	Secondary	Negative	Negative	Additive	Additive	Additive	Positive	Additive	Positive	Additive	Negative	Additive	Negative	Positive	Additive	Additive	Additive	Additive	Additive	Positive	Negative	Additive	Negative	Additive	Additive	Positive	Additive	Additive	Negative	Additive	Additive	Additive	Additive	Negative	Positive	Additive	Additive	Positive	Positive
Flavonoids, 3-Rha-7-Rha-Kae (577.6, 15.8)	Secondary	Additive	Additive	Negative	Additive	Additive	Positive	Additive	Positive	Additive	Negative	Additive	Negative	Positive	Additive	Additive	Additive	Additive	Additive	Positive	Negative	Additive	Negative	Additive	Positive	Additive	Additive	Additive	Negative	Additive	Additive	Additive	Additive	Additive	Positive	Additive	Additive	Positive	Positive
indole-3-carboxylate hex (323.30, 11.1)	Secondary	Additive	Additive	Negative	Additive	Negative	Positive	Additive	Additive	Additive	Negative	Additive	Negative	Positive	Additive	Additive	Additive	Additive	Additive	Positive	Negative	Positive	Negative	Additive	Additive	Additive	Additive	Negative	Negative	Additive	Additive	Additive	Additive	Negative	Positive	Additive	Additive	Positive	Positive
Glucosinolates, neoglucobrassicin or 4-methoxyglucobrassicin (477.3, 17.3)	Secondary	Additive	Additive	Additive	Positive	Additive	Positive	Additive	Additive	Additive	Negative	Additive	Negative	Positive	Additive	Additive	Additive	Additive	Additive	Additive	Negative	Positive	Additive	Additive	Positive	Positive	Positive	Additive	Negative	Additive	Additive	Positive	Additive	Negative	Additive	Additive	Additive	Positive	Positive
Benzenoids, protocatechoyl Xyl (285.2, 7.6)	Secondary	Additive	Negative	Negative	Additive	Negative	Positive	Negative	Negative	Negative	Negative	Negative	Negative	Additive	Negative	Additive	Negative	Additive	Additive	Additive	Negative	Additive	Negative	Additive	Additive	Additive	Negative	Negative	Negative	Negative	Additive	Additive	Additive	Negative	Additive	Additive	Additive	Additive	Positive
Possible flavonoid (565.19, 4.50)	Secondary	Additive	Negative	Negative	Additive	Negative	Additive	Additive	Negative	Additive	Negative	Additive	Negative	Positive	Additive	Additive	Additive	Additive	Additive	Additive	Negative	Additive	Negative	Additive	Additive	Additive	Negative	Negative	Negative	Negative	Additive	Additive	Additive	Negative	Positive	Additive	Additive	Positive	Positive
Glucosinolate (679.4, 17.0)	Secondary	Negative	Additive	Negative	Additive	Additive	Positive	Additive	Positive	Additive	Negative	Additive	Negative	Positive	Additive	Additive	Additive	Additive	Additive	Additive	Negative	Positive	Additive	Additive	Positive	Additive	Additive	Additive	Negative	Additive	Additive	Additive	Additive	Negative	Positive	Additive	Additive	Positive	Positive
Indolic.glucosinolate (477.2, 20.1)	Secondary	Additive	Additive	Negative	Additive	Negative	Additive	Additive	Additive	Additive	Additive	Additive	Additive	Positive	Negative	Additive	Additive	Additive	Additive	Positive	Negative	Additive	Negative	Additive	Additive	Additive	Additive	Negative	Additive	Additive	Additive	Additive	Additive	Additive	Positive	Additive	Additive	Additive	Positive
Kaempferol.Glc.Rha.Rha (739.5, 13.5)	Secondary	Additive	Additive	Additive	Additive	Additive	Positive	Positive	Positive	Additive	Negative	Additive	Negative	Positive	Additive	Additive	Additive	Additive	Additive	Positive	Negative	Positive	Additive	Additive	Positive	Additive	Additive	Additive	Negative	Additive	Additive	Additive	Positive	Additive	Positive	Additive	Additive	Positive	Positive
Unknown (371.2, 11.6)	Secondary	Negative	Negative	Additive	Positive	Additive	Additive	Additive	Positive	Additive	Additive	Additive	Negative	Positive	Additive	Additive	Additive	Additive	Positive	Additive	Negative	Additive	Additive	Additive	Positive	Positive	Additive	Additive	Negative	Additive	Additive	Additive	Positive	Additive	Positive	Additive	Negative	Additive	Positive

Table S5. Metabolites identified in the second project. 165 analytes from primary metabolism were identified and quantified using gas chromatography mass spectrometry (GC-MS). Metabolites induced by the temperature switch (21-17ºC) in necrotic hybrids were identified from this dataset.

Class	Name	MPIMP-ID	Sum Formula	KEGG-ID	Derivate
Acids	Benzene-1,4-dicarboxylic acid	M001710	NA	NA	Benzene-1,4-dicarboxylic acid (2TMS)
Acids	Benzoic acid	M000347	C7H6O2	C00180	Benzoic acid (1TMS)
Acids	Benzoic acid, 4-hydroxy-	M000463	C7H6O3	C00156	Benzoic acid, 4-hydroxy- (2TMS)
Acids	Boric acid	M001531	NA	NA	Boric acid (3TMS)
Acids	Citric acid	M000069	C6H8O7	C00158	Citric acid (4TMS)
Acids	Dehydroascorbic acid	M000082	NA	NA	Dehydroascorbic acid (2MEOX) BP
Acids	Fumaric acid	M000067	C4H4O4	C00122	Fumaric acid (2TMS)
Acids	Glutaric acid, 2-hydroxy-	M000809	C5H8O5	C03196	Glutaric acid, 2-hydroxy- (3TMS)
Acids	Glutaric acid, 2-oxo-	M000571	C5H6O5	C00026	Glutaric acid, 2-oxo- (1MEOX) (2TMS) MP
Acids	Glycolic acid	M000886	C2H4O3	C00160	Glycolic acid (2TMS)
Acids	Lactic acid	M000100	C3H6O3	C00186	Lactic acid (2TMS)
Acids	Maleic acid	M000076	C4H4O4	C01384	Maleic acid (2TMS)
Acids	Malic acid	M000065	C4H6O5	C00149	Malic acid (3TMS)
Acids	Malic acid, 2-methyl-	M000066	C5H8O5	C02612	Malic acid, 2-methyl- (3TMS)
Acids	Piperidine-2-carboxylic acid	M000528	NA	NA	Piperidine-2-carboxylic acid (1TMS)
Acids	Pyrrole-2-carboxylic acid	M000896	NA	NA	Pyrrole-2-carboxylic acid (2TMS)
Acids	Pyruvic acid	M000071	C3H4O3	C00022	Pyruvic acid (1MEOX) (1TMS)
Acids	Salicylic acid	M000220	C7H6O3	C00805	Salicylic acid (2TMS)
Acids	Shikimic acid	M000607	C7H10O5	C00493	Shikimic acid (4TMS)
Acids	Succinic acid	M000074	C4H6O4	C00042	Succinic acid (2TMS)
Alcohols	Benzylalcohol	M000422	C7H8O	C00556	Benzylalcohol (1TMS)
Amino Acids	Alanine	M000026	C3H7NO2	C00041	Alanine (3TMS)
Amino Acids	Alanine, 3-cyano-	M000466	C4H6N2O2	C02512	Alanine, 3-cyano- (2TMS)
Amino Acids	Alanine, beta-	M000027	C3H7NO2	C00099	Alanine, beta- (3TMS)
Amino Acids	Asparagine	M000013	NA	NA	Asparagine (2TMS)
Amino Acids	Aspartic acid	M000033	C4H7NO4	C00049	Aspartic acid (3TMS)

Amino Acids	Glutamic acid	M000036	C5H9NO4	C00025	Glutamic acid (3TMS)
Amino Acids	Glutamine	M000032	NA	NA	Glutamine [-H2O] (2TMS) MP
Amino Acids	Glycine	M000031	C2H5NO2	C00037	Glycine (3TMS)
Amino Acids	Isoleucine	M000017	C6H13NO2	C00407	Isoleucine (2TMS)
Amino Acids	Lysine	M000014	C6H14N2O2	C00047	Lysine (3TMS)
Amino Acids	Methionine	M000018	C5H11NO2S	C00073	Methionine (2TMS)
Amino Acids	Ornithine	M000028	C5H12N2O2	C00077	Ornithine (3TMS)
Amino Acids	Phenylalanine	M000011	C9H11NO2	C00079	Phenylalanine (1TMS)
Amino Acids	Proline	M000029	NA	NA	Proline [+CO2] (2TMS)
Amino Acids	Pyroglutamic acid	M000037	C5H7NO3	C02238	Pyroglutamic acid (2TMS)
Amino Acids	Serine	M000015	C3H7NO3	C00065	Serine (3TMS)
Amino Acids	Serine, O-acetyl-	M000024	C5H9NO4	C00979	Serine, O-acetyl- (2TMS)
Amino Acids	Threonine	M000016	C4H9NO3	C00188	Threonine (3TMS)
Amino Acids	Valine	M000030	C5H11NO2	C00183	Valine (2TMS)
Fatty Acids	Hexadecanoic acid	M000483	C16H32O2	C00249	Hexadecanoic acid (1TMS)
Fatty Acids	Octadecanoic acid	M000485	C18H36O2	C01530	Octadecanoic acid (1TMS)
Fatty Acids	Tetradecanoic acid	M000480	C14H28O2	C06424	Tetradecanoic acid (1TMS)
N- Compounds	Agmatine	M000234	NA	NA	Agmatine [-NH3] (3TMS)
N- Compounds	Arginine	M000835	NA	NA	Arginine [-NH3] (2TMS)
N- Compounds	Ethanolamine	M000096	C2H7NO	C00189	Ethanolamine (3TMS)
N- Compounds	Indole-3-acetonitrile	M000593	NA	NA	Indole-3-acetonitrile (1TMS)
N- Compounds	Octylamine	M000934	NA	NA	Octylamine (2TMS)
N- Compounds	Putrescine	M000186	C4H12N2	C00134	Putrescine (4TMS)
N- Compounds	Spermidine	M000106	C7H19N3	C00315	Spermidine (4TMS)
N- Compounds	Uracil	M000456	C4H4N2O2	C00106	Uracil (2TMS)
Phenylpropanoids	Sinapic acid, cis-	M000648	C11H12O5	NA	Sinapic acid, cis- (2TMS)
Phenylpropanoids	Sinapic acid, trans-	M000010	C11H12O5	C00482	Sinapic acid, trans- (2TMS)
Phosphates	Ethanolaminephosphate	M001131	NA	NA	Ethanolaminephosphate (4TMS)
Phosphates	Fructose-6-phosphate	M000510	C6H13O9P	C00085	Fructose-6-phosphate (1MEOX) (6TMS) MP
Phosphates	Glucose-6-phosphate	M000513	C6H13O9P	C00092	Glucose-6-phosphate (1MEOX) (6TMS) MP
Phosphates	Glycerol-3-phosphate	M000328	C3H9O6P	C00093	Glycerol-3-phosphate (4TMS)

Phosphates	Glycerophosphoglycerol	M000834	C6H15O8P	C03274	Glycerophosphoglycerol (5TMS)
Phosphates	Mannose-6-phosphate	M000711	C6H13O9P	C00275	Mannose-6-phosphate (1MEOX) (6TMS) MP
Phosphates	Phosphoric acid	M000075	H3O4P	C00009	Phosphoric acid (3TMS)
Phosphates	Phosphoric acid monomethyl ester	M000507	NA	NA	Phosphoric acid monomethyl ester (2TMS)
Polyhydroxy Acids	Ascorbic acid	M000001	NA	NA	Ascorbic acid (4TMS)
Polyhydroxy Acids	Dehydroascorbic acid dimer	M000082	C6H6O6	C05422	Dehydroascorbic acid dimer (2MEOX) MP
Polyhydroxy Acids	Erythronic acid	M000454	C4H8O5	NA	Erythronic acid (4TMS)
Polyhydroxy Acids	Galactonic acid	M000596	C6H12O7	C00880	Galactonic acid (6TMS)
Polyhydroxy Acids	Gluconic acid	M000508	C6H12O7	C00257	Gluconic acid (6TMS)
Polyhydroxy Acids	Gluconic acid-1,5-lactone	M000638	C6H10O6	C00198	Gluconic acid-1,5-lactone (4TMS)
Polyhydroxy Acids	Glyceric acid	M000073	C3H6O4	C00258	Glyceric acid (3TMS)
Polyhydroxy Acids	Lyxonic acid-1,4-lactone	M001180	NA	NA	Lyxonic acid-1,4-lactone (3TMS)
Polyhydroxy Acids	Threonic acid	M000078	C4H8O5	C01620	Threonic acid (4TMS)
Polyhydroxy Acids	Threonic acid-1,4-lactone	M000595	C4H6O4	NA	Threonic acid-1,4-lactone (2TMS)
Polyols	Arabitol	M000588	C5H12O5	C01904	Arabitol (5TMS)
Polyols	Erythritol	M000054	C4H10O4	C00503	Erythritol (4TMS)
Polyols	Glycerol	M000053	C3H8O3	C00116	Glycerol (3TMS)
Polyols	Inositol, myo-	M000060	C6H12O6	C00137	Inositol, myo- (6TMS)
Polyols	Ribulose + Xylulose	M000879	NA	NA	Ribulose + Xylulose (1MEOX) (4TMS) MP
Polyols	Sorbitol	M000055	C6H14O6	C00794	Sorbitol (6TMS)
Polyols	Threitol	M000469	C4H10O4	NA	Threitol (4TMS)
Sugar Conjugates	alpha-D-Galactopyranosyl-(1,4)-D-galac	M001185	NA	NA	“alpha-D…” (1MEOX) (8TMS) MP
Sugar Conjugates	Galactinol	M000673	C12H22O11	C01235	Galactinol (9TMS)
Sugar Conjugates	Salicylic acid-glucopyranoside	M001182	NA	NA	Salicylic acid-glucopyranoside (5TMS)
Sugars	Fructose	M000606	C6H12O6	C00095	Fructose (1MEOX) (5TMS) BP

Sugars	Galactose	M000043	C6H12O6	C00124	Galactose (1MEOX) (5TMS) MP
Sugars	Glucose	M000040	C6H12O6	C00031	Glucose (1MEOX) (5TMS) BP
Sugars	Lyxose	M000576	C5H10O5	C00476	Lyxose (1MEOX) (4TMS) MP
Sugars	Maltose	M000048	C12H22O11	C00897	Maltose (1MEOX) (8TMS) MP
Sugars	Mannose	M000633	C6H12O6	C00936	Mannose (1MEOX) (5TMS) MP
Sugars	Raffinose	M000049	C18H32O16	C00492	Raffinose (11TMS)
Sugars	Rhamnose	M000590	C6H12O5	C00507	Rhamnose (1MEOX) (4TMS) MP
Sugars	Sucrose	M000044	C12H22O11	C00089	Sucrose (8TMS)
Sugars	Tagatose	M000622	NA	NA	Tagatose (1MEOX) (5TMS) MP
Sugars	Trehalose, alpha,alpha'-	M000671	C12H22O11	C01083	Trehalose, alpha,alpha'- (8TMS)
Sugars	Xylose	M000579	C5H10O5	C00181	Xylose (1MEOX) (4TMS) MP
MSTs	A112003-101	M000000	NA	NA	A112003-101
MSTs	A116014-101	M000000	NA	NA	Unknown#bth-pae-013
MSTs	A139006-101	M000000	NA	NA	A139006-101
MSTs	A138004-101	M000000	NA	NA	A138004-101
MSTs	A142003-101	M000000	NA	NA	A142003-101
MSTs	A143003-101	M000000	NA	NA	A143003-101
MSTs	A144007-101	M000000	NA	NA	similar to Aspartic acid (2TMS)
MSTs	A145008-101	M000000	NA	NA	A145008-101
MSTs	A145016-101	M000000	NA	NA	NA145016 (classified unknown)
MSTs	A145015-101	M000000	NA	NA	NA145015
MSTs	A147001-101	M000000	NA	NA	A147001-101
MSTs	A147005-101	M000000	NA	NA	A147005-101
MSTs	A147011-101	M000000	NA	NA	NA147011 (classified unknown)
MSTs	A148006-101	M000000	NA	NA	A148006-101
MSTs	A151008-101	M000000	NA	NA	A151008-101
MSTs	A155014-101	M000000	NA	NA	D155405
MSTs	A157003-101	M000000	NA	NA	A157003-101
MSTs	A159002-101	M000000	NA	NA	A159002-101
MSTs	A160018-101	M000000	NA	NA	Unknown#sst-cgl-037
MSTs	A161007-101	M000000	NA	NA	A161007-101

MSTs	A163004-101	M000000	NA	NA	A163004-101
MSTs	A167005-101	M000000	NA	NA	A167005-101
MSTs	A165011-101	M000000	NA	NA	D165453
MSTs	A167004-101	M000000	NA	NA	A167004-101
MSTs	A167003-101	M000000	NA	NA	A167003-101
MSTs	A170001-101	M000000	NA	NA	NA170001 (classified unknown)
MSTs	A171003-101	M000000	NA	NA	A171003-101
MSTs	A171005-101	M000000	NA	NA	A171005-101
MSTs	A171025-101	M000000	NA	NA	D171803
MSTs	A174005-101	M000000	NA	NA	A174005-101
MSTs	A174001-101	M000000	NA	NA	NA174001
MSTs	A175008-101	M000000	NA	NA	A175008-101
MSTs	A176001-101	M000000	NA	NA	NA176001 (classified unknown)
MSTs	A176010-101	M000000	NA	NA	A176010-101
MSTs	A178003-101	M000000	NA	NA	A178003-101
MSTs	A180004-101	M000000	NA	NA	NA180004
MSTs	A185003-101	M000000	NA	NA	A185003-101
MSTs	A187005-101	M000000	NA	NA	A187005-101
MSTs	A191007-101	M000000	NA	NA	A191007-101
MSTs	A190021-101	M000000	NA	NA	A190021-101
MSTs	A196006-101	M000000	NA	NA	A196006-101
MSTs	A199004-101	M000000	NA	NA	A199004-101
MSTs	A203003-101	M000000	NA	NA	A203003-101
MSTs	A209004-101	M000000	NA	NA	A209004-101
MSTs	A211001-101	M000000	NA	NA	NA211001
MSTs	A213001-101	M000000	NA	NA	NA213001
MSTs	A214003-101	M000000	NA	NA	A214003-101
MSTs	A214004-101	M000000	NA	NA	A214004-101
MSTs	A217007-101	M000000	NA	NA	A217007-101
MSTs	A222008-101	M000000	NA	NA	D222462
MSTs	A228001-101	M000000	NA	NA	A228001-101

MSTs	A227008-101	M000000	NA	NA	NA227008
MSTs	A000512-101	M001430	NA	NA	similar to Sinigrin_A
MSTs	A000512-101	M001430	NA	NA	similar to Sinigrin_B
MSTs	A240004-101	M000000	NA	NA	A240004-101
MSTs	A250001-101	M000000	NA	NA	A250001-101
MSTs	A251003-101	M000000	NA	NA	A251003-101
MSTs	A254002-101	M000000	NA	NA	A254002-101
MSTs	A255012-101	M000000	NA	NA	Unknown#sst-cgl-119
MSTs	A260006-101	M000000	NA	NA	D260482
MSTs	A276008-101	M000000	NA	NA	A276008-101
MSTs	A278005-101	M000000	NA	NA	NA278005
MSTs	A279005-101	M000000	NA	NA	A279005-101
MSTs	A278013-101	M000000	NA	NA	D278931
MSTs	A300001-101	M000000	NA	NA	similar to Galactinol
MSTs	A302003-101	M000000	NA	NA	A302003-101
MSTs	A308003-101	M000000	NA	NA	A308003-101
MSTs	A311002-101	M000000	NA	NA	A311002-101
MSTs	A313001-101	M000000	NA	NA	A313001-101
MSTs	A317003-101	M000000	NA	NA	A317003-101
MSTs	A324001-101	M000000	NA	NA	A324001-101
MSTs	A329006-101	M000000	NA	NA	A329006-101